

**Proceedings of the Belgian and Dutch National Groups of IABSE  
Young Engineers Colloquium 2023 - YEC2023**



Construction site of the immersed tunnel segments, Zeebrugge, Belgium

**Ghent, Belgium**



**International Association for Bridge and Structural Engineering**



**Proceedings of the Belgian and Dutch National Groups of IABSE  
Young Engineers Colloquium 2023 - YEC2023**

**Editor:**

A. Outtier, Ghent University, Ghent, Belgium

**Organised by:**

Belgian and Dutch National Groups of IABSE

Published by: IABSE - Jungholzstrasse 28 - 8050 Zurich, SWITZERLAND

ISBN 978-3-85748-197-0



## Young Engineers Colloquium 2023 - YEC2023

### Organising and Scientific Committee

prof. dr. ir. H. (Hans) De Backer, Ghent University, Belgium  
dr. ir. A. (Ane) de Boer, Municipality of Amsterdam, The Netherlands  
prof. ir. B. (Bart) De Pauw, TUCRAIL, Brussels, Belgium and Ghent University, Belgium  
dr. ir. V. (Vincent) de Ville de Goyet, Bureau Greisch, Belgium  
ir. A. (Alain) Dumortier, Bureau Greisch, Belgium  
ing. B. (Bruno) Godart, Gustave Eiffel University, IFSTTAR, Champs/Marne, France  
ing. B.H. (Bert) Hesselink, Royal Haskoning DHV, The Netherlands  
ir. F. (Frank) Maatje, Bouwen met Staal, The Netherlands  
ir. P. (Pierre) Mingeot, Besix, Belgium  
ir. A. (André) Orcési, MTECT/SG, France  
dr. ir. A. (Amelie) Outtier, Ghent University, Belgium  
prof. ir. H.H. (Bert) Snijder, Eindhoven University of Technology, The Netherlands  
ir. S. (Sander) Van Alphen, Movares, The Netherlands  
prof. dr. ir. Ph. (Philippe) Van Bogaert, Ghent University, Belgium  
Mr. L. (Luc) Waeghe, Janson Bridging, France

### Awards Committee

dr. ir. A. (Ane) de Boer, Municipality of Amsterdam, The Netherlands  
dr. ir. V. (Vincent) de Ville de Goyet, Bureau Greisch, Belgium  
prof. ir. H.H. (Bert) Snijder, Eindhoven University of Technology, The Netherlands  
prof. dr. ir. Ph. (Philippe) Van Bogaert, Ghent University, Belgium

### Support staff

A (Amelie) Outtier  
L. (Lien) De Backer



## Sponsors

YEC2023 would not have been possible without our sponsors. Their contribution to YEC2023 is gratefully acknowledged. Our sponsors are (in alphabetical order):



BESIX  
<https://www.besix.com>



Bureau Greisch  
<https://www.greisch.com>



Gemeente Amsterdam  
<https://www.amsterdam.nl>



IMD Raadgevende Ingenieurs  
<https://imdbv.nl/>



ProRail  
<https://www.prorail.nl>



Royal HaskoningDHV  
<https://www.royalhaskoningdhv.com>



TUC RAIL  
<https://www.tucrail.be>



Willemen Groep NV  
<https://www.willemen.be>



## **Preface by the President of IABSE, Dr. Tina Vejrum**

This Young Engineers Colloquium jointly organized by the Belgian and the Dutch group of IABSE promises to become a very exciting and valuable event where students and young professions get the opportunity to present their work, exchange ideas, inspire each other, meet seniors from the profession, make new contacts and expand their network.

The YEC events build on two fundamental core values of IABSE: The importance of young professionals in pushing for development and the need for international collaboration to achieve real change. The Belgian and Dutch groups of IABSE have a long tradition of co-organizing successful events and inviting the international community of professionals working with the built environment to participate and share their knowledge. This will be two intense days of learning and discussing of innovative ideas that will ultimately shape our future sustainable and liveable societies.

## **Preface by the Chair of the Belgian National Group of IABSE, Hans De Backer**

This will be the third time that the Belgian and Dutch group of IABSE organize a Young Engineers Colloquium together. After the first successful edition in Eindhoven in 2019, the second one had to be organized strictly online due to the COVID-19 pandemic in 2020. Because of that, I am extremely happy that we can once again plan for an onsite event, where we offer Young Engineers the chance to show their work and initial work experience to their peers. But it is not limited to that. They can also to interact with more experienced members of the structural engineering field and this within the international framework of IABSE. I look forward to welcoming everybody, young engineers, and experienced engineers to the city of Ghent, within the aula of my alma mater, Ghent University.

## **Preface by the Chair of the Dutch National Group of IABSE, Bert Hesselink**

On 24 and 25 November 2023 the Belgian and the Dutch National Group of IABSE will be the joint hosts of a colloquium aimed at young engineers. The Dutch National Group is proud to be part of this initiative.

YEC2023 builds on the long history of trade and collaboration between Belgium and the Netherlands and on the strong common engineering tradition. Offering a unique opportunity for young professionals to meet and exchange ideas across borders, the initiative truly reflects the international spirit of IABSE.

Students, young engineers and experienced professionals, who act as mentors and beacons of our profession, are warmly welcomed to participate actively in an inspiring day which will serve as an introduction to the vibrant community of IABSE and its activities.

The Young Engineers Colloquium is supported by the British National Group of IABSE and by the French National Group of IABSE



## General preface

The Belgian and Dutch National Groups of IABSE have jointly organized the Young Engineers Colloquium 2023 (YEC2023) on November 24<sup>th</sup> and 25<sup>th</sup>. This was already the third edition, which was thankfully once again an in-person event, taking place in Ghent at the historic Aula of Ghent University. This edition was supported by the neighbouring national groups of France and the United Kingdom. The YEC2023 is especially meant for young engineers to exchange knowledge internationally. The colloquium is open to all professionals interested in structural engineering regardless their age, but apart from the keynote speaker, all presenters are young engineers under 35 years of age.

This colloquium offers young engineers an exciting opportunity to present their work to an audience of fellow engineers from the structural engineering sector. It provides attendees with an overview of current research topics as well as challenging engineering and construction projects and is an excellent platform to share experiences among experienced and young engineers.

IABSE stands for International Association for Bridge and Structural Engineering and is the international professional and scientific association active in the field of structural engineering. IABSE offers a platform for structural engineers to exchange information and to learn from each other at the international level. IABSE covers all aspects of structural engineering in all materials. The structures comprise, besides bridges, also buildings and all kinds of civil engineering structures. For more information see: [www.iabse.org](http://www.iabse.org). The Dutch and Belgian National Groups of IABSE are sister associations of the main IABSE organization which is based in Zurich, Switzerland.

Apart from the keynote paper, two-page papers were prepared by the colloquium participants and collected in these proceedings. These papers may contain student projects, PhD research as well as engineering and construction projects. In the spirit of IABSE, these proceedings contain contributions on buildings, bridges and any other civil engineering structure and in any material.

The Belgian and Dutch National Groups of IABSE have a strong tradition in organizing and co-organizing local as well as international events. The local activities of the National Groups are quite important in encouraging young engineers to join this international IABSE community with fellow structural engineers from all over the world. We hope it incites them to participate in the international conferences as well.

On behalf of the Organising and Scientific Committee,

Hans De Backer



## Content

### Keynote paper

Case study for a KPI-based Quality Control system of roadway bridges

*José C. Matos, N.Son Dang*..... 14

### Session 1

Construction and calibration of digital twins for metallic truss bridges

*Carla Menuet, Théo Bailly* ..... 22

Methods of automating design optimisation

*Trevor Spanenburg*..... 24

Structural design automation of a cut and cover tunnel

*Kelvin Roovers*..... 26

A new finite element for joints based on the components method

*BODSON Romain, de Ville de Goyet Vincent, GOLEA Tudor*..... 28

Parametric modelling to improve sustainability in design

*Eloïse Denis, Stef Feyers, Simon Van Gompel* ..... 30

Full dynamic train-track-bridge interaction calculation to verify passenger comfort on the Lembeek high-speed rail viaduct

*Nick Gerard* ..... 32

Simulated aleatory traffic for fatigue design of steel bridges

*Marco Lucio Cerquaglia, Yves Duchêne, Vincent de Ville de Goyet* ..... 34

Fatigue recalculation of the Gallieni bridge over the Rhone in Lyon

*Amine Laklalech and Jimmy Jacquot*..... 36

Shear and Wheel Loading on Bolted Connectors for Composite Bridge Decks

*Angeliki Christoforidou, Jelco Köhlenberg, Abishek Baskar, Job ter Kuile, Marko Pavlovic* ..... 38



## Session 2

Re-use of prefabricated prestressed bridge girders in the Netherlands	
<i>Danny Jilissen, Rob Vergoossen</i> .....	40
Proof load testing prestressed concrete girders for reuse	
<i>Jose Eduardo Paredes Pineda</i> .....	42
Wind Tunnel Tests and Normative Approaches of the ARC MAJEUR Subject to Vortex Shedding	
<i>Adrien Palm, Yves Duchêne</i> .....	44
Dynamic analysis of a hybrid steel-GFRP footbridge	
<i>LB Cornelissen</i> .....	46
Development of fully precast lightweight steel-UHPFRC composite bridge	
<i>Xiujiang Shen</i> .....	48
Influence of a timber outrigger system on cross laminated timber core buildings	
<i>F.F. Janssens</i> .....	50
Circularity in bridge engineering	
<i>Sharon Deceuninck</i> .....	52
Renewal of a Station Roof: Using Bio-based Materials	
<i>Tijmen Scharff</i> .....	54
Effect of modal coupling on the assessment of footbridge vibrations	
<i>Thibaud Bastin, Vincent de Ville de Goyet, Yves Duchêne</i> .....	56
Optimization of construction sequence by anchoring cofferdam to tunnel	
<i>Wouter Lambrechts</i> .....	58
Pile group effect: calculation and impact on design of high-rise buildings	
<i>Niko Verschaeve</i> .....	60
Piling disease in Amazonehaven	
<i>Reza Nejad</i> .....	62
Automation in diaphragm wall design of project Oosterweel Junction	
<i>Heng Fang, Bart Rombauts, Benjamin Tytgat</i> .....	64



### Session 3

Structural design and analysis of Tour Triangle	
<i>Maarten Van Craenenbroeck</i> .....	66
Structural Assessment of Historical Verbundträger Bridge Decks	
<i>Berber Renckens, Ane de Boer</i> .....	68
Construction of the new Verbindingsbrug in Zeebrugge	
<i>Steffie Rooms</i> .....	70
Structural assessment of masonry arches	
<i>Thomas Harrewijn</i> .....	72
Risk management on historical quay walls in Amsterdam	
<i>Rick Voortman</i> .....	74
Lock Renovation in Auvelais (Belgium) – Miter Gates	
<i>Dubucq Robin, Bonivers Michaël</i> .....	76
Pont Patton – Ettelbrück – Luxemburg	
<i>Koen Calleyl</i> .....	78
Structural Assessment of Historic Masonry Cellars in Utrecht	
<i>Peter Vos</i> .....	80
Assessing concrete structures after repair: a chloride ingress forecasting model	
<i>Karel Van Den Hende, Stef Helderweirt, Wouter Botte, Stijn Matthys and Robby Caspeele</i> .....	82
Modern trends in Bridge Health Monitoring (BHM)	
<i>Muhammad Farjad Sami, Hans De Backer, Amelie Outtier</i> .....	84
Research: Use of innovative techniques in bridge inspections	
<i>Thomas Plumet</i> .....	86
Renovating the IJ-viaduct while keeping Amsterdam Central Station in operation – A case study	
<i>Laura van der Hoeven</i> .....	88
Cycling bridge ‘Vijfstraten’: using parametric design in bridge engineering	
<i>Ronan Pieters</i> .....	90



## List of authors

Bailly, T. ....	22
Baskar, A. ....	38
Bastin, T.....	56
Bodson, R. ....	28
Bonivers, M. ....	76
Botte, W. ....	82
Calleyl, K.....	78
Caspeepe, R. ....	82
Cerquaglia, M. L.....	34
Christoforidou, A. ....	38
Cornelissen, L.....	46
De Backer, H.....	84
de Boer, A.....	68
de Ville de Goyet, V.....	28, 34, 56
Deceuninck, S. ....	52
Denis, E. ....	30
Dubucq, R.I.....	76
Duchêne, Y.....	34, 44, 56
Fang, H. ....	64
Feyers, S. ....	30
Gerard, N. ....	32
Golea, T. ....	28
Harrewijn, T. ....	72
Helderweirt, S.....	82
Jacquot, J.....	36
Janssens, F.....	50
Jilissen, D.....	40
Köhlenberg, J.....	38
Laklalech, A. ....	36
Lambrechts, W. ....	58
Matos, José C. ....	14
Menuet, C.....	22
Nejad, R.....	62
Outtier, A.....	84



<i>Palm, A.</i> .....	44
<i>Paredes, J. E.</i> .....	42
<i>Pavlovic, M.</i> .....	38
<i>Pieters, R.</i> .....	90
<i>Plumet, T.</i> .....	86
<i>Renckens, B.</i> .....	68
<i>Rombauts, B.</i> .....	64
<i>Rooms, S.</i> .....	70
<i>Roovers, K.</i> .....	26
<i>Sami, M. F.</i> .....	84
<i>Scharf, T.</i> .....	54
<i>Shen, X.</i> .....	48
<i>Son Dang, N.</i> .....	14
<i>Spannenburg, T.</i> .....	24
<i>ter Kuile, J.</i> .....	38
<i>Tytgat, T.</i> .....	64
<i>Van Craenenbroeck, M.</i> .....	66
<i>Van Den Hende, K.</i> .....	82
<i>van der Hoeven, L.</i> .....	88
<i>Van Gompel, S.</i> .....	30
<i>Vergoossen, R.</i> .....	40
<i>Verschaeve, N.</i> .....	60
<i>Voortman, R.</i> .....	74
<i>Vos, P.</i> .....	80



# Case study for a KPI-based Quality Control system of roadway bridges

José C. Matos, N.Son Dang

ISISE, University of Minho, Guimarães, Portugal

Contact: [sondn@civil.uminho.pt](mailto:sondn@civil.uminho.pt)

## 1 Abstract

It has increasingly become challenging for civil engineers to change their strategy from developing new facilities to maintaining the existing aging infrastructures. Aiming to sustain their service performance throughout the operational stage. Especially for the roadway bridges, which are simple typical structures but very critical to the growth of the socioeconomic system. This research aims to suggest a quality control framework for managing highway bridges utilizing key performance indicators (KPIs). In this regard, case studies are being undertaken for several bridges, most located in European countries. The performance indicators (PIs) and goals (PGs) are formed during this. Then, following the assessment of the vulnerable zone, the derivation KPIs from those PIs are introduced and developed while considering various maintenance situations and time functions. The presentation includes a curated case study focusing on a steel truss bridge. This case study demonstrates the potential for developing a long-term strategy for managing highway bridges on a lifecycle level.

**Keywords:** Roadway Bridge; Quality Control; Key Performance Indicators; Spider Diagram; Decision-Making.

## 1. Introduction

Current research presents several national and municipal bridge management systems (Shim et al., 2017, 2019; Dang et al., 2018, 2020). Their architectural frameworks are similar, but their condition assessment techniques differ (Tran et al., 2023; Nhamage et al., 2023). These changes can affect maintenance decisions. The highway bridge management process helps identify maintenance needs more consistently. Performance indicators and maintenance strategy planning help establish the procedure. It increases the need for quality control (QC) systems to ensure that products and services meet or exceed user and community standards. Road infrastructure asset management and QC go together (Matos et al., 2017, 2020, 2023). They are public services, but the state or a private-public partnership can manage them. Both instances require efforts to improve system quality and reduce unexpected expenditures. The standardized approach unites maintenance management formats from diverse networks and nations yet allows them to be integrated with the design because they are already operational. First, quantify performance factors to produce roadway bridge assessment recommendations. These assessment actions have reference periods. Step two is establishing performance standards. Finally, a road bridge QC plan

guideline and benchmark implementation examples can be created.

Performance indicators (PI) have been studied in bridge condition assessment (“Fib Model Code for Concrete Structures 2010,” 2013; Ugwu & Haupt, 2007). It permits quality control (QC) programs to compare measured PIs to pre-specified performance goals (PG). PIs, especially KPIs, allow to define goals to create QC programs that ensure bridge-quality service. Bridge management techniques can be enhanced by quantifying and assessing bridge performance and quality specifications to ensure an expected performance level, improving asset management of aging bridges. Management systems commonly employ lifecycle analysis (Yang & Frangopol, 2019). For structural condition evaluation, deterministic performance prediction models explain the future condition through a functional association between structural condition characteristics, such as structural age, and mechanical, chemical, and thermal loading processes (Dhada et al., 2020; Hanley et al., 2016). Such models require precise variable information to implement. Analyzing indicators for assessment frameworks and quantification procedures is crucial.

Thus, performance indicator quantification methodologies must be recommended for assessing roadway bridges. These assessment actions need reference periods. Then, set performance standards. That would lead to a quality control plan for roadway

bridges, and these plans emphasize advanced deterioration prediction methods. Sustainable roadway bridge management, which evaluates environmental, economic, and social performance indicators throughout the life cycle, is also essential. By quantifying and assessing bridge performance and quality standards to ensure an expected performance level, bridge management methods will be much enhanced, improving asset management of aging bridges in Europe.

## 2 Performance indicators and goals

### 2.1 Performance indicators

Code standards partially cover mechanical and technical qualities and deterioration behavior, which the indicators capture. Natural aging, material quality, service life design, sustainable, environmental, economic, and social indicators, and performance profiles are considered. A flexible European performance indicator database meets country-specific needs. Safety, serviceability, availability, prices, and environmental efficiency are measured.

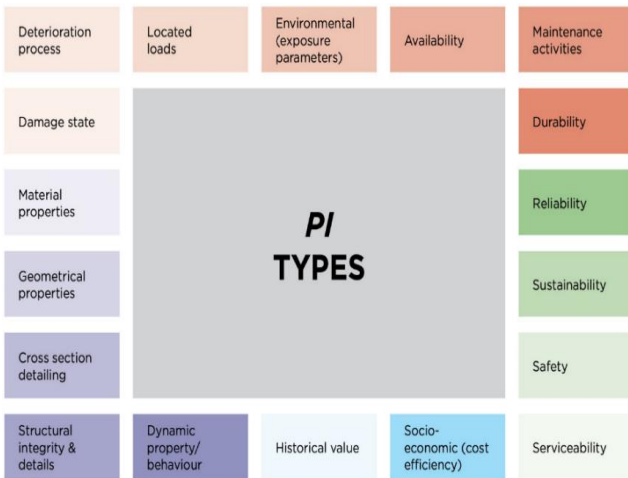


Figure 1. Possible clusters of research-based performance indicators

### 2.2 Performance goals

Figure 2 connects Performance Indicators to Performance Goals at component, system, and network levels. A multi-objective system sets bridge and network performance targets. This study covers five performance aspects: Reliability; Availability; Economy; Environment; Traffic Safety. Multi-criteria decision-making (MCDM) ranks alternatives using inputs, benefit/cost information, and decision-maker/stakeholder opinions. However, performance metrics and goal setting differ across Europe.

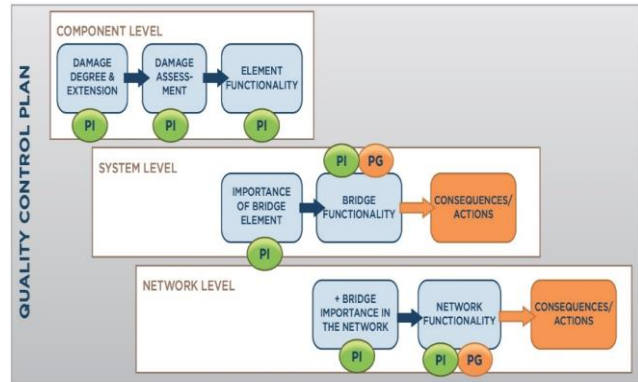


Figure 2. The assessment procedure from component to the system and network level is based on the PIs and PGs

## 3 Quality Control Plan

### 3.1 Bridge assessment and Quality Control ontology

Safety and serviceability are apparent KPIs for existing bridges, and durability, stability, affordability, and utility can be added. This paper proposes KPIs (qualitative, between the ordinal scale of 1-5). Safety and serviceability are examined separately, and availability includes serviceability. Spider Net diagrams show performance (Figure 3a). KPI values in the green zone improve bridge performance.

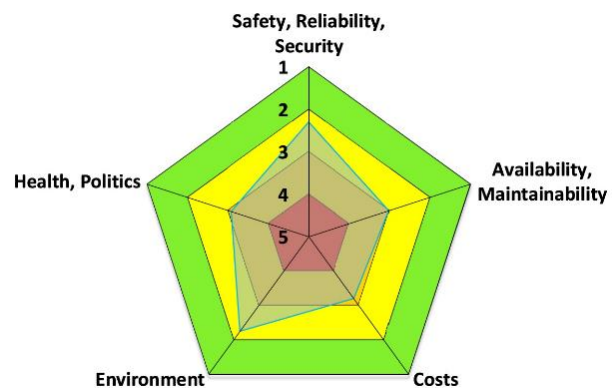


Figure 3. The 'Spider Diagram' for bridge assessment

QC will analyze KPIs for alternative maintenance scenarios based on inspection/investigation or prediction to find the best practical one. Ecosystem, economy, and time-based KPIs are helpful. Bridge damage procedures are single or multiple; therefore, knowing about them is essential for performance prediction, preventive maintenance, and rehabilitation. Damage processes are slow and observable (with adequate inspection) or non-observable (handled by an appropriate maintenance strategy). Better damage process information, graded

by kind, intensity, extent, location, cause, and impacted material, helps optimize inspection and maintenance procedures.

PIs assess bridge fitness. A crack width > 0.4 mm may indicate reinforcing yield from poor resistance or overloading. Unlike an observation, a PI interprets its effect on bridge performance. Some observations are symptoms; therefore, they don't affect static KPIs (Reliability and Safety). In a dynamic situation, symptoms may immediately affect relevant KPIs (Availability and Economy). This study examines Design & Construction, Observations, Damage Processes, and Symptoms in the QCP framework.

This research uses modern codes' dependability index definition of safety and serviceability, which relates to the target likelihood of a bridge's fitness for purpose during its service life. If existing bridges are unrestricted, reliability evaluation can be economically beneficial. Based on experience and data, a basic reliability assessment can be performed for review. Design documentation can identify relevant failure mechanisms and sensitive zones. Vulnerable zones in bridge structures are where damage most affects safety and serviceability and can be caused by numerous failure modes. Figure 3b shows an Entity Relationship Diagram of the critical entities' broad framework ontology (ERD). The "crowfoot with a circle" represents one-to-zero relationships, whereas the "crowfoot" represents one-to-many relationships.

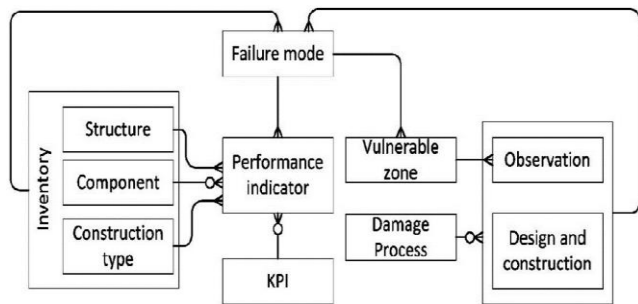


Figure 4. The ontology of a Quality Control Framework

### 3.2 Development of KPIs over time

This research scales all KPIs from 1-5, with 1 being the best and 5 the worst. "Availability," "Environment," and "Economy" KPIs must be scaled from 1-5 in native units. "Availability" is the system's uptime. Each time instant can have a value of 0 or 1. "Availability" can be evaluated by vehicle category-specific journey time, which can be monetized as user expenses. A qualitative "Availability" value can be established

based on road importance and alternate routes when models or information are missing. "Economy" follows suit. It normalizes KPIs. As mentioned, a "spider diagram" helps illustrate KPIs. When time is of interest, the time axis can be inserted orthogonally on the diagram plane to each KPI's axis. It creates a "performance tube" (Figure 5).

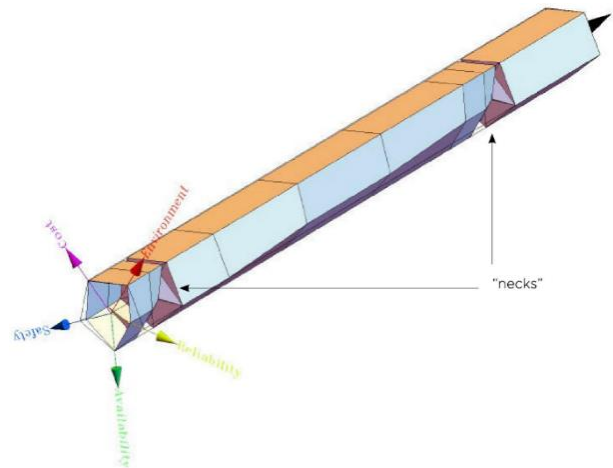


Figure 5. Generation of a Performance Tube over time for the KPIs

Serviceability and safety failure types can be analyzed separately on multiple "Reliability" axes. It simplifies maintenance decisions and accounts for failures due to severe deterioration and hazards. "Necks" in the diagram indicate low performance, whereas "complete" pentagon cross-sections indicate good performance. The volume between the "full" pentagon and the "performance tube" could be a performance deficit to be minimized. Using Net Present Value (NPV), monetized KPIs compare future and current events. Non-monetized KPIs divide opinion. Several research on social preference for non-monetized qualities like emotions and values face this difficulty, yet bridge KPIs have some economic influence. Thus, the KPIs "Reliability," "Availability," and "Safety" will be discounted using NPV, like the cash flow and maintenance intervention costs. Today, these KPIs matter more than in one, two, or ten years, and thus, short-term therapies may be costlier but more beneficial. The NPV is divided by the NPV estimated if all KPIs were equal to one across the research period to normalize the KPIs. These long-term KPIs are "average."

### 3.3 Quality Control framework

Static and dynamic quality control steps are planned (see Figure 6). Preparation, inspection, and KPI snapshots make up the first, and the second approach involves determining service life, KPI development, and the best maintenance scenario.

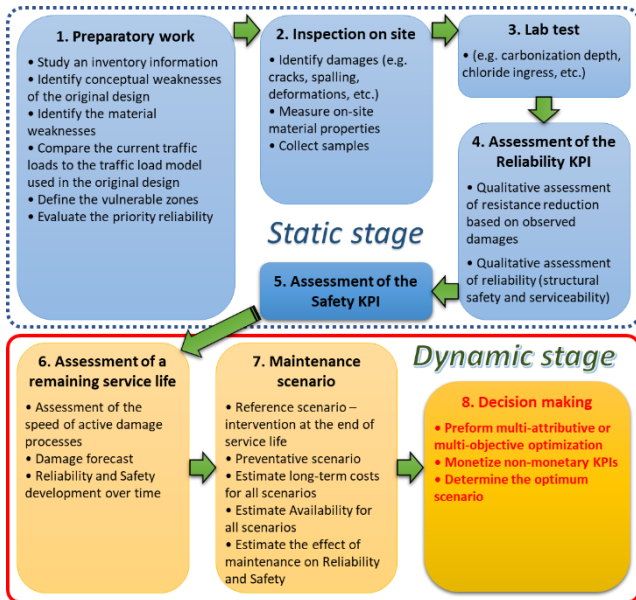


Figure 6. The steps in the QC Framework.

## 4 Case study for the steel truss bridge

This research examines a 1956 36m single-span half-through steel truss bridge with a reinforced concrete slab. Road 9779 crosses the Jordan River between Qiryat Shmona and Israel's Golan Heights. The 2012 average daily traffic was 6800, with no heavy vehicle data. Heavy army trucks often pass the bridge. The historical drawing depicts mass-reinforced concrete abutments with four rows of hammered piles penetrating the foundation. Since the pile was built in 1956, it might be steel or wood. The substructure

consists of two reinforced (found during investigations) enormous concrete abutments with a deadman block at the back and tension-buried girders.



Figure 7. Steel truss bridge, Israel.

### 4.1 Key performance indicators

KPIs are based on team expertise and Israeli bridge inspection experience (figure 8). Bridge failure modes and signs are estimated. Two life cycle techniques examine the lifetime costs, dependability, availability, and safety of selected truss bridges in the following "100 years". The first method assumes no bridge repairs save pavement ones, and bridge flaws develop until a component or system failure, and only the relevant part or system is fully repaired. A second preventative method considers the initial significant bridge restoration and a later periodical set of timely treatments to prevent defect development and structure degradation. Seismic retrofitting is not required in this circumstance.



Structure type	Group	Component	Material	Design & Construction	Failure mode	Location/ Position	Damage /Observation	Damage process	KPI	Performance Indicator component level		Performance value		Estimated failure time [years]
										R	S	R	S	
TB	Structural elements	Main Trusses	Steel	1954	Truss Bending failure mode	Upper chord compression zone	Corroded plates	Corrosion	Reliability (Structure safety)	2.3	4.1	4.1	2.1	40
						Corroded rivet	Corrosion	2.3		40				
						Lower chord tension zone	Corroded plates	Corrosion		2.3				40
						Corroded rivet	Corrosion	2.3		40				
					Truss Shear failure mode	Diagonals	Corroded plates	Corrosion		2.3				40
							Corroded rivet	Corrosion		2.3				40
							Accidental damage	Impact		2.0				20(?)
					Global buckling of truss upper chord	Connection of truss verticals with deck cross girder	sheared rivet	Fatigue		4.1				15
							Out of plane movement of lower connection plate	Fatigue		4.1				20
							Cross girders	Steel		1954				Bending
		web plate buckling	Bearing area over main truss	Rivets are partially sheared	Fatigue	4.1			20					
		Bending	Along the girder	Corroded rivet	Corrosion	2.1			40					
		Deck slab	Reinforced concrete	1954	Bending	HMS/bottom	delamination	Corrosion	Reliability	2.1	2.1	30		
					Falling chunks	bottom	Spalling	Corrosion	Safety (Life and limb)	2.1	2.1	30		
					Bending	HMH	Efflorescence	Leaching	(Symptom) (2.1)					
		Bearings	Steel	1954	Bearing Failure	Abutment 1 (west)	Corrosion	Corrosion	Reliability	2.0	4.0	40		
		Bearings	Steel	1954	Bearing Failure	Abutment 1 (west)	Bearing restrained no movement due to corrosion and debris	Corrosion	Reliability	4.0		20		
		Bearings	Steel	1954	Bearing Failure	Abutment 11 (east)	Loss of rotation ability due to Corrosion	Corrosion	Reliability	3.0		20		
		Abutment	Reinforced concrete	1954		Abutment 1 (west)	Spalling and delamination at closing wall	Joint leaking	Reliability	3.0	3.0	20		
		Abutment	Reinforced concrete	1954	Bearing Failure	Abutment 1 (west)	closing wall with horizontal crack	Closing of joint	Reliability	3.0		20		
		Wing wall	Reinforced concrete	1954		Wing wall	Horizontal cracking		Reliability	2.1	3.3	-		
		Wing wall	Reinforced concrete	1954		Wing wall	Spalling	Corrosion	Reliability	3.3		-		
		Wing wall	Reinforced concrete	1954		Wing wall	Surface abrasion	Abrasion	(Symptom)	3.3		-		
		Expansion Joint	steel	1954	Closing	EJ 1 (west)	Closing of EJ	Deck movement	Reliability	3.0	3.0			
		Pedestrian Deck slab	Reinforced concrete	1954	HMH	Over transvers supporting truss	Transvers cracks	Not active	Reliability	2.3	2.3	20		
		Pedestrian Deck slab	Reinforced concrete	1954	Falling chunks	South Edge	Spalling	Corrosion	Safety (Life and limb)	3.3	3.3	20		
Safety barrier	Steel	1954	Falling of the deck	Safety barrier	Broken, missing parts	Impact	Safety (Life and limb)	3.0	3.0	10 (?)				
Pedestrian Handrail	Steel	1954	Falling of the deck	Handrail anchoring	Corrosion of structural steel	Corrosion	Safety (Life and limb)	2.7	2.7	30				
Curb	Reinforced concrete	1954	Falling chunks	Curb side	Spalling, delaminations	Corrosion	Safety (Life and limb)	3.3	3.3	20				
Pavement	Asphalt	Estimated 2005	Sudden disturbance to driver	Expansion joints overlay	Open transvers cracks	Joint reflection cracking	Safety (Life and limb)	3.3	3.3	5				

Figure 8. KPIs for the steel truss bridge, Israel.

## 4.2 Scenario

### 4.2.1 Reference scenario (figure 9)

Only periodic pavement repairs are done on the reference approach. This strategy develops the flaw to bridge failure. Next, assume the following structure faults development and failure times: Pavement collapse in five years owing to expansion joint cracks and potholes will diminish driver safety and raise the risk of accidental impact load impacting the primary truss members. (the reference example requires pavement layer restoration); Accidental damage will collapse the steel safety barrier in 10 years; Due to rivet fatigue, the vertical truss member-cross girder connections are projected to fail in 15-20 years. Based on the faults detected, this problem will progress. It reduces the FEM's safety factor against upper compressed chord global buckling; Based on site climate and present corrosion condition, corrosion

will affect bridge components for 30–40 years. Spalling at the bottom of the slab edges and curbs will likely create unsafe circumstances for boat service users traveling below the bridge in 15-20 years. The pedestrian handrail anchoring is corroding and expected to collapse in 30 years.

### 4.2.2 Preventative scenario (figure 10)

Preventive maintenance is one of several life cycle techniques. The method assumes the bridge will be fully restored, bringing its reliability index to 'as new'. The intervention will happen two years after design. This massive intervention establishes a 10-year preventive intervention strategy, the 20-year and 40-year periodic intervention expenses. The region bridge maintenance contractor contract process determines costs. Lifecycle: Immediate bridge repair comprises Complete concrete elements repair, concrete curb replacement, joints connection repair



including about 400 rivets and plate replacement, overall bridge painting, new expansion joints, bearing rehabilitation, safety barrier replacement with end blocks, pedestrian handrail rehabilitation, pedestrian deck overlay, new waterproofing, and asphalt overlay. Cost includes temporary traffic arrangement. Upper-layer asphalt paving and safety barrier restoration are part of the 10-year intervention based on actual accidents. Temporary traffic arrangements cost. The 20-year intervention involves 10 years +

total concrete surface treatments, overall painting system renewal, in-depth NDT of the truss connections before repainting, and EJ rehab/replacement. The cost includes temporary traffic arrangements. The 40-year intervention includes 20 years + rivet replacement (estimated 500 units), bearing rehabilitation/replacement, deck waterproofing system renewal, and temporary traffic arrangement costs.

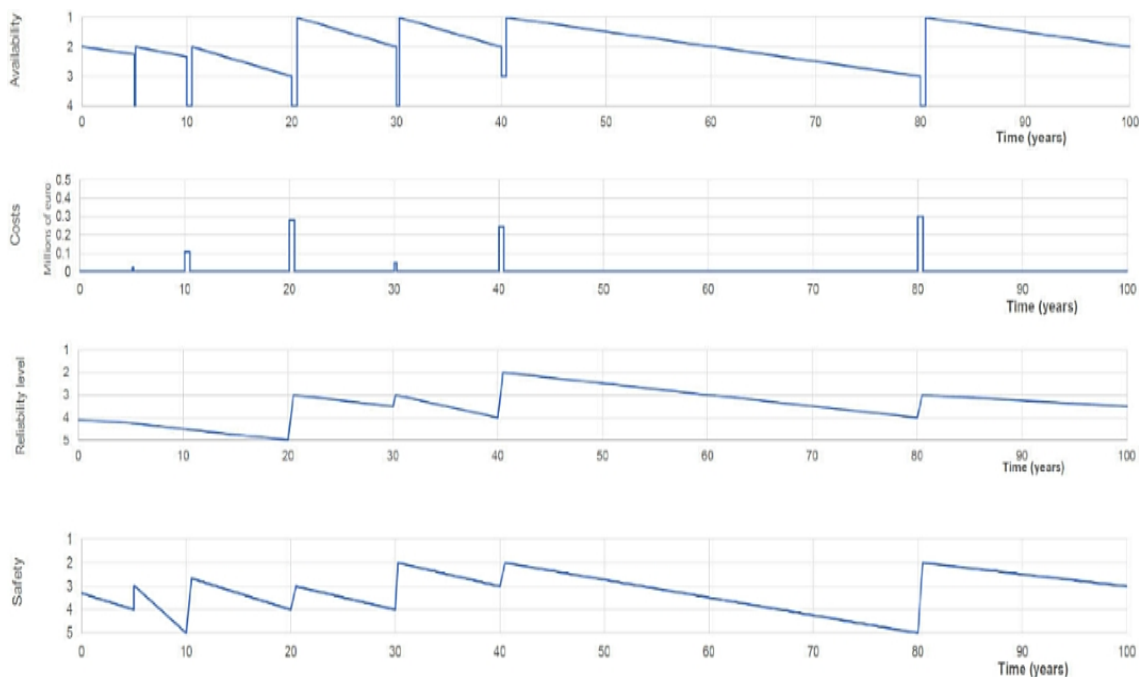


Figure 9. Evolution of key parameters under reference scenario.

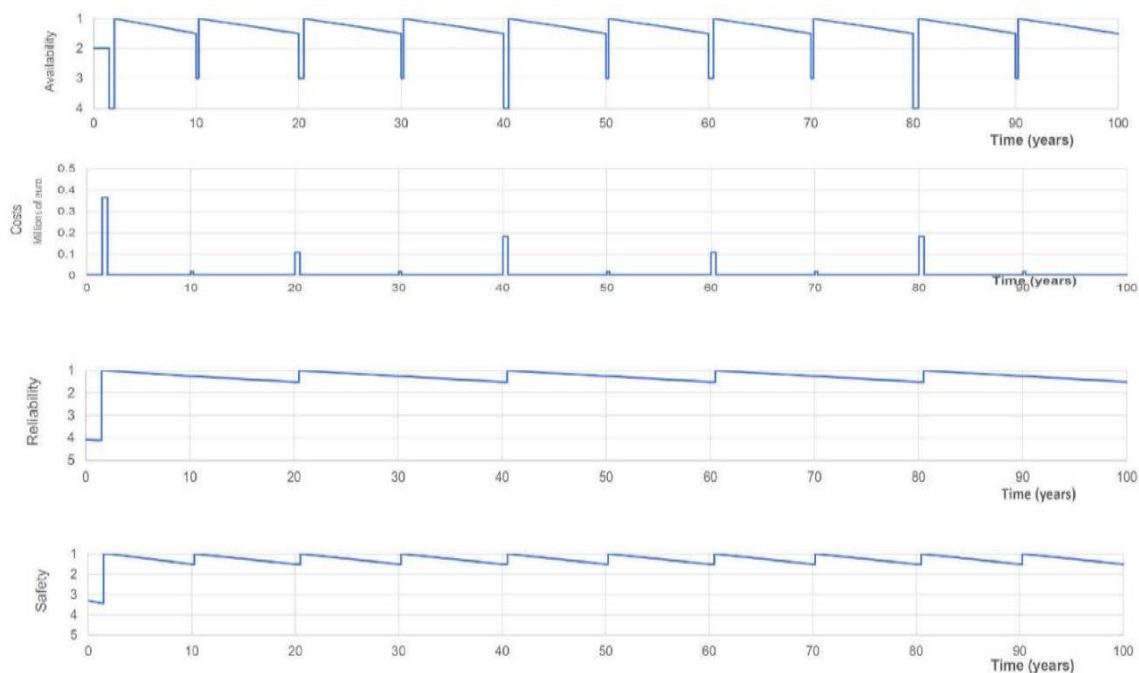


Figure 10. Evolution of key parameters under the preventative scenario.

### 4.3 Comparison

This "spider diagram" compares the two ways. The analysis suggests a preventative method for this truss bridge. Though more expensive, all other indicators are better. Over time, reliability and safety remain excellent.

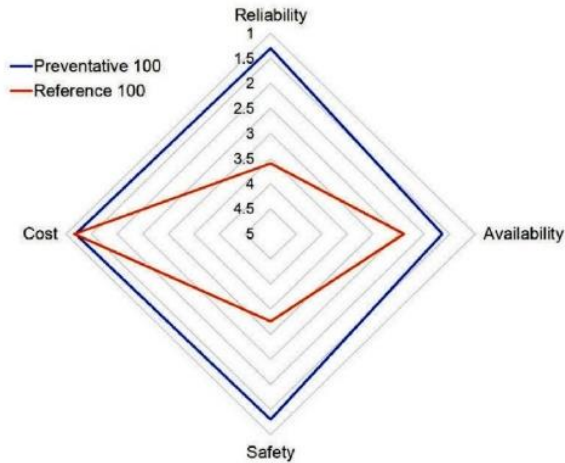


Figure 11. Spider diagram for the referenced vs. preventative approach

## 5 Conclusions

This article proposed a KPI-based roadway bridge quality control framework. Performance indicators, vulnerable zone assessment, KPI derivation from PI, and KPI development through time with diverse scenarios are provided for the difficult situations. Finally, a case study introduces and proves a 2-step quality control framework, resulting in a strong performance in establishing the roadway bridge's long-term preventative maintenance policy. Conclusions:

- Primary inspection data plan high-quality and timely transportation infrastructure repair. Thus, individual object maintenance costs can be assessed, laying the groundwork for a cost-effective roadway or highway item maintenance strategy. Transferring data and information from design documents and construction to management and operation is crucial to transportation infrastructure management.
- Advanced research, scientific understanding, and mathematical and statistical models can improve roadway infrastructure longevity and degradation prediction. It should gather, analyze, and grade bridge durability data, and visual condition assessment should be related to findings. After that, estimates of

how long an element stays in a condition can be revised. Then, typical repairs can be connected to bridge condition.

- Civil engineering needs sustainability indicators. Society needs to evaluate products' economic, environmental, and social impacts.

## Acknowledgments

The authors would like to acknowledge COST TU1406 Research Project: Quality specifications for roadway bridges, standardization at a European level (tu1406.eu), and now, to EuroStruct – European Association for the Quality Control of Bridges and Structures (eurostruct.org). Also, they would like to acknowledge the international R&D projects SAFEWAY - GIS-based infrastructure management system for optimized response to extreme events on terrestrial transport networks (safeway-project.eu), SIRMA – Strengthening Infrastructure Risk Management in the Atlantic Area (sirma-project.eu), and the national R&D projects InfraCrit (management system for critical infrastructures), GIIP (management system for port infrastructures), and GOA.BI – GOA Bridge Management System – Bridge Intelligence.

## References

- [1] Shim, C.S.; Dang, N.S.; Lon, S.; Jeon, C.H. (2019). Development of a bridge maintenance system for prestressed concrete bridges using 3D digital twin model. *Struct. Infrastruct. Eng.*, 15, 1319–1332
- [2] Shim, C.S.; Kang, H.; Dang, N.S.; Lee, D. (2017). Development of BIM-based bridge maintenance system for cable-stayed bridges. *Smart Struct. Syst.*, 20, 697–708
- [3] Dang, N. S., Rho, G. T., & Shim, C. S. (2020). A master digital model for suspension bridges. *Applied Sciences*, 10(21), 7666.
- [4] Dang, N. S., & Shim, C. S. (2018). BIM authoring for an image-based bridge maintenance system of existing cable-supported bridges. *IOP Conference Series: Earth and Environmental Science*, 143(1), 012032.
- [5] Dang, N. S., & Shim, C. S. (2020). BIM-based innovative bridge maintenance system using augmented reality technology. *Lecture Notes in Civil Engineering*, 54, 1217–1222.
- [6] Dhada, M., Hadjimetriou, G. M., & Parlikad, A. K. (2020). Predicting Bridge Elements Deterioration, using Collaborative Gaussian



- Process Regression. *IFAC-PapersOnLine*, 53(3), 348–353
- [7] fib Model Code for Concrete Structures 2010. (2013). *Fib Model Code for Concrete Structures 2010*, 1–402
- [8] Hanley, C., Matos, J. C., Kelliher, D., & Pakrashi, V. (2016). Integrating multivariate techniques in bridge management systems for lifecycle prediction
- [9] Matos, J. C., Casas, J. R., & Fernandes, S. (2017). COST TU1406 - An overview of European standardization on quality control of road bridges. *IABSE Conference, Vancouver 2017: Engineering the Future - Report*, 304–311.
- [10] Matos, J. C., Fernandes, S., Sousa, H. S., Coelho, M., Teixeira, E., Moscoso, Y., & Tinoco, J. (2020). From quality control to decision-making on the management of bridges and structures: What's next? *JOURNAL OF MATERIALS AND ENGINEERING STRUCTURES*, 7, 551–559.
- [11] Ugwu, O. O., & Haupt, T. C. (2007). Key performance indicators and assessment methods for infrastructure sustainability—a South African construction industry perspective. *Building and Environment*, 42(2), 665–680.
- [12] Yang, D. Y., & Frangopol, D. M. (2019). Lifecycle management of deteriorating civil infrastructure considering resilience to lifetime hazards: A general approach based on renewal-reward processes. *Reliability Engineering & System Safety*, 183, 197–212.
- [13] Matos, J. C., Fernandes, S., Tran, Q.M., Nguyen, T.Q., Baron, E., Dang, N.S. (2023). Developing a Comprehensive Quality Control Framework for Roadway Bridge Management: A Case Study Approach Using Key Performance Indicators. *Applied Sciences* 13 (13), 7985
- [14] Tran, Q.M., Sousa, H.S., Matos, J.C., Fernandes, S., Nguyen, T.Q., Dang, N.S. (2023). Finite Element Model Updating for Composite Plate Structures Using Particle Swarm Optimization Algorithm. *Applied Sciences* 13 (13), 7719
- [15] Pooraskarparast, B., Bento, A., Baron, E., Matos, J.C., Dang, N.S., Fernandes, S. (2023). Fluid–Soil–Structure Interactions in Semi-Buried Tanks: Quantitative and Qualitative Analysis of Seismic Behaviors. *Applied Sciences* 13 (15), 8891
- [16] Tran, Q.M., Sousa, H.S., Ngo, V.T., Nguyen, D.B., Nguyen, T.Q., Nguyen, X.H., Baron, E., Matos, J.C., Dang, N.S. (2023). Structural Assessment Based on Vibration Measurement Test Combined with an Artificial Neural Network for the Steel Truss Bridge. *Applied Sciences* 13 (13), 7484
- [17] Nhamage, I.A., Dang, N.S., Horas, C.S., Martins, J.P., Matos, J.C., Calçada, R. (2023). Performing Fatigue State Characterization in Railway Steel Bridges Using Digital Twin Models. *Applied Sciences* 13 (11), 6741



# Construction and calibration of digital twins for metallic truss bridges

**Carla Menuet, Théo Bailly**

*Strains, Paris, Île-de-France, France*

Contact: [carla.menuet@strains.fr](mailto:carla.menuet@strains.fr)

## Abstract

This paper presents the study carried out as part of the Gerico Project, which aims to provide bridges managers with insights on their bridges' health thanks to a calibrated numerical model. Modal parameters identification as well as load tests are used to update a numerical finite element model. This model is then used to simulate structural health disorders.

**Keywords:** Numerical model updating – Digital twins – Steel bridge – Modal analysis – load tests simulation

## 1 Introduction

The Gerico (**G**estion des **R**isques par ponts **C**onnectés / Risk management with smart bridges) Project is part of a larger group of projects, financed by the French state and managed by the CEREMA (French public establishment) as part of the call for project "Ponts Connectés / Smart bridges".

The overall objective is to build bridges' digital twins that can be used to evaluate and monitor the structures' health. Model updating is conducted using tools like operational modal analysis and loads tests.

Two steel bridges are under study: the Haut Village bridge and the Grand Pont de Mauves. This paper focuses on the Haut Village bridge.

The Gerico project is carried out by a consortium composed of the following entities: OSMOS, SCE, STRAINS, Loire Atlantique Department, and the city of Angers.

## 2 Context

### 2.1 The Haut Village Bridge

The Haut Village Bridge is a 225 m pulled iron cage bridge dating from 1882. Only the first span remains from the original bridge. The 4 other spans were destroyed during World War II and rebuilt in two stages in modern steel. It is thus a very heterogenous bridge with 2 typologies of truss built from 2 different material and 3 typologies of bearing structure (2 types of concrete slabs for the post-war spans and vaults for the original span).



*Figure 1. Haut Village Bridge*

### 2.2 Presentation of the global model

The model used is a FEM model based on beam elements for all steel components and shell elements for concrete slabs or vaults. The software used for the modeling and computation is Pythagore®.

### 2.3 Measurements

The bridge was instrumented for a period of several months, in order to evaluate the sensitivity of the measurements to seasonal evolution.

An identification of modal parameters of the bridge (frequencies and mode shapes) was conducted using operational modal analysis. Accelerometers as well as optical cords were used to measure vibrations. Optical cords were also used during the load-tests-based calibration described in §4.

### 3 Modal identification based calibration [1]

The mode shapes and natural frequencies retrieved from the operational modal analysis were compared to those extracted from a modal analysis conducted with the FEM software. The Modal Assurance Criterion (eq. 1) was used to form pairs between experimentally and numerically identified natural modes of the structure.

$$MAC(\Phi_1, \Phi_2) = \frac{(\Phi_1 \cdot \Phi_2)^2}{(\Phi_1 \cdot \Phi_1)(\Phi_2 \cdot \Phi_2)} \quad (1)$$

A study of the sensitivity of the modal parameters to several parameters of the FEM model such as material characteristics (Young modulus, density...) or support condition (longitudinal stiffness of roller bearing devices) was conducted.

Finally, a scouring disorder of one of the center piers was introduced in the model and its influence on modal parameters was identified. The scouring was modeled by a reduction of the longitudinal axis rotation stiffness at the base of the pier.

The ability to locate the damage with an analysis based on the co-ordinate modal assurance criterion (COMAC) was investigated.

### 4 Load-tests-based calibration

Another approach was explored for the calibration of the model, based on the exploitation of load tests performed on the bridge. In this approach, strains measured with the optical cords were compared to results obtained with the model. A semitrailer-type vehicle weighing 10 t was used for the tests. A total of 16 passages were performed, providing a large amount of data.

In the model, the convoy was simulated by moving static charges corresponding to the axletrees. Strains were deduced from the stresses extracted at each step using the relation linking strain, stress, geometrical and mechanical characteristics of the steel component.

Numerically extracted strains were systematically superior to measurements, especially around assembling pieces where sections are increased. This observation led to the construction of detailed local models in order to represent the mechanical behavior of the structural node in a more accurate way. These models were built using an inhouse 3D FEM software.

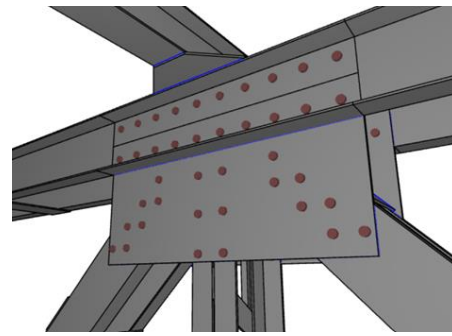


Figure 2 : Local model of section T11 S4, upstream, top

The forces used in the local model were extracted from the global model using the timestep generating the maximum strain. The calculation resulted in strains closer to the measures than the ones obtained with the global model.

### 5 Conclusion

Finite element model updating based on modal parameters and static behavior was conducted.

Comparison between static strains measured during load tests and strains extracted from numerical simulation first showed higher strains in the numerical model than what was measured. The use of a 3 dimensional local model shed light on the 3 dimensional behavior of stresses in the area where the cord was installed. This explained why the beam elements behavior did not fit the measurements.

Comparison of the modal parameters experimentally and numerically identified resulted in the frequency of numerical modes being approximately 10% lower than those of measured modes. The sensitivity analysis allowed to explore ways to reduce this gap by modifying some parameters of the numerical model.

Finally, the study of the influence of a scourge on the dynamical behavior of the bridge showed a reduction of the frequency of transversal modes but no impact on vertical modes. For a continuous bridge like the Haut Village bridge, the scouring of one pier affects the mode shapes over all spans, the COMAC analysis thus fails to locate precisely the damage. However, natural modes showing transversal displacement where there was not before can be a sign of scouring.

### References

- [1] M. I. Friswell et J. E. Mottershead, Finite Element Model Updating in Structural Dynamics, Kluwer Academic Publishers, 1995.



## Methods of automating design optimisation

**Trevor Spannenburg**

Antea Nederland B.V., Heerenveen, NL

Contact: [trevor.spannenburg@anteagroup.nl](mailto:trevor.spannenburg@anteagroup.nl)

### Abstract

Computational design can be used to automate the design process and optimisation. Two existing methods in computer sciences have been used to solve the optimisation of a structural design. The first method is smart filtering, in which the solution space is reduced based on the structural analysis of a smaller subset until an optimum has been found. In the second method, artificial intelligence in the form of a genetic algorithm is used to optimise the design.

**Keywords:** design automation; computational design; pile foundation; artificial intelligence; genetic algorithm, sheet pile; optimisation; tunnel entrance.

## 1 Introduction

The world is currently undergoing a digital transformation. New technologies are improving efficiency of methods and processes in different fields of work. These effects are also occurring in the field of structural engineering. Automation of actions is becoming more common in design processes. One form of automation is computational design. This paper will discuss two examples of the implementation of computational design. In both cases, optimisation of the design itself has been automated.

## 2 Automating the design process

Automation of the design process is already happening since the introduction of computers. The level of automation however is what differs. Automation can already be programming a simple function that add two values. A more sophisticated level of automation could be parametric design. With this form of automation, a design is made based on several input variables and prescribed relationships. The design is manipulated by changing the input variables, rather than direct manipulation. Parametric design has proven to be a useful tool for the engineer, as it allows for a faster exploration of multiple design solutions. However, this exploration of the solutions would still be done manually. The next step in automation is computational design, in which the searching for the optimal solution is automated.

With computational design, software is used to not only generate designs, but also analyse them and eventually come up with the optimal solution. How the software explores the solution space, can differ per application. Two examples of search methods will be discussed here.

### 2.1 Smart filtering - sheet-piling structure

The first case concerns the design of sheet-piling structures with grouted anchors. The structural design is made up of 12 parameters that all can vary, with examples such as the type of sheet-pile and the length of the anchor. The design has to fulfil a set of requirements concerning safety and serviceability, for which the performance is expressed in unity checks (or factor of safety). Examples of such unity checks would be deflection of the sheet-pile, or stresses within the anchor. Each design parameter can have different influences on different unity checks. Increasing the stiffness of the sheet-pile can lower the deflection, but increase the stresses in the sheet-pile itself. Hence, changing a design parameter can have both a positive and a negative effect.

As stated, the structural design consists of 12 parameters. Varying all these parameters results in a large set of possible designs to analyse. Exploring the solution space is an iterative process that would be labour-intensive when done manually. However, the search method can be simplified to an algorithm, which in turn can be used by the computer to automatically optimise the design. In this case, a search method coined *smart filtering* has been applied for sheet-piling structures. With this method, the solution space can iteratively be reduced based on a structural analysis of a small subset, until an optimal solution in terms of costs has been found that fulfils all requirements, with cost being either money, carbon footprint or ECI. The logic to reduce the solution space has been programmed into the software.

The search method starts with creating a discretised set of the solution space, consisting of multiple design variables such as the length of the sheet-pile. Secondly, a small subset is selected from the solution space. A structural

analysis is performed on this small subset, from which the different performances (unity checks) are obtained per design. Example: when a certain design has too much horizontal deflection, shortening the length of the sheet-pile will not help. Hence, all similar designs that have a shorter sheet-pile length can be removed from the solution space. This removal process can be executed simultaneously for all design parameters. In this case, weaker designs are removed from the solution space. Another example: another design has been analysed as well, and it has been observed it fulfils all requirements. In turn, all designs which have a higher cost, are eliminated from the solution space; these designs are proven to not be the optimum. In short, *smart filtering* iteratively explores the solution space and reduces it based on the following principles:

1. When a design has proven to not fulfil the requirements, eliminate all weaker designs according to logic;
2. When a design has proven to fulfil all requirements, eliminate all designs with higher costs.

In test cases, solution spaces numbering in trillions of possibilities have been explored with under a thousand real calculations. This has proven to be an increase in performance compared to *brute forcing*.

## 2.2 Genetic design - pile foundation tunnel entrance

In the second case, the design of a pile foundation for tunnel entrances has been automated. An example of such a design is presented in Figure 11. In this case, artificial intelligence in the form of a genetic algorithm has been used to automate the optimisation of the pile foundation. This method has been dubbed *genetic design*.

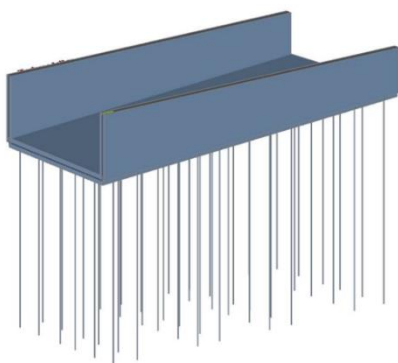


Figure 1. Example structural model tunnel entrance including pile foundation

The software starts by generating a random set of designs. Parameters that are varied are the length and type of pile, as well as the spacing of the piles. Each

design is then analysed on its structural performance. Next, the best-performing designs are combined for a new randomly generated set of solutions, a so-called generation. Each design of this new generation is a copy, with small randomised changes. Examples of these changes can be longer piles or a smaller centre-to-centre distance near the edge. New generations are continuously produced until an optimum has been found. Meanwhile, the results of each generation is logged to allow for traceability, which means the algorithm is a glass-box solution. In comparison to the smart filtering of the previous case, genetic design does not require the programming of logic in its search method. The exploration of the solution space is solely done based on the results.

This method has been applied for the design of an underpass at the station of Groningen. A design had already been made for the pile foundation using conventional methods. Through the use of genetic design, a reduction in carbon footprint of 20%, as well as a reduction in cost of 30%, was obtained in comparison to the initial design.

## 3 Conclusions

Computational design can be used in several ways. In this paper, two methods have been discussed. The first method, smart filtering, reduces the solution space based on pre-programmed logic set up by the engineer. The decision-making of the algorithm is thus transparent, a so-called glass box. The second method uses a genetic algorithm to explore the solution space. The advantage of this method is that it requires no pre-programmed logic. It is therefore suitable for situations where the influence of design variables on the performance is unknown. Depending on the case, different methods of computational design can be used. In all cases, computational design can provide several advantages, such as reduced costs, lower carbon footprint and a quicker design cycle.

# Structural design automation of a cut and cover tunnel

**Kelvin Roovers**

BESIX Engineering, Brussels, BE

Contact: [kelvin.roovers@besix.com](mailto:kelvin.roovers@besix.com)

## Abstract

The structural design of the Nordhavn tunnel required creating many similar analytical models in multiple engineering applications. In an unconnected software landscape this process involves numerous repetitive modelling and copy-pasting tasks that are time consuming and prone to error. Custom computer routines and parametric models were developed at BESIX Engineering to automate the structural design workflow and data exchange between applications. The present paper discusses the Nordhavn tunnel project and the custom developments that have greatly increased the efficiency and flexibility of the digital design process.

**Keywords:** parametric design, automation, infrastructure, tunnel, cut&cover, reinforced concrete design

## 1 Introduction

The Nordhavn tunnel is a 1,4 km long road tunnel to be constructed in the North of Copenhagen, Denmark. BESIX has been awarded the Design & Build of this tunnel together with Danish partner MT Højgaard. The tunnel will be constructed using the cut and cover method and runs under water for a length of 700m (Figure 1). The design of the temporary structures is done by our inhouse engineering department, while the design of the permanent reinforced concrete tunnel structure has been subcontracted. However, as it is the mission of the BESIX engineering department to protect the company from design risks, we have created a verification model to validate the tunnel design.

The tunnel has a variable elevation and its rectangular cross-section comprises two tubes that widen near the exit ramps. Various design parameters change along the length of the tunnel, including:

- slab and wall thicknesses;
- roof and floor spans;
- anchor dimensions, positions and prestress;
- water, soil and building loads;

Eleven out of 54 tunnel segments were deemed critical and selected for analysis. First the internal forces of the structural elements were computed in 2D analytical models using the software Scia Engineer. Afterwards the governing internal forces in each structural element were extracted to determine the minimum required reinforcement using the software IDEA StatiCa. The algorithmic modelling tool Grasshopper ties together the different parts of the

digital design workflow thanks to parametric models and automated data flows. These custom developments, resulting from a close collaboration between the design engineer and computational designer, are presented in the following paragraphs.



Figure 1: 4D model of the Nordhavn tunnel with temporary structures

## 2 Parametric tunnel section

The internal forces in each structural element of a tunnel segment are determined using 2D analytical models (Figure 2). In a first step, a representative tunnel segment was modelled and analysed using the built-in functions of the chosen FEM software package. Once properly validated, the process needed to be repeated for the other tunnel segments. This highly repetitive task comprises numerous error-prone copy-pasting actions that do not contribute to improving engineering insights of the structure. Hence, the process of modelling and calculating the other tunnel segments has been automated using a Grasshopper script. For each of the 54 unique tunnel segments, the variable loads have been derived and gathered in a single spreadsheet table together with the variable structural dimensions and properties (as defined in the subcontractor's design). Next, this data is inserted

into the original analysis model using an XML formatted text file. Calculations are run in an automated background process and the results exported to a spreadsheet to be used as the basis for the design of the reinforcement.

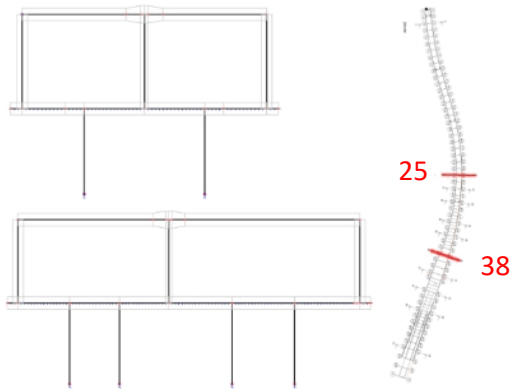


Figure 2: 2D analysis models of two tunnel segments

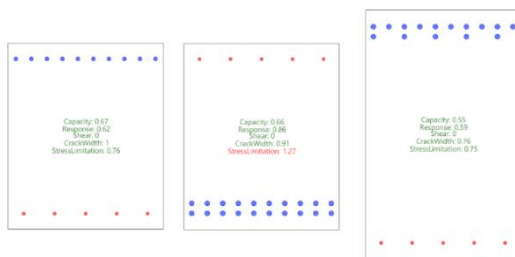


Figure 3: Example of analytical reinforced concrete cross sections with unit checks for a roof span of tunnel segment 38.

### 3 Rebar design automation

Given the internal forces in walls, roof and floor slab resulting from the 2D analysis, the minimum required transversal reinforcement has been determined at the critical element sections: at the position of maximum bending near the supports and along the span of the element. Starting from the minimum reinforcement specified in the basis of design, a selection of predefined rebar layouts is tested one by one in order of preference until the first layout is found that passes all design checks. This straightforward procedure is automated to obtain the required reinforcement for all elements of a tunnel segment in less than a minute.

Per critical element section, the Grasshopper script creates a reinforced cross section representing a one meter long strip of the tunnel (Figure 3). The governing forces are inserted from the analytical model. XML formatted text files are again used for data exchange with the analysis software. An overview of the resulting rebar layouts and unit checks is exported to a spreadsheet for validation and for reporting purposes.

### 4 The super-powered engineer

The presented developments were conducted in close collaboration between the design engineer — responsible for design decisions, setting up the mock-up of the analysis model and validation of results— and the computational designer —with the coding skills needed to automate the requested processes and establish the data connections between the different software. This fruitful collaboration gives rise to digital workflows where the engineer loses as little time as possible on repetitive work that brings little added value and personal gratification.

Experience shows that the time and resources invested in these custom developments can quickly be returned. A first parametric development might indeed take longer than the familiar way of working. But already from the second or third application, reuse of code and knowledge leads to development times not exceeding those of more traditional modelling approaches. In addition, this way of working increases resilience to design changes — greatly reducing time lost by rework— and facilitates studying design alternatives —aiming to lower cost and environmental impact of our designs.

### 5 Conclusions

The inhouse design works for the permanent structure of the Nordhavn tunnel had as purpose to validate the subcontractor’s design. Hence, the main dimensional parameters were fixed and the design process posed limited engineering challenges. The repetitive nature of the task would nevertheless make it time consuming and prone to error. We’ve developed parametric models and established automated software connections to easily run variations of the same principle. These developments enable us to go through the reinforcement design process of a tunnel segment in a matter of minutes, leaving plenty of time for validation. In addition, the scripts make it easy to rerun the structural analysis in case of modifications or to analyse additional tunnel segments if deemed necessary. We’re continuously expanding our development efforts, gradually increasing the scope of the automated process. The aim is to obtain reliable rebar ratios as early as possible in the design process to predict the true cost and impact of design decisions.

### 6 Acknowledgements

The presented work was made possible thanks to the help from colleagues of the BESIX engineering department, including Pierre Mengeot, Toby Barnett, Hasan Ismail, Gaëtan de Caritat and Jasper Bosmans

# A new finite element for joints based on the components method

**BODSON Romain Ir., de Ville de Goyet Vincent dr. Ir.**

Bureau d'études GREISCH, Liège, Belgium

**GOLEA Tudor Ir.**

University of Liège, UEE, Belgium

Contact: [rbodson@greisch.com](mailto:rbodson@greisch.com)

## Abstract

Design of steel joints based on the components method (CM) according EC3 is an alternative to complex finite element model analysis for the characterisation of joint's behaviour ( $M-\phi$  curve) due to its simplicity of utilisation. However, some important issues are not considered in components method, i.e.: group effects, components interactions and variation of shear force along the height of column web panel. Based on recent research [1], this paper introduces a new unified finite element based on components mechanical model and incorporate the key aspect described before.

**Keywords:** Joints; Components Method; Bolted Connections; Finite Elements; Mechanical models

## 1 Introduction

Semi-rigid connections can be modelled by a mechanical model using several springs and rigid connections, taking into consideration some key aspects such as the group effects, components interactions and variation of shear force along the height of column web panel [1,2]. Each spring has its own *DoF* and a non-linear constitutive law that corresponds to a component, established most of the time according to EC3.

Then, a static condensation of each internal *DoF* is performed to obtain an equivalent spring with only 4 nodes  $X$  3 *DoF*'s to characterise behaviour of any joint's connections.

## 2 Finite element implementation

### 2.1 Mechanical model

Based on models developed by considering key aspects of joints behaviour, a 2 sides beams-column connection can be represented by the mechanical model given in Fig.1 (just one side is represented due to the symmetry).

Each spring represent a set of components acting in tension or compression, group effects effect are taken into account with fuses elements (H in red).

Column Web panel in Shear (CWS) is modeled with a plane beam stiffness matrix element with shear deformation for each sub-panel (cws<sub>i</sub> in blue). Then, linear constraint elements are present to ensure that section remains locally plane (grey vertical lines). We also add constrains to impose that the rigid connections on each side of the fuse remain parallel. This mechanical model can capture the behavior of the whole joint connections.

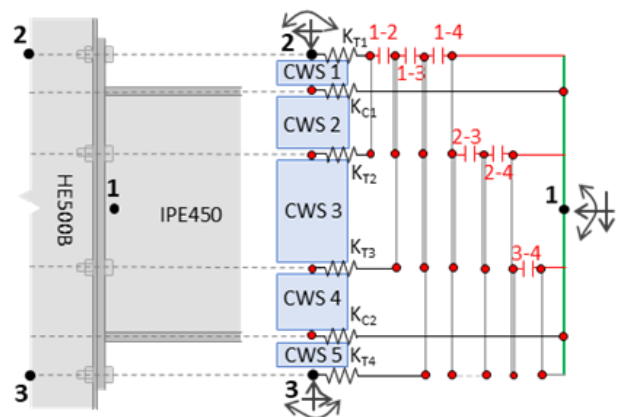


Figure 1. 2 Beams-column joint connections

### 2.2 Static condensation

Basically, the mechanical model has 4 connections nodes with the rest of the structure, ie: *external nodes* (black nodes n°1;2;3 -Fig.1, nodes n°4 not visible due to symmetry). The other nodes are *internal nodes* (red nodes -Fig.1). To develop an equivalent "super" single spring, we perform a static

condensation including the linear constraints, resulting in a stiffness matrix between the 4 external nodes. This gives us a plane finite element with only 4 nodes X 3 DoF's.

Finally, as each spring law are non-linear, the condensation is repeated at each iteration. We also operate a decondensation to evaluate the state of each spring and the out-of-balance forces.

### 2.3 Validation

Based on these developments, this finite element is implemented in the FINELG software. The results of a 2 double-side specimen (as in Fig.1) tested [1] under cyclic loading with unbalance moments on each sides are compared with the new FEM results. The failure occurs when the column web in shear (CWS) reaches its resistance.

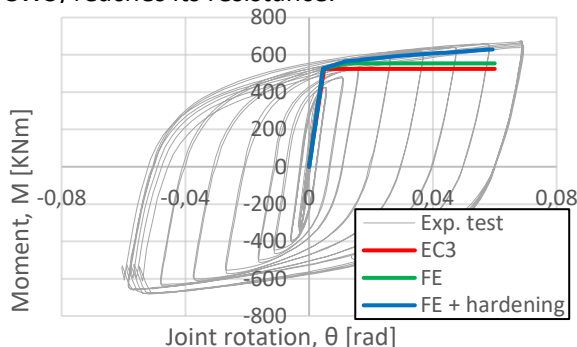


Figure 2.  $M-\theta$  curve (right joint)

According to EC3, the behavior of the CWS component is modelled with only one spring. In our FE, each individual sub-panel are modelled separately. This allows a gradual activation of the plasticity in each sub-panel subjected to shear forces. This explains why our FE gives a plastic moment resistance 5,6% higher than EC3 (Fig.2)

The central sub-panel of the CWS reaches its plasticity for  $M_{pl,rd} = 525$  kNm, which corresponds to the plastic bending moment predicted by EC3 (red curve). At this point, a plastic redistribution occurs between adjacent sub-panels of the CWS, leading to a redistribution of internal forces within the connection. This results in an increase in the applied bending moment until plasticity has propagated to the adjacent CWS sub-panels. When all sub-panels or adjacent components are yielded, we reach the plateau observed in Fig.2 (in green). Fig.3 shows this effect. After the first yielding of the central sub-panel CWS, a reserve exists to reaches  $M_{pl,rd}$ .

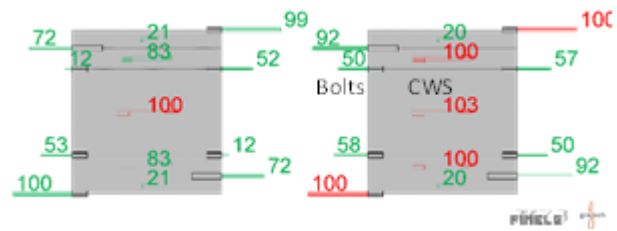


Figure 3. Ratio between force/plastic resistance – first yielding (left) & collapse load  $M_{pl,rd}$  (right)

The curve (FE + hardening (in blue)) represents the case where a hardening is added to the behaviour law of subpanel (CWS). This adjustment gives in a closer match to the experimental test.

### 3 Conclusions

A new general finite element was implemented to model the behaviour of any beam-column joint based on the components method. Each component is modelled as a non-linear spring, group effects are considered through fuses elements and variation of shear forces in CWS is also included. So, the overall behaviour of joint is fully characterised.

It is shown that, compared to EC3, considering each CWS separately increases the accuracy of the connection's behaviour, thus enabling a more precise characterization of the failure mode.

In future, components interaction will also be added to complete our finite element.

### 4 Acknowledgements

This work was funded by the Service Public de Wallonie as part of the FINELG2020 project.

### 5 References

- [1] Golea, T. (2023). A generalised mechanical model for the characterisation of steel joints. Eurosteel 2023 (pp. 1222-1227). Amsterdam: ce/papers.
- [2] Mathieu, J. (2020). Développement d'un modèle novateur de caractérisation du comportement précis d'assemblages de construction métallique et mixte acier-béton. Ulg: Liège.



# Parametric modelling to improve sustainability in design

Eloïse Denis, Stef Feyers, Simon Van Gompel

BESIX Engineering Department, Brussels, Belgium

Contact: [eloise.denis@besix.com](mailto:eloise.denis@besix.com), [stef.feyers@besix.com](mailto:stef.feyers@besix.com), [simon.vangompel@besix.com](mailto:simon.vangompel@besix.com)

## Abstract

Nowadays, a structural design does not only need to be feasible and cost-effective, but it also needs to limit the environmental impact. Environmental regulations are more and more to be considered. This paper presents a workflow in which the complete calculation process is considered as one parametric model. The result obtained is a summary table of the possible design solutions, including the embodied carbon calculated according to a life cycle assessment (LCA). This enables the designer to optimise the sustainability in design. This workflow is then applied to a case study on Schijnpoorttunnel, part of the Oosterweel project.

**Keywords:** parametric design; sustainability; LCA; embodied carbon; Schijnpoorttunnel

## 1 Introduction

BESIX Engineering Department adds value to the design of a project using the latest trends in calculation methods, one of which is parametric modelling. This is a design approach where the calculation model is defined as a set of pre-defined rules which describe the correlations between the different elements of a model. By doing so, when one of the input parameters is changed, the complete model will adapt accordingly, including the automated set of calculations performed in different software. This enables the designer to examine different possible solutions and optimise the design according to specific design requirements.

One of the requirements that is becoming increasingly important, is to include sustainability aspects in the design choices. A calculation method that can be used to evaluate the environmental impact of a project throughout its entire life cycle, is a Life Cycle Assessments (LCA). In an LCA, the quantities of the used materials are multiplied by its environmental impact factor.

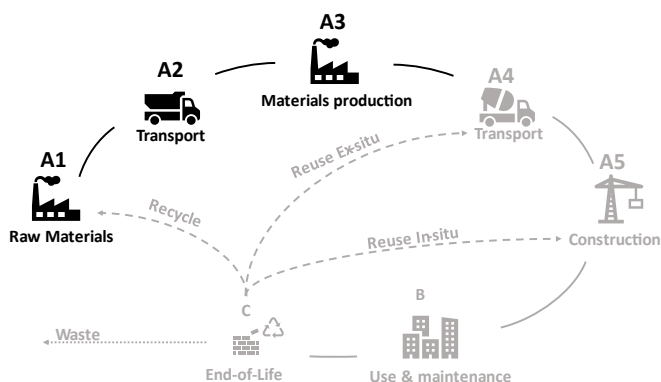


Figure 1-1: Life Cycle Assessment

## 2 Workflow

In this article, a workflow is presented where the complete calculation process is considered as one parametric model. This workflow is translated into a Grasshopper script, which allows to connect the different steps of a design in an automated manner.

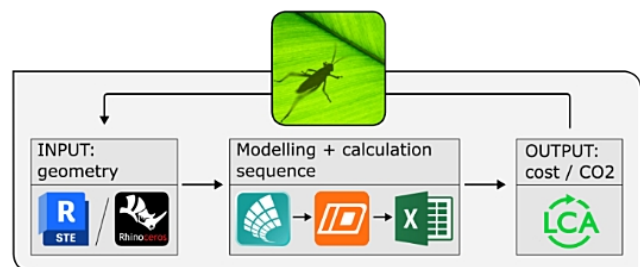


Figure 2-1: Workflow

The first step is to obtain the geometry, either by extracting it from a Revit model or by building it in Rhino. This geometry is then translated into a FEM-model and the additional information, such as loads and supports, is defined. The governing results are extracted and copied to an IDEA Statica file, where different reinforcement layouts are tested. All possible solutions are summarized in Excel and the required quantities are calculated.

These quantities are multiplied by their environmental impact factor and their price factor. The last step is to assess the obtained solutions.

For the sustainability parameter, the focus in this workflow is embodied carbon included in steps A1 to A3 of the LCA. These steps are linked to the material selection and are considered as the most determining one's with reliable information available at the design stage.

### 3 Case study – Schijnpoorttunnel

#### 3.1 Description of the project

This case study focuses on the post-tensioned roof of Schijnpoorttunnel, a part of the Oosterweel project in Antwerp. Currently, feasibility and sensitivity analysis are ongoing, considering all the geometrical boundary conditions in a dense urban environment.

#### 3.2 Analysis and results

For this analysis, three governing cross-sections CS1 – CS2 – CS3 (as shown in figure 3-1) have been considered. A 1D isolated model of the roof is used to withdraw the internal forces, considering as well geometrically feasible post-tensioning lay-outs. These are checked and then implemented in de template IdeaStatica files.

For every section the following parameters are considered as a variable: concrete thickness, reinforcement configuration, amount and the eccentricity of the post-tensioning strands.

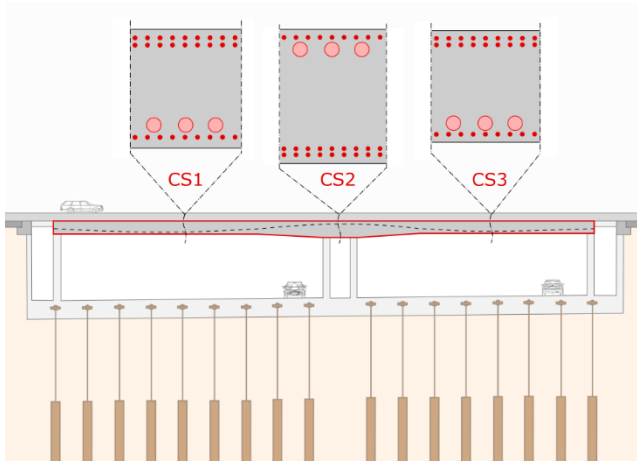


Figure 3-1: Roof of Schijnpoorttunnel

Adopting this workflow leads to an improved understanding of the structure. For example, analysis shows that increasing the eccentricity of the strands allows to reduce the number of strands, but also requires more passive reinforcement (as accidental explosion loads are to be considered). The results of the workflow reveal the relative importance and influence of the different parameters.

The results of the analysis show that it is not possible to have the best option for every investigated section, as the post-tensioning cables need to be installed over the full width of the tunnel. As a result, the number of strands has to be the same in all sections.

In figure 3-2, a graph is shown with the results for cross-section CS1. It gives the amount of CO<sub>2</sub> and the relative increase of the direct construction cost for different configurations. We see that the best options are having a thickness of 1,5 m.

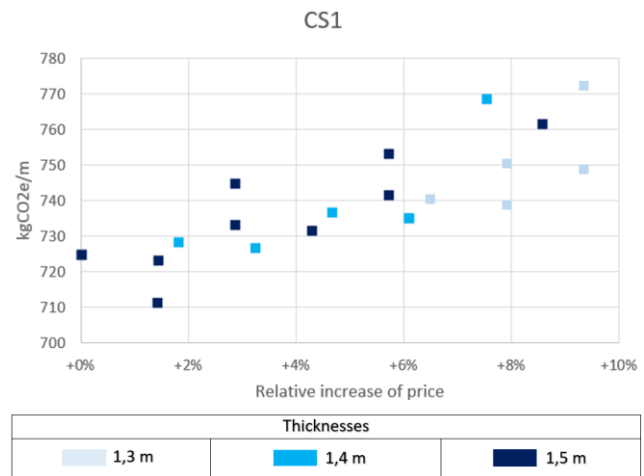


Figure 3-2: Carbon footprint and cost impact for the results of CS1

#### 3.3 Integral design

The presented sensitivity analysis considers only the roof structure of the tunnel, of which each cross-section is analysed separately. This allows to determine the most optimal configuration within the pre-defined set of parameters. However, to obtain the complete design of the tunnel, the design choices should be made integrally, by considering all boundary conditions and requirements into account.

The insights from the sensitivity analysis reveal the governing parameters and their relative influence. This allows the designer to make further design considerations in a well-founded and fundamental manner.

### 4 Conclusions

The workflow is an innovative manner of incorporating the fundamental steps of a structural design, as well as the new environmental constraints that are slowly emerging via regulations such as the RE2020 (France) and MPG (The Netherlands).

This methodology gives the designer the ability to make well-founded and responsible design choices to optimize the design. It can be implemented for other (sub)structures by adjusting the script of the parametric model with the project specific boundary conditions.

*BESIX is part of the joint venture TM ROCO carrying out the works of Oosterweel 3b on behalf of Lantis.*

# Full dynamic train-track-bridge interaction calculation to verify passenger comfort on the Lembeek high-speed rail viaduct

Nick Gerard

TUC Rail, Brussels, Belgium

Contact: [nick.gerard@tucrail.be](mailto:nick.gerard@tucrail.be)

## Abstract

In order to verify the accelerations of train carriage and bridge deck, a FEM is made of both train and track/bridge. A reference calculation is made to compare the results of the calculation with measurements carried out inside the vehicle.

**Keywords:** train-track interaction, accelerations, dynamics

## 1 Introduction

Currently on the high-speed line between Belgium and France there are stretches where velocity is limited to 160 km/h. No specific dynamic verification was required in the original calculation. Authorities wish to increase the velocity up to 220 km/h. To do so, acceleration limits are applicable on the bridge deck level as well as in the train carriages. This paper will focus on the train carriage accelerations in the reference case where the train drives 160 km/h in order to compare the model with measurements carried out in the train vehicle.

## 2 Viaduct lay-out

The viaduct consists out of multiple isostatic concrete U-shaped bridge decks with a length of 19 m. The stiffness of the bridge deck  $EI$  equals 16,9 GNm<sup>2</sup>, the divided weight of the structure is 6,6 t/m and the ballast: 6,03 t/m. This results in a first bending mode at 4,96 Hz. The first torsional mode has an eigenfrequency of 8,32 Hz.

Following flowchart from figure 6.9 NBN EN 1991-2: 2004, a dynamic calculation is required but only bending modes should be considered. As such when performing the calculation, a 2D model can be used.

## 3 Design criteria and modelling

### 3.1 Design criteria

As the bridge already exists, acceleration limit for the train vehicles was set to 2 m/s<sup>2</sup> which corresponds to an acceptable comfort limit.

### 3.2 Track model

A finite element model was built in python. Three major zones are to be distinguished, an approach zone from where the vehicle will start, a bridge zone and an end zone. A detail of the model is schematically shown in Figure 1.

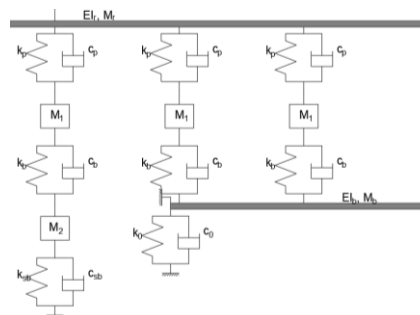


Figure 1 schematic view of the FEM

The properties of this model are given in Table 1.

Table 1 properties of the track model [1]

	[kg]		[N/m]		[Ns/m]
$M_r$	60	$k_p$	600e+6	$c_p$	30e+3
$M_2$	**	$k_b$	832e+3	$c_b$	264e+3
$M_1$	*	$k_{sb}$	22e+6	$c_{sb}$	104e+3
$M_b$	6600	$k_0$	2e+9	$c_0$	2e+7
$EI_r$	12.7e+6 [Nm <sup>2</sup> ]		$EI_b$		16.9e+9 [Nm <sup>2</sup> ]

\*mass of the sleeper: 324 kg, mass of ballast 312 kg

\*\*mass of ballast + mass of subballast 420 kg

A rail beam element is modelled continuous from start to end. Below the rail a spring and damper are attached as railpad towards a node representing the sleeper. Below the sleeper a ballast spring/damper is modelled and connected to a node with the mass of

the ballast and partly the subballast. Below this node a spring/damper for the subballast is installed. In the zone of the bridge the spring/damper of the ballast is connected to the bridge directly. The bridges are modelled as beam elements, 4 consecutive bridges were modelled.

### 3.3 Train model

For the Train model, the axis distances of a Thalys train were used, the model of a bogie with the carriage mass on top is given in Figure 2.

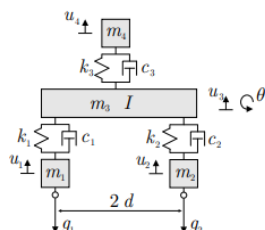


Figure 2 Spring/mass/damper train model [2]

With properties listed in Table 2, where there is no difference between indices 1 and 2.

Table 2 Properties of the train model

	[kg]		[N/m]		[Ns/m]
$M_4$	22 384	$k_3$	$2.5e+6$	$c_3$	$2e+3$
$M_3$	4313	$k_1$	$2.5e+6$	$c_1$	1
$M_1$	1816	$k_H$	$2.8e+9$		
$I$	1500 [kgm <sup>2</sup> ]				

### 3.4 Coupling

The system needs to be solved iteratively for each timestep. The contact forces are applied on the track model resulting in the displacements of each contact point. These displacements are applied to the train models resulting on its turn in contact forces. This is repeated until the difference in force applied to the track model and calculated in the train model is less than 1% of the quasi-static load. The system is solved with direct time integration, Newmark's method.

## 4 Results

The calculated accelerations in the cabin are shown in Figure 3. From this calculation follows that the maximum acceleration in the cabin is about  $0,4 \text{ m/s}^2$ . when comparing this value to the measured accelerations in Figure 4, they correspond very well and the overall behaviour is comparable. The graph that should be compared with the measurements is the green one, carriage 3. This is the first carriage behind the engine vehicle and the position of

measurement in de train.

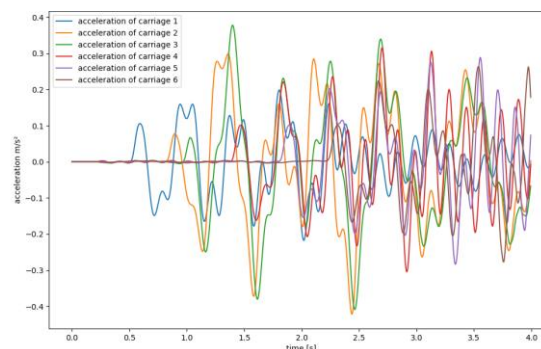


Figure 3 Calculated accelerations in the train

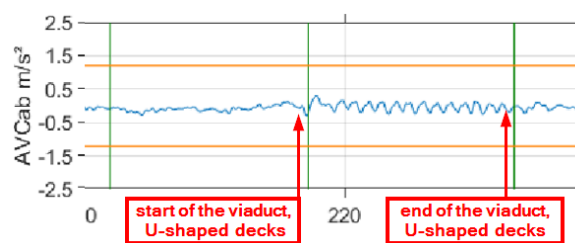


Figure 4 Measured accelerations in the train cabin

The order of magnitude from the calculation is in line with the one from measurements. When entering the viaduct, the largest peak acceleration occurs, after which accelerations seem to decay. Worth mentioning is that the train properties are from a 'French' chassis and measurements from a 'Belgian' chassis. Also for the track properties there can be a large scattering.

## 5 Conclusion and Acknowledgements

A FEM was presented in order to verify if speed can be increased on the Lembeek viaduct. Due to large number of uncertainties, there are differences between measurements and FEM. As the overall trend seems to agree, the calculation will now be carried out with increased velocities.

The author wishes to thank Marleen Ade (Infrabel) for the provision of the properties of the Thalys vehicle as well as the measurement data.

## References

- [1] Nielsen J. A hybrid model for prediction of ground-borne vibration due to discrete wheel/rail irregularities. *Journal of Sound and Vibration*. 2015; 345: 103-120.
- [2] François S. Trillingen ten gevolge van de Thalys hogesnelheidstrein op lijn L2 Brussel-Keulen: in situ metingen en numerieke voorspellingen. Masterthesis, Leuven; 2000



# Simulated aleatory traffic for fatigue design of steel bridges

Marco Lucio Cerquaglia dr. ir., Yves Duchêne dr. ir., Vincent de Ville de Goyet dr. ir.

Bureau Greisch, Allée des noisetiers 25, 4031 Liège

Contact: [mlcerquaglia@greisch.com](mailto:mlcerquaglia@greisch.com)

## Abstract

This work presents recent developments in the fatigue design of bridges submitted to aleatory traffic loads. Synthetic traffic loads are generated according to prescribed probability density functions representative of real traffic. A Montecarlo approach is used to estimate the damage induced on the structure. Lorries weight and inter-distances, as well as traffic composition, are generated in an aleatory way. Different traffic regimes (free-flow vs jammed), depending on the time of the day, are also accounted for. A critical analysis of the traffic parameters is performed.

**Keywords:** Fatigue, damage, bridges, Montecarlo, aleatory traffic

## 1 Introduction

Nowadays, steel road bridges also need to fulfill fatigue requirements. The aim of the approach presented here is to perform fatigue design according to Eurocode fatigue model 5 [1] (p.53) but replacing real-life measurements by Finite Element computations. Synthetic traffic loads are generated according to prescribed probability density functions representative of the real traffic. A Montecarlo approach is then employed to estimate the damage induced on the structure, based on Eurocode SN curves [2] (p.15). This work takes inspiration from the PhD thesis of Baptista [3].

## 2 Aleatory traffic generation

### 2.1 Traffic parameters

During off-peak hours, traffic is considered as free flow, while during rush hours it is considered as an alternating sequence of free-flow (10 minutes) and jammed phases (5 minutes).

According to [3] (p.141-143), free-flow traffic can be characterized through a Gamma distribution, while jammed traffic can be modelled through a Beta distribution.

We consider 32000 vehicles per day per lane, with a constant flux,  $Q$ , of 1800 vehicles per hour. By hypothesis, trucks represent 25% of vehicles in slow lanes and 10% in fast lanes. For each type of truck, a bi-normal distribution (with known average and standard deviation) is employed to model the uncertainty on the weight (cf. data recorded in Brothal [3] (p.137)). A relative frequency is also given for each type.

### 2.2 Inter-distances and weight generation

The generation of the distances between vehicles proceeds according to the following steps:

1. Choose the type of lane (slow vs fast). This dictates the proportion of trucks amongst the total amount of vehicles.
2. Perform a time loop over the day with time step size  $\Delta t$ .
3. At each time step, choose the type of traffic to be modelled, free flow vs jammed (this depends on the time of the day).
4. Since the flux of vehicles is supposed constant, the number of vehicles is  $N_{veh} = Q \times \Delta t$ . For illustration purposes, let us suppose that  $N_{veh} = 9$ .
5.  $N_{veh}$  aleatory values of distances are generated from the probability density function corresponding to the current traffic type (Figure 1(a)). A minimum distance can also be imposed to avoid unphysical interpenetration. In this way an ensemble of  $N_{veh}$  vehicles, with wanted distances  $d'_i$ , has been generated. At this stage, it has not yet been decided which of these vehicles are cars and which are trucks.
6. The type of lane determines how many of these vehicles are trucks, and the number of trucks of each type can also be set, since their frequency of occurrence is known. The position of the trucks in the ensemble of  $N_{veh}$  vehicles is assigned aleatorily. Vehicles that are not trucks are cars (Figure 1(b)).
7. For the computation, cars can be eliminated since their contribution to fatigue damage is

neglected, and distances  $d_i$  between trucks can be computed as mere sums of the  $d'_i$  between two successive trucks (Figure 1(c)).

8. Finally, a random weight can be assigned to each truck based on the normal distribution corresponding to its type (Figure 1(d)). So far, only global effects are considered, and trucks are modeled as concentrated loads.
9. Steps 3 to 8 are repeated for each time step until the end of the time loop.

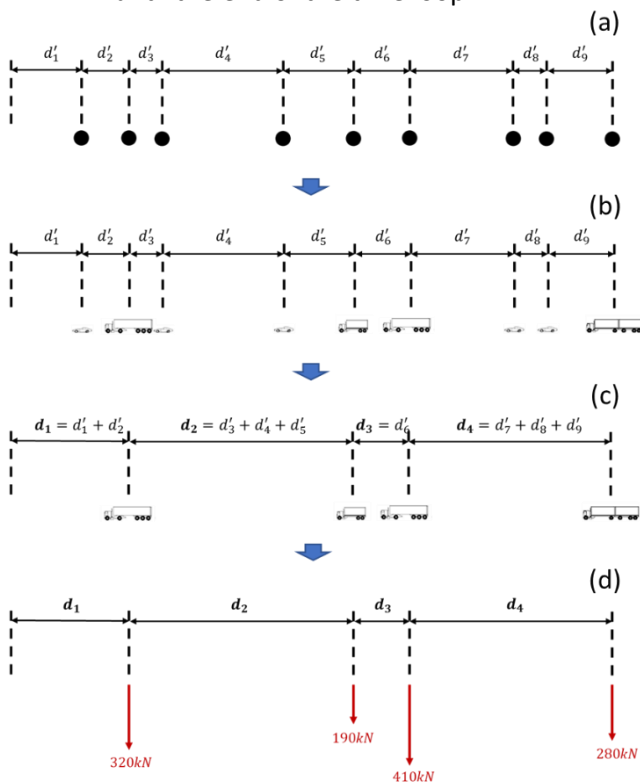


Figure 1. Aleatory traffic generation procedure.

### 3 Influence of traffic parameters on damage

Once the aleatory traffic loads are generated, damage at a given point on the structure can be computed [2] (pp.13-18). However, the traffic parameters proposed in [3] lead to an incoherence between the simulated travel time and the imposed observation window. As in [3] (p.141), we employ a Gamma distribution for free-flow traffic, but we consider a mean distance between vehicles of 60m (instead of 120m) and a free-flow traffic speed of 90km/h (vs 80km/h) for trucks. With this new set of parameters, consistency between total travel time and the imposed observation window is recovered. A comparison between the traffic parameters employed in [3] and those proposed in this work, in terms of total damage over 250 days, is presented in Figure 2 for different span lengths of an idealized

bridge. A detail with fatigue class 100 and a sinusoidal influence line are considered. The two sets of parameters lead to comparable damages for span lengths up to ~50m. For shorter spans, inter-distances play a minor role since damage is mostly due to local effects related to the passage of one truck at a time. For longer spans, the difference becomes more important and grows with the influence line length.

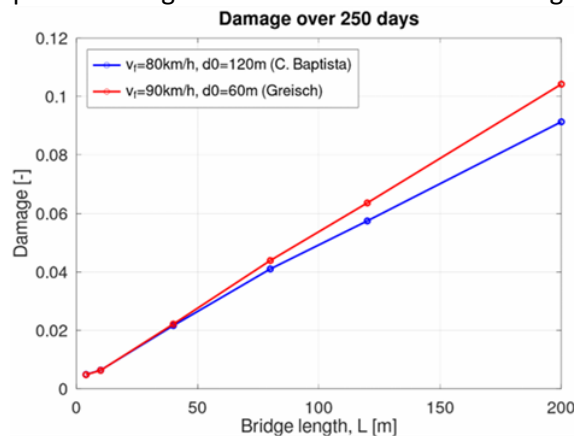


Figure 2. Damage sensitivity to traffic parameters.

### 4 Conclusions

In this work we presented a method to estimate fatigue damage on steel bridges, considering aleatory traffic loads. Synthetic traffic loads are generated numerically and then applied on a finite element model of the structure to deduce aleatory stress histories, according to a Montecarlo approach. The statistical model used for the traffic is the one proposed in [3], however we propose to use different parameters than [3] to ensure consistency between travel time and the imposed observation window. It was shown that no meaningful difference on the resulting damage exists for influence lines up to ~50m. On the contrary, differences of up to ~15% have been observed for longer influence lines (up to 200m). However, we must highlight that these are preliminary results, based on an idealized problem.

### Acknowledgements

This research is supported by the Walloon Region (Belgium) through convention n. 8096 "Finelg2020".

### References

- [1] EN 1991-2, Eurocode 1: Actions on structures - Part 2: Traffic loads on bridges; 2003.
- [2] EN 1993-1-9, Eurocode 3: Design of steel structures - Part 1-9: Fatigue; 2005.
- [3] Baptista, C. *Multiaxial and variable amplitude fatigue in steel bridges*. PhD Thesis. École Polytechnique Fédérale de Lausanne ; 2016

# Fatigue recalculation of the Gallieni bridge over the Rhone in Lyon

**Amine Laklalech and Jimmy Jacquot**

EGIS, Paris, France

Contact: [amine.laklalech@egis-group.com](mailto:amine.laklalech@egis-group.com)

## Abstract

The Gallieni Bridge, situated in Lyon and spanning the Rhône River, connects Quai Claude Bernard with Quai du Docteur Gailleton, linking the 7th and 2nd arrondissements of the city. Presently, this bridge serves as a passage for two tramway lines and road traffic. The TEOL project, or Tramway Express de l'Ouest Lyonnais, aims to establish a fresh tramway route between Tassin-Alaï and Lyon-Jean Macé. This upcoming route is planned to utilize the existing tramway infrastructure, commencing in 2032. This has raised concerns about the bridge's capacity to handle the additional tramway traffic. In light of this, an assessment was conducted to evaluate the feasibility of incorporating the new tramway onto the bridge. Initially, a diagnostic phase involved gathering and analyzing existing data and bridge drawings to comprehend the structure's behavior. Subsequently, the focus shifted to assessing the bridge's capability to withstand the augmented loads (existing traffic plus the new tramway) both statically and in terms of fatigue.

**Keywords:** Diagnosis, Tramway, Fatigue, Static, Steel, Reinforcement.

## 1 Introduction

Built in 1965, it is a three-span steel bridge (57.65 m - 89.50 m - 57.65 m) with a total length of 204.8 meters and a width of 29.8 meters. It is composed of seven full-web girders of varying heights, interconnected by lattice girders. The tramway lines T1 and T2 have been brought in service in 2002.



Figure 1. Views of the current state of the Gallieni Bridge

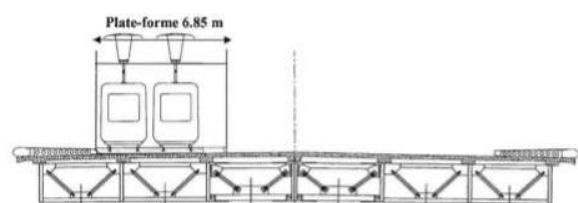


Figure 2. Cross section of the functional profile

No modification of this functional profile is considered for the calculations.

After gathering all the technical information and drawings during the diagnosis phase, the objective was to calculate the capacity of the bridge to withstand the new loads given in the scenarios of circulation of the tramway lines T1, T2 and TEOL given by the operator.

Three scenarios have been assessed regarding the lifespan of the bridge:

- **1965-2065:** Lifespan of 100 years.
- **1965-2075:** Lifespan of 110 years.
- **1965-2057:** Lifespan of 92 years.

The need for reinforcements to endure the fatigue loads generated by the introduction of the new tramway line was assessed for each scenario.

## 2 Methodology

This chapter aims to present the different stages enabling the in-depth feasibility study to be carried out.

1. Determination of calculation assumptions and operating scenarios: Lifespan of the structure, type of tramway, frequency of tramway passage, traffic speed, road traffic assumptions and lifespan objective of the bridge.
2. Modelling of the bridge on a 3D software based on the existing drawings.

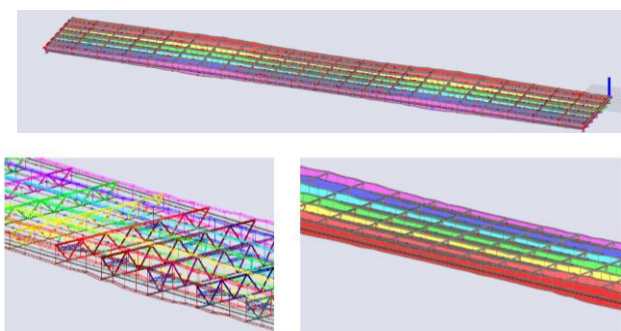


Figure 3. Views of the 3D model of the Gallieni bridge

3. Static assessment of the structure's integrity after the passage of new tram convoys, adhering to Eurocodes.
4. Fatigue verification of the structure for beams P1, P2, P3 and P4 carried out using [1].
  - a. Determination fatigue detail classes
  - b. Assessing the influence of road traffic on the structural fatigue resistance.
  - c. Assessing the influence of tramway traffic on the structural fatigue resistance.
  - d. Calculation of the accumulation of damage using the following equation:

$$\text{Endommagement} = \sum \frac{n_i}{N_i} \leq 1 \quad (1)$$

$$\Delta\sigma = \left(\frac{5}{N}\right)^{\frac{1}{5}} \cdot \left(\frac{2}{5}\right)^{\frac{1}{5}} \cdot \frac{C}{\gamma_{MF}} \quad \text{d'où l'on tire } N = \frac{5 \cdot \left(\frac{2}{5}\right)^{\frac{5}{3}} \cdot C^5}{(\Delta\sigma)^5 \cdot \gamma_{MF}^5}$$

5. Determination of the potential reinforcement of the structure for each scenario.

### 3 Results

#### 3.1 Static verification

Table 3. Results of static verification

Beam	$\sigma_{\max}$ , upper flange	$\sigma_{\max}$ , lower flange
P1	340,2 MPa	355 MPa
P2	346,6 MPa	345,1 MPa
P3	327,5 MPa	336 MPa
P4	313 MPa	325,8 MPa

The maximal stress obtained is inferior to 355 MPa.

#### 3.2 Fatigue verification

##### 3.2.1 Scenario 1: 1965-2065

Table 2. Total damage induced by fatigue loads

Beam	Nmax, upper flange	Nmax, lower flange
P1	109 %	109 %
P2	120 %	107 %
P3	73 %	88 %
P4	15 %	15 %

##### 3.2.2 Scenario 2: 1965-2075

Table 3. Total damage induced by fatigue loads

Beam	Nmax, upper flange	Nmax, lower flange
P1	127 %	127 %
P2	143 %	122 %
P3	88 %	108 %
P4	18 %	18 %

##### 3.2.3 Scenario 3: 1965-2057

Table 4. Total damage induced by fatigue loads

Beam	Nmax, upper flange	Nmax, lower flange
P1	90 %	90 %
P2	99 %	90 %
P3	58 %	88 %
P4	12 %	12 %

### 3.3 Conclusions and discussion

From a static standpoint, the Gallieni bridge can withstand the loads induced by the new TEOL Tramway. Fatigue calculation reveals that the beams under the tramway platform need reinforcements in scenario 1 and 2. However, in scenario 3, the bridge can handle the new loads without any need for reinforcements. These findings emphasize the critical role of the assumptions provided by the operator in determining whether reinforcements are necessary. Also, this study shows that the fatigue recalculation of an existing steel bridge that was not meant to accommodate railway traffic initially is a complex subject. Furthermore, this study underscores the complexity of recalculating fatigue for an existing steel bridge that was originally not designed for railway traffic. It is important to note that further investigations are required to ensure that the steel structure does not exhibit any cracks, which could indicate the onset of fatigue deterioration.

### References

- [1] Guide de conception et de justification des ponts métalliques et mixtes-résistance à la fatigue (SETRA/SNCF/CTICM)

# Shear and Wheel Loading on Bolted Connectors for Composite Bridge Decks

Angeliki Christoforidou, Jelco Köhlenberg, Abishek Baskar, Job ter Kuile, Marko Pavlovic  
Delft University of Technology, Delft, The Netherlands

Contact: [a.christoforidou@tudelft.nl](mailto:a.christoforidou@tudelft.nl)

## Abstract

Composite sandwich panels, recognized for their lightweight design, durability, and fatigue resistance, have been progressively utilized in bridge construction since the 1990s. However, their deployment in larger highway bridges remains constrained by the need for slip-resistant connectors that ensure hybrid interaction without compromising strength. This paper introduces and examines the injected steel reinforced resin (iSRR) connector, which integrates bolting and injection techniques. Through extensive experimental campaigns, which included cyclic shear, compressive loading, and static tests, the iSRR connector showed enhanced performance. It registered an 18% higher shear resistance compared to traditional M27, 10.9 grade bolts. Additionally, it surpassed the compressive resistances, achieving at least 2.5 times the standard load. The connector also exhibited outstanding fatigue endurance, surviving millions of loading cycles. This study underscores the iSRR connector's potential as a robust solution for hybrid structures integrating composite sandwich panels.

**Keywords:** composite to steel connection, fatigue, compression, shear, bolts, iSRR connector.

## 1 Introduction

Composite sandwich panels, known for their durability and lightweight, have become integral in bridge construction since the 1990s. However, their use in high-load highway bridges is limited due to the absence of reliable slip-resistant connectors.

Traditional connection methods, like adhesive bonding and various bolt types, have not consistently met long-term strength and reliability needs, highlighting the necessity for a more robust solution.

A connection method, proposed in [1], integrates adhesive bonding, bolting, and injection techniques. Previous studies have confirmed its performance in static pull-out and push-out tests. This paper focuses on investigating the connector's fatigue performance when subjected to shear and compressive wheel loading. Suggestions in the design of the iSRR connector are given to meet several application requirements which are supported by experimental results.

## 2 Design configurations of iSRR joint

To fabricate the iSRR connector illustrated in Figure 1 (a), a sizable, near-cylindrical cavity within the composite deck needs to be created. The mechanical connector is placed

in the hole that is later injected with an injectant material called steel reinforced resin (SRR), thus deriving the nomenclature 'iSRR connector'. The injection process can be conducted either in situ during onsite assembly or as a prefabrication procedure in a manufacturing facility. Bolts are preloaded onsite to preclude any potential slippage resulting from the bolt-hole clearance within the steel girder.



(a) Without spherical plate (b) With spherical plate

Figure 1. iSRR connector geometries

An alternative iSRR connector configuration introduces a spherical plate mechanism as shown in Figure 1 (b). This plate, whose diameter equates to the center-to-center distance of the webs of the panel, functions to distribute the compressive forces originating from vehicular wheel loads from the webs directly to the steel girder. This results in less bending of the bottom facing and thereby reduces the likelihood of delamination of the bottom laminate of the sandwich web core panel.

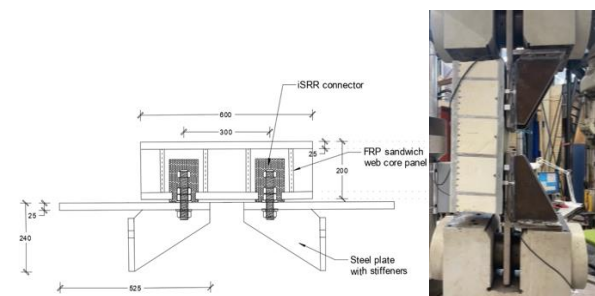
### 3 Experimental campaign

#### 3.1 Description of test setups

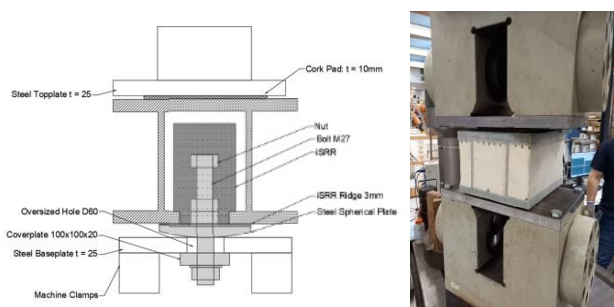
Cyclic shear and compressive loading are applied on the iSRR connectors with M27 bolts of 10.9 grade. Once the cyclic tests are resumed, the same setups are used to apply static loading with a rate of 0.04 mm/sec. All tests are conducted in machine, with capabilities for loading up to  $\pm 600$  kN and 800 kN for cyclic and monotonic loading, respectively.

The shear loading experimental setup is depicted in Figure 2 (a) and it utilizes the iSRR connector design of Figure 1 (a). This setup evaluates a single lap joint, bridging a composite deck panel and a steel end detail, under fully reversed cyclic loading with a maximum load level of 80 kN. Linear Variable Displacement Transducers (LVDTs) are monitoring the relative slip increase between the steel plate and the composite deck at the connections' height.

Local wheel loading is also applied to the connection with the spherical plate and the setup is shown in Figure 2 (b). The wheel load is simulated by the incorporation of a cork pad. The vertical displacement per load cycle is measured by LVDTs. Compressive loading of a minimum load equal to 90 kN is applied.



(a) Shear loading



(b) Wheel loading

Figure 2. Loading test setups

#### 3.2 Experimental results

The connectors sustained 3 million cycles of shear loading without any visible sign of damage but with a displacement range increase of 0.5 mm as shown in Figure 3. Similarly, the iSRR connector with the spherical plate

reached 2 million cycles of compressive loading without any sign of damage and no displacement range increase.

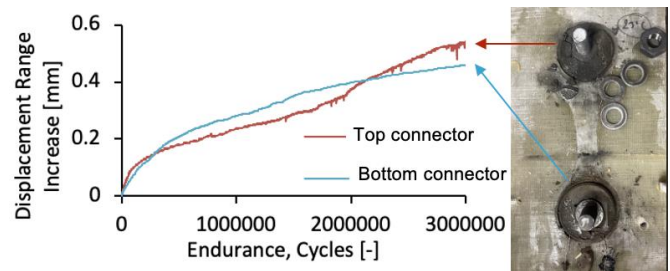


Figure 3. Cyclic shear performance of iSRR connectors

The static experiments show that the iSRR connector's maximum shear resistance reaches 270 kN. This is an 18% increase over the M27, 10.9 bolt's shear resistance, which is limited by bolt shearing. Additionally, the iSRR connector demonstrates a local compressive resistance exceeding 501 kN, a value 2.5 times greater than the applied load from LM2 of NEN [2]. This indicates the capacity to sustain even higher loads, a potential limited by delamination in the bottom face of the sandwich panel which led to web failure.

### 4 Discussion

The two distinct design adaptations of the iSRR connector respond to varied onsite demands: one prioritizing cyclic shear performance and the other focusing on effectively managing cyclic wheel loads. The upcoming phases of the project will generate force against cycles at various temperatures, and the iSRR joint will be tested under moisture.

### 5 Conclusions

The iSRR connector registered an 18% higher shear resistance over conventional M27, 10.9 bolts and a local compressive resistance at least 2.5 times higher than the relevant load from Eurocode. Finally, it demonstrated excellent fatigue performance with no sign of failure after millions of cycles of loading. All these prove that the iSRR connector is a viable solution in hybrid structures utilizing composite sandwich panels.

### References

- [1] Csillag F, et.al. Tensile and shear resistance of bolted connectors in steel-FRP hybrid beams. In YEC 2019: proceedings of the Belgian-Dutch IABSE young engineers colloquium. 2019; 50-51
- [2] NEN-EN 1991: Eurocode 1: Actions on Structures - Part 2: Traffic loads on bridges. Section 4.3.3, PAR (1), 2015



## Re-use of prefabricated prestressed bridge girders in the Netherlands

**Danny Jilissen, Rob Vergoossen**

*Royal HaskoningDHV, Rotterdam, Zuid-Holland, the Netherlands*

Contact: [danny.jilissen@rhdhv.com](mailto:danny.jilissen@rhdhv.com)

### Abstract

The Dutch construction industry aims to cut CO<sub>2</sub> emissions by 49% and recycle all concrete waste by 2030. Reusing structural elements faces challenges due to the lack of guidelines. Efforts are underway to develop protocols. Initiatives like the Hoog Burel overpass project demonstrate successful element reuse, significantly reducing CO<sub>2</sub> emissions. Costs remains a challenge for wider adoption, but scaling up reuse of prefabricated prestressed bridge girders has been initiated.

**Keywords:** Re-use, circular construction, prefabricated concrete girder, overpass, prestress, bridge.

## 1 Introduction

The Dutch construction industry plays a pivotal role in the country's resource consumption and energy usage, accounting for approximately half of all raw materials and 40% of total energy expenditure. Furthermore, it is a major contributor to waste production (40%) and CO<sub>2</sub> emissions (35%). In response to this, the Dutch Concrete Agreement, endorsed by the government, has set ambitious targets to slash CO<sub>2</sub> emissions by 49% compared to 1990 levels, while also mandating that all concrete waste be recycled into new concrete by 2030. To meet these goals, the industry is exploring innovative solutions, and one promising approach is the reutilization of structural elements from bridges and overpasses from functional obsolete structures in new projects.

## 2 Removing barriers

Reuse has two important barriers: There are no guidelines and there is a knowledge gap.

### 2.1 No guidelines

Despite the apparent simplicity of the reuse strategy, its practical implementation faces several barriers. One of the most significant challenges is the absence of standardized protocols and guidelines specifically tailored to the reuse of structural elements. Presently, the Eurocodes, which form the basis for construction standards, predominantly focus on new construction, leaving a notable gap in guidance for reuse. To address this, various guidelines have been formulated, including CB'23 and NTA 8713 Reuse of structural steel. A CROW guideline for the reuse of structural prefab concrete elements was also recently

published. General considerations in the reuse of precast concrete elements are shown in this guideline. This guideline provides an overview of the steps to be taken and provides guidance on the important steps. Some steps include collecting data, the usefulness and necessity of research into the elements to be reused, disassembly from the donor project, transport and storage, processing of elements and considerations for matchmaking and application in the new project. In addition, there is a specific appendix with recommendations for reuse of prefabricated prestressed bridge girders. Furthermore, on an international scale, the FIB ModelCode 2020 is pioneering the pre-codification of end-of-life scenarios and reuse, marking a historic milestone in the industry.

### 2.2 Disseminating of knowledge

At present, the deconstruction of structural elements from existing structures carries a higher cost compared to conventional demolition practices. Consequently, a willing party must provide pre-financing to facilitate the dismantling process instead of the typical practice of converting these elements into concrete aggregate. Contractors, typically entrusted with both demolition and construction tasks, will only find the reuse of these elements economically viable if they are assured of their future use or sale. Additionally, when constructing a new viaduct, it is imperative that reused elements are guaranteed to be released in a timely manner and furnished with a quality declaration after disassembly, modification, and, if necessary, repair. Achieving this level of certainty necessitates a structural assessment, which also demands pre-financing. In cases where a client holds significant control over a region's infrastructure, they are well-

positioned to oversee the pre-financing and matching processes. By doing so, they can incentivize dismantling and reuse through contractual arrangements and gain insight into expiring constructions and the need for new ones.

Currently, there is no existing stock of deconstructed elements. However, as elements are gradually deconstructed from various bridges and overpasses over time, a stockpile will naturally accrue. Ideally, this stock will comprise elements of varying lengths, skew angles, and load-bearing capacities. This diversity will facilitate the most efficient matching of elements with the prerequisites of new overpasses slated for construction.

### 2.2.1 Pilot project Hoog Burel

The Dutch Ministry of Infrastructure, Rijkswaterstaat, has issued a Strategic Business Innovation Research (SBIR) directive to the market, inviting proposals for Circular Viaducts in pursuit of their target to achieve climate neutrality and full circularity by 2030. A consortium led by Royal HaskoningDHV, advocating for the reuse of prefab girders, was selected to develop a tested prototype following a feasibility study that confirmed its viability.

In Groningen, a large-scale transformation of the southern ring road is underway. When tasked with demolishing the KW21 Europaplein viaduct, the contractor opted for a circular construction approach. Instead of complete demolition and conversion into aggregate, 26 prefabricated prestressed girders from the main spans were salvaged and repurposed. In the SBIR project, the team identified the replacement of the 60-year-old Hoog Burel overpass over the A1 motorway as an opportunity for incorporating reused girders. Although the girders from the Groningen viaduct were available, they required modification to match the specifications of the Hoog Burel project. Challenges included the absence of original fabrication drawings and the need for indirect support to accommodate the required construction joints. A series of tests on bored cylinders were conducted in the laboratory to assess strength, chloride ingress, carbonation, and alkali-aggregate reaction. The results indicated outstanding performance, with minimal ingress of aggressive agents even after four decades.



Figure 1. Placement of the reused bridge girders

This demonstrated the potential for these elements to maintain structural integrity for centuries. The successful adaptation of these girders, despite the additional challenges, resulted in a substantial environmental benefit, reducing CO2 emissions by 96% compared to newly cast girders. Hoog Burel is the first overpass of Rijkswaterstaat that was constructed with reused bridge girders (Figure 11) and was opened to traffic on March 1, 2023.

### 2.2.2 Scaling up reuse

Rijkswaterstaat is widening the A9 between the Badhoevedorp and Holendrecht junctions. In addition, Rijkswaterstaat is deepening the A9 near Amstelveen over a length of 1.6 km. During the widening and deepening of the A9, the current viaducts will be functional obsolete. This releases many elements and materials that are suitable for reuse. The partners of Liggers2.0, in collaboration with Rijkswaterstaat and the consortium Closing the Loop, are currently investigating the potential reuse of girders from the A9 motorway project. An agreement was recently concluded with Rijkswaterstaat to dismantle about 450 girders from this project instead of demolishing them. There is also the chance of further scaling up to almost 1,000 bridge girders. It is currently being investigated whether a large part of these bridge girders can be used in the replacement and renovation project of the A44 of Rijkswaterstaat. At the same time, research is also being conducted into setting up a large storage and modification depot. The bridge girders from the A9 could then be transported here.

## 3 Conclusions

Despite the potential environmental benefits of reusing structural elements, they remain more expensive than traditional demolition and new production. Standardization and optimization are imperative for widespread adoption and economic viability. This shift towards greater circularity is a crucial step in moving away from a disposable society.



# Proof load testing prestressed concrete girders for reuse

**Jose Eduardo Paredes Pineda**

*Nebest B.V., Vianen, The Netherlands; TU Delft, Delft, The Netherlands*

Contact: [jose.paredes@nebest.nl](mailto:jose.paredes@nebest.nl)

## Abstract

In the Netherlands, demolished girder bridges contrast with the construction of new ones. A circular viaduct is achievable with the high-quality reuse of prestressed concrete inverted-T girders. Proof load testing demonstrates that the girders can be reused when non-compliant with design rules through conventional assessment. A load testing setup and protocol are being developed for experimental assessment of the shear resistance of these structural components.

**Keywords:** concrete bridges, prestressed concrete, assessment, proof load testing

## 1 Introduction

Every year about 40 new concrete girder bridges are built in the Netherlands. In contrast, around 7 girder bridges were demolished per year between 2001-2019 [1]. These bridges are far away from reaching their technical service life. Nearly 60 bridges will be demolished between 2024-2036, almost 3000 prefabricated concrete girders will be crushed into concrete rubble.

The consortium Closing the Loop (CtL) is designing a circular viaduct for Rijkswaterstaat as part of their transition towards a circular economy. CtL aims on the high-quality reuse of these girders within the superstructure of the viaduct. This model not only reduces environmental impact but also secures part of the demand for new girders with the stock in existing infrastructure. Methods of assessment can ensure they meet structural resistance requirements as there are no design standards for new bridges built with reused girders.

## 2 Literature review

### 2.1 Levels-of-approximation framework

The assessment is performed with models that are approximations of reality. The fib Model Code 2010 introduced the levels-of-approximation (LoA) framework for assessment of concrete structures. If the resistance is found to be insufficient, the accuracy of the assessment can be progressively refined through a higher level of approximation. The most simple method is the verification of the cross-sectional capacity to withstand the design solicitations. If this approach shows insufficient resistance, the next step is to obtain the load effects from a linear finite element model [2].

The girders intended for reuse fail to meet the criteria for new bridges through conventional assessment. Traffic load model 1 prescribes higher loads and the shear resistance model from Eurocode 2 results in lower capacities, than the original design criteria. The girders were designed with the fully prestressed philosophy, with little to no shear reinforcement, relying on the concrete for shear. Thus, the girders show insufficient shear capacity and do not have the required amount of stirrups. Nonlinear finite element models are a more sophisticated method but are excluded for designing new concrete bridges. Previous research of prestressed concrete girders (from bridges built in the 1960-80s or lab specimens built with the specifications from such bridges) demonstrated that code provisions underestimate the shear resistance [3, 4, 5, 6, 7, 8].

### 2.2 Proof load testing

Load testing is the measurement of the structural response to controlled and predefined loadings without changing the elastic response [9]. Proof load testing is the is a direct demonstration of the capacity of the structure to withstand the design solicitations.

## 3 Method

This research intends to develop a proof load testing methodology for assessing the shear resistance of salvaged inverted-T girders from decommissioned bridges.

### 3.1 Test structure

The dataset of girders to be demolished is analysed to dimension the test structure (Figure 1). The applied loads in the studies define a range of the test load that the system can be expected to deliver. The steel structure delivers a force up to 3000 kN, accommodates girders up to 20 m in

length and 1500 mm in height, and its self-balancing feature enables on-site testing (Figure 2).

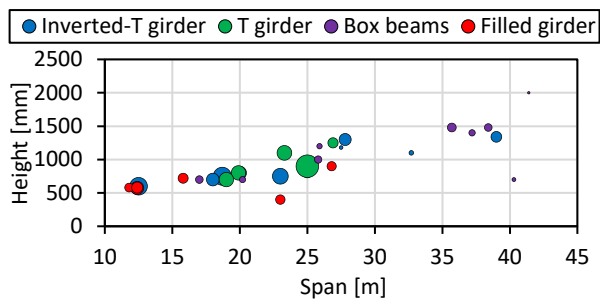


Figure 1. Number of girders per type, span length and height to be demolished (2024-2036)

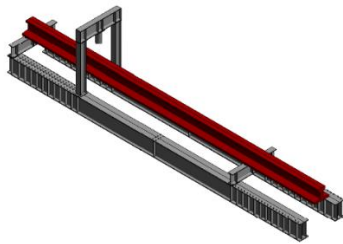


Figure 2. Test structure

### 3.2 Loading application

The target proof load is applied at the location of the critical cross-section identified from analytical assessment. The load is applied through a hydraulic actuator in an area equal to the wheel print of the design tandem. The magnitude of the load is selected to give the same cross-sectional effects as the governing load combinations. The load is applied in a monotonic loading protocol with 4 load levels: baseline (sensor calibration), SLS, ULS and ULS with a transfer factor.

### 3.3 Stop criteria

Stop criteria are parameters monitored in real-time which indicate irreversible damage. Stop criteria are derived from mechanical models of the shear failure mechanisms and validated with failure tests. The parameters to measure are deflections, applied load and concrete strains.

### 3.4 Sensor plan

The selection of measurement techniques is based on the resolution and rate at which the physical parameters are to be measured during testing.

## 4 Discussion

In contrast to the trend of cyclic protocols, a monotonic protocol is proposed as the former checks the linearity of the structural response when cracking is allowable. However, cracking in prestressed girders without stirrups is not allowable as it can lead to sudden failure.

The experimental tests consist of a proof load test followed by a failure test. The evolution of damage monitored validate the stop criteria and loading scheme by comparison with the expected behavior from analytical and numerical models. The difference between the failure load and the target proof will indicate the safety margin.

## 5 Conclusions

This research addresses how to repurpose concrete girder bridges for new construction. A rigorous proof load testing methodology is under development, and encompasses a structure for on-site testing, load application scheme, stop criteria for damage prevention, and a measurement plan.

## 6 References

- [1] Rijkswaterstaat, *Eindrapport Haalbaarheidsonderzoek Hergebruik Prefabliggers (in Dutch)*, 2020.
- [2] E. Lansoght, "Assessment of existing concrete bridges by load testing: barriers to code implementation and proposed solutions," *Structure and Infrastructure Engineering*, vol. 19, no. 12, 2023.
- [3] S. Ensink, C. van der Veen, D. Hordijk, E. Lansoght, H. van der Ham and A. de Boer, "Full-size field test of prestressed concrete T-beam bridge," in *Structural Faults & Repair 2018 and European Bridge Conference 2018: 15 -17 May 2018*, Edinburgh, UK, 2018.
- [4] S. Ensink, C. van der Veen and A. de Boer, "Shear tests on large prestressed concrete T-beams," in *Proceedings of fib symposium 2016: Performance-based approaches for concrete*, Cape Town, SA, 2016.
- [5] E. Lansoght, G. I. Zarate Garnica, F. Zhang, M. -K. Park and H. Sliedrecht, "Shear Experiments of Prestressed Concrete Bridge Girders," *ACI Structural Journal*, vol. 118, no. 3, pp. 117-130, 2021.
- [6] G. P. Osborn, P. J. Barr, D. A. Petty, M. W. Halling and T. R. Brackus, "Residual Prestress Forces and Shear Capacity of Salvaged Prestressed Concrete Bridge Girders," *Journal of Bridge Engineering*, vol. 17, no. 2, pp. 302-309, 2012.
- [7] A. Higgs, P. J. Barr and M. W. Halling, "Comparison of Measured and AASHTO LRFD-Predicted Residual Prestress Forces, Shear and Flexural Capacities of High-Strength Prestressed-Concrete Bridge Girders," *Journal of Bridge Engineering*, vol. 20, no. 1, 2015.
- [8] W. Zhou, H. Li and W. Zhang, "Experimental behavior of the shear strength of full-scale precast prestressed double tees," *Journal of Building Engineering*, 2021.
- [9] AASHTO, *The manual for bridge evaluation with 2016 interim revisions*, Washinton DC: American Association of State Highway and Transportation Officials, 2016.

# Wind Tunnel Tests and Normative Approaches of the ARC MAJEUR Subject to Vortex Shedding

Adrien Palm, Yves Duchêne

Bureau Greisch, Liège, Belgium

Contact: [apalm@greisch.com](mailto:apalm@greisch.com)

## Abstract

The sculpture called “Arc Majeur” is a curved steel structure with a height of 60 meters and a 2,25 meters square section. Due to its slenderness, the structure is very sensitive to vortex induced vibrations (VIV). The initial design of the structure with the Eurocode is compared to wind tunnel tests of an aeroelastic model. These tests, performed afterward, validate the design and improve the safety margin of the structure. Both approaches show that a tuned mass damper (TMD) is necessary to damp the vibrations for structural safety reasons and fatigue lifetime, but experimental results allow a lower damping.

**Keywords:** vortex induced vibrations; wind tunnel tests; aeroelastic model; Arc Majeur

## 1 Introduction

Imagined in the 1980s by the artist Bernar Venet, the “Arc Majeur” (Figure 1) is erected in Belgium. The arc is not a continuous circular arch but a two-curvilinear-segments arc. It culminates 60 m above the motorway.



Figure 1. The “Arc Majeur” during erection

The structure is designed by Greisch office and can withstand wind gusts up to 52 m/s at ULS. The square section of the arc ( $b = 2,25$  m) produces VIV for a wind speed around  $V_{cr} = 16$  m/s. To reduce the vibration amplitudes, the main arc is equipped with a TMD, with a mass of 1500 kg, placed at its top. This paper compares VIV effects according to the Eurocode [1] to wind tunnel tests. These tests are carried out at the University of Liège with professors Andrienne T. and Denoël V.

## 2 Vortex Induced Vibrations

As the first critical wind speed of VIV is lower than the average wind speed on site, there is a risk of VIV. The amplitudes of vibration must be compared to the

maximum admissible displacements at the top of the arc: 0,44 m for structural integrity and 0,34 m for fatigue state. Aeroelastic properties of the arc without TMD are the following for in-plane response: the natural frequency  $f_0 = 0,86$  Hz, the structural damping  $\xi = 0,32$  %, the mass ratio  $M = \frac{m_s}{m_{air}} = 332$ , the numbers of Strouhal  $S_t = \frac{f_0 \cdot b}{V_{cr}} = 0,12$ , Scruton  $S_c = \frac{4 \cdot \pi \cdot \xi \cdot m_e}{\rho_{air} \cdot b^2} = 10,3$ , and Skop-Griffin  $SG = 2 \cdot \pi \cdot S_t^2 \cdot S_c = 0,93$ .

### 2.1 Eurocode approach

The amplitudes of vibration according to the method 2 of the Eurocode 1991-1-4 [1] and ANB [2] are equal to 1,15 m for a damping ratio  $\xi = 0,32$ % and 0,32 m for a damping ratio  $\xi = 3,0$ %. The TMD provides an equivalent damping ratio of 3,6% and ensures both the structural integrity and the fatigue resistance.

### 2.2 Wind tunnel tests

Aeroelastic tests are performed in the wind tunnel facility of the University of Liège [3]. They allow to evaluate the vibration amplitudes and the lock-in range for different Scruton numbers by varying the damping of the model. This paper focus on the tests in a low turbulent wind in the direction of the motorway. The effects of wind turbulence, curvature and wind orientation are investigated [4] but are not presented here. The Figure 2 shows the aeroelastic model. It is made of an aluminium tube core and 3D printed outer volumes in plastic. The following

similitudes are respected: the geometrical, the mass ratio, the Strouhal and the Scruton similitudes.



Figure 2. aeroelastic model in wind tunnel

The VIV responses of the model in a low turbulent flow are presented in Figure 3 in terms of relative amplitude  $Y_F/b$  as a function of the reduced velocity  $V_r = V/(f_0 \cdot b)$ , for five different Scruton numbers.

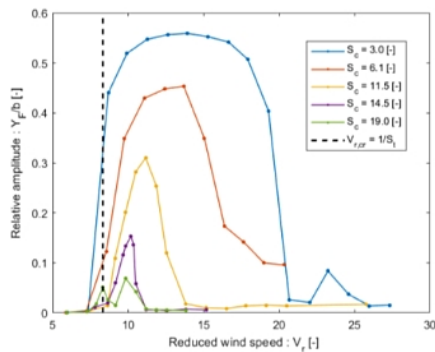


Figure 3. VIV response for different Scruton numbers

These results are summarized in terms of maximum relative amplitude as a function of Scruton number in Figure 4 with the blue curve. These tests predict a vibration amplitude of  $Y_F = 0,34 b = 0,77 m$  the “Arc Majeur” without TMD ( $S_c = 10,3$ ) and a lock-in range from  $V = V_r \cdot f_0 \cdot b = 16$  to  $26 m/s$ .

### 2.3 Comparison of both approaches

For validation of the present experimental results, they are compared, to references tests from the literature and to the experimental Skop-Griffin curve in black, in Figure 4.

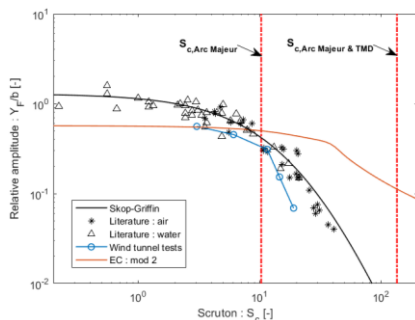


Figure 4. Comparison: tests, Eurocode, literature

According to Figure 4, the transition zone between high and low vibration amplitudes occurs for lower Scruton numbers according to the tests results (in blue) than with the Eurocode (in red).

To check the fatigue lifetime, stresses variations at critical points are compared to the S-N curves given by the Eurocode EN 1993-1-9. The numbers of cycles are estimated with Hansen's formula [2]. Figure 5 displays the fatigue lifetime as a function of the damping ratio. Based on the Eurocode, a minimum critical damping ratio of 2,75% is necessary to ensure a lifetime of 50 years. Based on wind tunnel tests, a damping ratio of 0,46% would be sufficient.

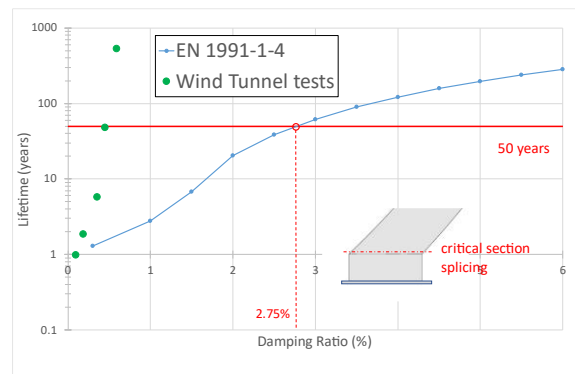


Figure 5. Lifetime vs. critical damping ratio  $\xi$

### 3 Conclusions

Firstly, the arc has been designed according to the recommendations of the Eurocode 1991-1-4. Then, aeroelastic tests in a wind tunnel showed that the transition zone between self-exciting response (at high amplitude of vibrations) and forcing response (at low amplitude) appears at too high Scruton number with the Eurocode method 2. So, according to the wind tunnel tests, the structural damping provided by the TMD could be lower and still ensure the safety of the structure.

### References

- [1] Eurocode 1991-1-4. *Actions on structures- Part 1-4: General actions – Wind actions*. April 2005.
- [2] NBN 1991-1-4 ANB. *Eurocode 1 - Part 1-4: National annex*. 2010 (F).
- [3] ULiège, *The University of Liège Wind Tunnel Facility: Technical description*, 2009, <https://www.wind-tunnel.uliege.be>.
- [4] Palm A., Duchêne Y., de Ville de Goyet V., Denoël V., Andrienne T., *Design, Wind Tunnel Tests, Normative and Theoretical Approaches of the ARC MAJEUR Subject to Vortex Shedding*. Eurodyn 2023, Delft, 2023

# Dynamic analysis of a hybrid steel-GFRP footbridge

LB Cornelissen MSc.

Royal HaskoningDHV, Rotterdam, The Netherlands

Contact: [lieuwe.cornelissen@rhdhv.com](mailto:lieuwe.cornelissen@rhdhv.com)

## Abstract

The city of Gothenburg is planning a new footbridge over the old city moat (Vallgraven). The design of this bridge is a collaboration of Systra AB and Royal HaskoningDHV. The bridge incorporates a Glass Fiber-Reinforced Polymer (GFRP) deck and steel girders. Due to the light weight and slender design a dynamic analysis for pedestrian comfort is needed. Results show a maximum acceleration of  $0.60 \text{ m/s}^2$ , affirming the bridge's suitability. Not all aspects of influence to pedestrian vibrations are currently included in the methods of analysis. The author calls for refining guidelines and monitoring post-construction behavior to enhance future designs.

**Keywords:** Engineering; vibrations; footbridge; FRP; steel; hybrid.

## 1 Introduction

The city of Gothenburg is planning a new footbridge over the old city moat (Vallgraven). The bridge (Figure 1) consists of two steel main girders (red), two steel cross girders and a deck. Originally, a steel deck was considered, but due to poor soil conditions a lighter Glass Fiber-Reinforced Polymer (GFRP) deck was chosen.

Lightweight footbridges are known to be sensitive to vibrations. A dynamic analysis is used to assess the accelerations caused and experienced by pedestrians.

## 2 Design

The architectural design of the bridge is made by architect Malin Mirsch of Systra AB, Sweden. The structural design in a collaboration between Systra AB and Royal HaskoningDHV, The Netherlands.



Figure 1 Impression of the bridge

### 2.1 Materials and geometry

Cross-sections of the bridge are shown in Figure 2 and Figure 3. The main and cross girders are constructed of S355 construction steel, while the deck is made of GFRP webcore sandwich panels. The webs in the deck, as indicated in Figure 3, are quasi-isotropic (QI) laminates,

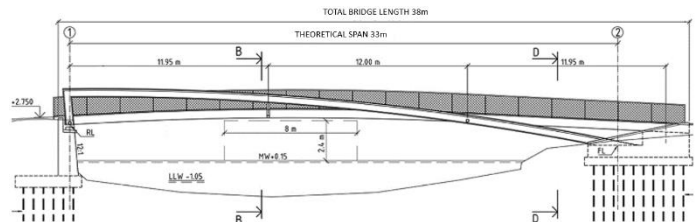


Figure 2 Longitudinal cross-section

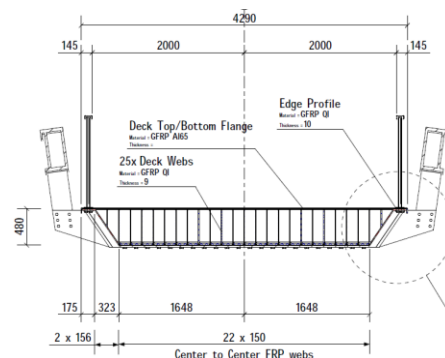


Figure 3 Transverse cross section B

the flanges are anisotropic (AI) laminates. The GFRP material properties are presented in Table 2-1 GFRP Material properties. The three GFRP deck sections are supported at the abutments and by two hat-profile cross girders. The deck sections are rigidly connected to the cross girders by a bonded and bolted connection, with the bolts solely added for redundancy. The cross girders are supported by hangers to the main girders. At the abutments the deck is free to translate longitudinally, the main girders are clamped.

Property	unit	GFRP QI	GFRP AI	
Young's modulus	E	MPa	18600	26200
Poisson's ratio	$\mu$	-	0.33	0.32
Shear modulus	G	MPa	7100	5600
Nominal weight	$\gamma$	kN/m <sup>3</sup>	19	19
Elongation coefficient	$\alpha$	1/K	1.00E-05	1.00E-05
Young's modulus 90°	E <sub>90</sub>	MPa	18600	16300
Poisson's ratio 90°	$\mu_{90}$	-	0.33	0.17

Table 2-1 GFRP Material properties

## 2.2 Dynamic analysis

The goal of the analysis is to determine the maximum acceleration experienced by pedestrians. The method used is described in the European guideline for human induced vibrations [1]. The bridge comfort class is set at CL2, with a maximum vertical acceleration of 0,7 m/s<sup>2</sup>.

### 2.2.1 Eigenforms

The bridge is modelled in the FE software package SOFiStiK, which has a built-in module to calculate the natural frequencies and Eigenforms. The first two vertical Eigenforms are shown in Figure 5, the corresponding frequencies are;  $f_1 = 2.85 \text{ Hz}$ . and  $f_2 = 5.53 \text{ Hz}$ . The Eigenforms differ from a simply supported structure. Therefore, the simplified method, the single degree of freedom (SDOF) method as described in [1] p.29, is not applicable and a more detailed analysis by FEM is necessary.

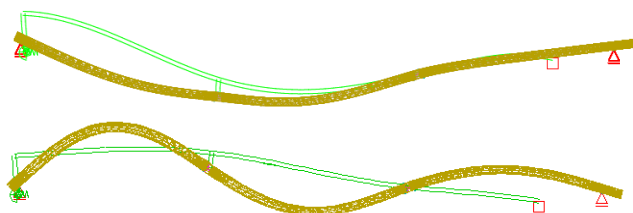


Figure 5 First (above) and second (below) vertical Eigenforms

### 2.2.2 Damping

The damping ratio (0,01) and the first two natural frequencies are used to determine the Rayleigh coefficients;  $rada$  – for mass proportional damping and  $radb$  – for stiffness proportional damping. No modal damping is used. The coefficients are determined as:

$$rada = w_1 \cdot w_2 \cdot \frac{(x_{i_1}w_2 - x_{i_2}w_1)}{w_2^2 - w_1^2} [1/sec] \quad (1)$$

$$radb = \frac{(x_{i_2}w_2 - x_{i_1}w_1)}{w_2^2 - w_1^2} [sec] \quad (2)$$

Where;  $w_1 = 2\pi f_1$ ;  $w_2 = 2\pi f_2$ ;  $x_{i_1} = x_{i_2} = 0.01$ .

### 2.2.3 Dynamic load

The dynamic load is a uniformly distributed harmonic load  $p(t) [N/m^2]$  that represents an equivalent pedestrian stream, as described in [1] p.27:

$$p(t) = P \cdot \cos(2\pi f_s t) \cdot n' \cdot \psi \quad (3)$$

Where;  $P \times \cos(2\pi f_s t)$  is the force due to a single pedestrian (280 N);  $f_s$  is the step frequency, equal to the first natural frequency of the bridge (2.85 Hz.);  $n'$  is the equivalent number of pedestrians (0.09);  $\psi$  is the footfall frequency reduction coefficient (0.125).

The dynamic load is applied in steps of 0.01 seconds and for a duration of 30 seconds. This duration is

sufficient to bring the bridge into the steady state vibration, as shown in Figure 6. Once the steady state is reached the maximum acceleration of the bridge can be determined.

## 2.3 Results

The deck displacement at each load step is plotted in Figure 6. The maximum acceleration during this analysis is 0,60 m/s<sup>2</sup>. This is below the comfort limit of 0,7 m/s<sup>2</sup> as set by the City of Gothenburg and falls within comfort class CL2, as per [1] p.15.

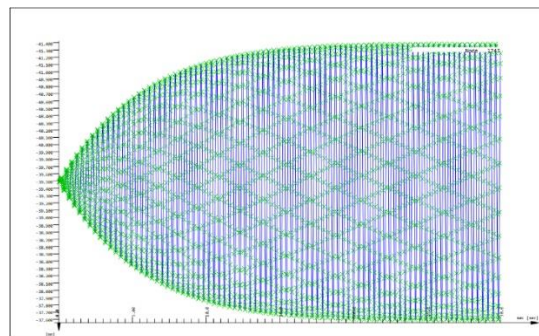


Figure 6 Maximum displacement of the deck

## 2.4 Discussion

Comfort level is often governing for the design of FRP bridges, while no comfort issues seems to occur in bridges which are designed with more flexibility. Question arises; Is there room for improvement of the guidelines? And, how can damping factors such as connections or the presence of handrails be included? To fine-tune the calculation methods it is recommended to monitor the vibrations of the bridge after completion.

## 3 Conclusions

A dynamic analysis of a newly designed footbridge in Gothenburg is performed by FEM to verify pedestrian comfort. The maximum acceleration of the bridge stays below the comfort class limit of 0.7 m/s<sup>2</sup>.

## References

- [1] Heinemeyer C, Butz C, Keil A, Schlaich M, Goldbeck A, Trometor S, Lukic M, Chabrolin B, Lemaire A, Martin P, Cunha A, Caetano E, authors Sedlacek G, Heinemeyer C, Butz C, Geradin M, editors. *Design of Lightweight Footbridges for Human Induced Vibrations*. EUR 23984 EN Luxembourg (Luxembourg): European Commission; 2009. JRC53442

# Development of fully precast lightweight steel-UHPFRC composite bridge

**Xiujiang Shen**

*Sustainable materials, VITO, Mol, Belgium*

Contact: [xiujiang.shen@vito.be](mailto:xiujiang.shen@vito.be)

## Abstract

Aiming at the full and proper exploitation of both steel and Ultra High Performance cementitious Fiber Reinforced Composites (UHPFRC) materials, a steel-UHPFRC composite girder bridge (3 × 30 m) is designed following a new concept as proposed by the author. The unique use of ① UHPFRC in both tension and compression and ② a half rolled section with continuous in-built steel dowels in combination with UHPFRC dowels (forming composite dowels as shear connectors) is highlighted. Compared with traditional steel-concrete composite structure, the steel usage and construction cost of the new structure can be reduced by 45% and 10%, respectively.

**Keywords:** composite structure; steel section; ultra-high performance fiber reinforced cementitious composite (UHPFRC); composite dowel

## 1 Introduction

The advance in structural materials and efficient design of structural elements are the keys to fulfil the concept of sustainability in modern civil engineering, where minor environmental impact and low economic costs are required. As an advanced cementitious material, Ultra High-Performance Cementitious Fiber Reinforced Composites (UHPFRC) has unique combination of extremely low permeability, high strength, and ductility [1,2]. A notable feature of UHPFRC under tension is the significant deformation capacity including hardening strain up to 5‰ with only multiple microcracks observed before reaching tensile strength [3,4]. Importantly, UHPFRC has a fatigue endurance limit of up to multimillions of cycles under both tension and compression [5–7]. These characteristics distinguish UHPFRC from traditional concrete and make it an ideal structural material for improving the structural performance, durability and sustainability of new or existing structures [8,9].

Recent research has highlighted the outperformance of steel-UHPFRC composite structure compared with traditional steel-concrete composite structures [10]. From the structural point of view, the main current challenges of the concept include: (1) proper geometry and arrangement of UHPFRC and steel components to fully utilize both materials; (2) reliable shear connectors to ensure efficient synergetic action between the two components. Several studies have been conducted to implement this concept in the form of steel-UHPFRC composite beam structures over last decade [10]. Nevertheless, the existing steel-

UHPFRC composite beam structures can still be further optimized.

## 2 Concept

In recent research, the author [11] proposed a new steel-UHPFRC composite beam structure, consisting of an inverted T-shaped steel component with in-built continuous steel dowels and a T-shaped UHPFRC component with steel reinforcement, as illustrated in Fig.1. The steel dowels are inserted into the web of T-shaped UHPFRC component, forming steel-UHPFRC composite dowel, to create connection between two components. Compared with traditional steel-concrete composite beams, the characteristics of the new structure (under positive bending moment) are:

1) The single-flange steel component, whose relative ineffective steel part near the neutral axis is removed, is arranged in the high tension zone to resist large part of the flexural tensile stress.

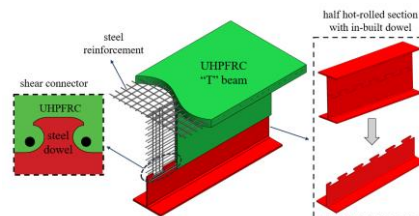


Figure 1. Schematic illustration of proposed steel-UHPFRC composite beam structure

2) Upper part (top flange mainly) of UHPFRC component is in compression zone to resist the entire compressive stress, and the lower part of UHPFRC web contributes to part of tensile resistance.

3) The hot rolled section with low residual stress during manufacturing is used and divided into two identical steel components with in-built continuous steel dowels by single cutting. Thus, no welding procedure is required, leading to fast fabrication and assembly, as well as reducing risk of fatigue failure.

### 3 Design

The Danjiang Bridge in Hunan Province, China, is the first continuous composite beam bridge that utilizes this concept. This bridge has span of  $3 \times 30$  m and a width of 11.75 m. The bridge superstructure is composed of 5  $\pi$ -shaped steel-UHPFRC composite beam with a standard width of 2.6 m. The composite beams are 1.2 m height with a UHPFRC deck thickness of 120 mm, UHPFRC web average thickness of 140 mm and a steel beam height of 430 mm. The details are shown in Fig.2, 3 and 4.

Compared with traditional steel-concrete composite structure, the steel usage and construction cost of the new structure can be reduced by 45% and 10%, respectively.

This construction of Danjiang Bridge is planned to start from January of 2024, and expected to be accomplished in December of 2024.

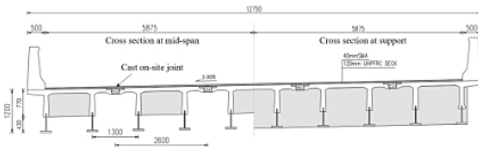


Figure 2. Details of steel-UHPFRC composite beam in Danjiang Bridge: Cross section of steel-UHPFRC composite beam

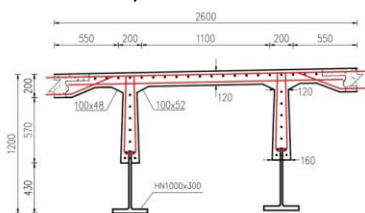


Figure 3. Details of steel-UHPFRC composite beam in Danjiang Bridge: Cross section of fully precast  $\pi$ -shaped unit

### 4 Conclusions

- (1) The unique use of ① UHPFRC in both tension and compression and ② half rolled section with in-built steel dowels in combination with UHPFRC dowels (forming composite dowels as shear connectors) is highlighted in the new steel-UHPFRC composite beam.
- (2) Compared with traditional steel-concrete composite structure, the steel usage and

construction cost of the new structure can be reduced by 45% and 10%, respectively.

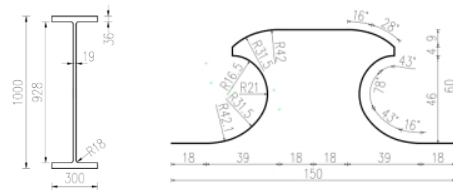


Figure 4. Details of steel-UHPFRC composite beam in Danjiang Bridge: hot-rolled section (left) and steel dowel (right)

### References

- [1] P. Richard, M. Cheyrezy, Composition of reactive powder concretes, *Cement and Concrete Research*. 25 (1995) 1501–1511.
- [2] R. Yu, P. Spiesz, H.J.H. Brouwers, Mix design and properties assessment of Ultra-High Performance Fibre Reinforced Concrete (UHPFRC), *Cement and Concrete Research*. 56 (2014) 29–39.
- [3] X. Shen, E. Brühwiler, Influence of local fiber distribution on tensile behavior of strain hardening UHPFRC using NDT and DIC, *Cement and Concrete Research*. 132 (2020) 106042.
- [4] X. Shen, E. Brühwiler, W. Peng, Biaxial flexural response of Strain-Hardening UHPFRC circular slab elements, *Construction and Building Materials*. 255 (2020) 119344.
- [5] T. Makita, E. Brühwiler, Tensile fatigue behaviour of ultra-high performance fibre reinforced concrete (UHPFRC), *Mater Struct*. 47 (2014) 475–491.
- [6] E. Parant, P. Rossi, C. Boulay, Fatigue behavior of a multi-scale cement composite, *Cement and Concrete Research*. 37 (2007) 264–269.
- [7] X. Shen, E. Brühwiler, Biaxial flexural fatigue behavior of strain-hardening UHPFRC thin slab elements, *International Journal of Fatigue*. 138 (2020) 105727.
- [8] E. Brühwiler, UHPFRC technology to enhance the performance of existing concrete bridges, *Structure and Infrastructure Engineering*. 16 (2020) 94–105.
- [9] B. Graybeal, E. Brühwiler, B.-S. Kim, F. Toutlemonde, Y.L. Voo, A. Zaghi, International Perspective on UHPC in Bridge Engineering, *Journal of Bridge Engineering*. 25 (2020) 04020094.
- [10] C.A. Benedetty, V.B. dos Santos, P.A. Krahl, A. Rossi, F. de A. Silva, D.C.T. Cardoso, C.H. Martins, Flexural and shear behavior of steel-UHPC composite beams: a review, *Engineering Structures*. 293 (2023) 116649.
- [11] Y. He, X. Shen, G. Chen, X. Shao, A new steel – UHPFRC composite beam with in-built composite dowels as connectors: Concept and design principles, *Engineering Structures*. 298 (2024) 117089.

# Influence of a timber outrigger system on cross laminated timber core buildings

F.F. Janssens

Biobased structures, Civil engineering, TU delft, Delft, Netherlands

**Contact:**

Florisdino@hotmail.com

## Abstract

A possible to solution to reduce emissions of the construction sector is to incorporate more timber in the design of a building. Multi-storey buildings in timber have gained increased interest with the development of cross laminated timber (CLT) products. This paper presents the possibility of increasing the lateral stiffness of a CLT core building by introducing a timber outrigger. Additional effects of the outrigger system have been investigated, such as the changes of forces in the connections. The findings in this paper are supported by extensive numerical models.

**Keywords:** stability system, CLT core, timber outrigger, wind-induced behaviour, lateral deflections, dynamic behaviour.

## 1 Introduction

The construction industry contributes significantly too global emissions. In response to the growing concern about climate change, new methods are being developed to reduce these emissions. Building with timber is one such approach, as it can be CO2 neutral if reforestation is practiced. Timber is a lightweight and flexible material compared to traditional construction materials like steel and concrete, which can result in high accelerations and deflections, negatively affecting user comfort.

Engineered wood products such as CLT and GLT make it possible to construct larger panel sizes and spans, which can lead to more efficient building design[1]. Many buildings utilize core systems to provide lateral stability and facilitate vertical transportation of goods and people[2]. Therefore, replacing a conventional concrete core with a CLT core could be a viable solution to reduce the building's environmental impact.

Timber, being a flexible material, often lacks the necessary stability to meet code requirements for deflection and acceleration in high-rise buildings[3]. Adding an outrigger, similar to those used in concrete and steel structures, can provide the solution to enhance user comfort. The outrigger transfers bending moments from the core to the columns around the core, reducing forces in the core and increasing overall stiffness[4]. However, it is unclear what the influence of the addition of a timber outrigger on a CLT core building is and how such a system can be improved. Therefore the purpose of this research is to evaluate the impact of a timber outrigger on a CLT core building, and

provide guidance for structural engineers on how to improve the structural behaviour of such a system.

## 2 Addition of a timber outrigger to a CLT core

The impact of adding an outrigger is evaluated through comparison of numerical case studies. Case A consists of a CLT core as the lateral stability system. Case B consists of a CLT core with timber outriggers. A sensitivity analysis is performed on different design aspects for each case. In Case A, the influence of core joint design is analysed, while in Case B, the impact of outrigger design parameters is evaluated. For a fair comparison of deflections, accelerations and force transfer, both Case A and B are designed based on ULS requirements. Finally, Case C is an optimized design based on the results of the sensitivity analyses. The different stability systems of the case studies as previously mentioned can be seen in Figure 1.

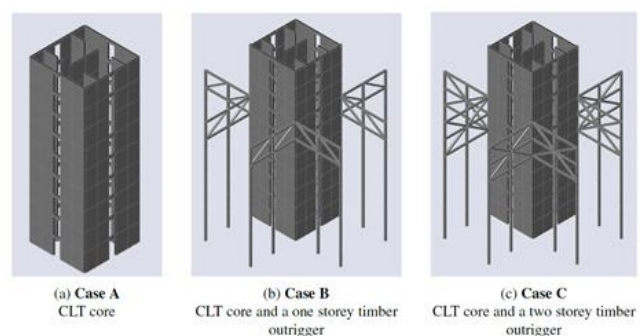


Figure 1. Numerical models of the different stability systems

By introducing a timber outrigger to a CLT core building bending moments are transferred from the core to the column, partially restricting rotation of the core. This will have the following effects on the behaviour of the structure. Firstly, the deflections due to lateral wind loading are reduced due to the increased global stiffness. In Figure 2 the maximum lateral deflection of the three different case studies is shown. In which the maximum lateral deflection of case A is reduced by 14% and 35% for case B and C respectively.

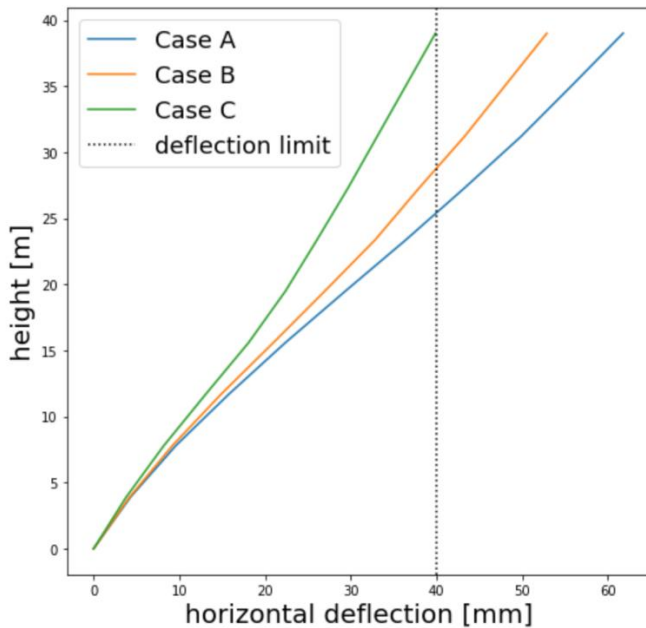


Figure 2. Lateral deflection of the different case studies.

Secondly, the increased stiffness of the structure will result in a reduction of peak lateral acceleration. The peak lateral acceleration of case A is reduced by 10% and 25% for case B and C respectively compared to case A. Thirdly, by transferring loads from the core to the columns the strength requirements on the connections of the core are reduced. Finally, by introducing a timber outrigger system to a CLT core building horizontal forces are generated in the core at outrigger level, which should be accounted for in the design phase of the vertical core joints. Increasing the stiffness of the outrigger will further reduce deflections, peak lateral acceleration and strength requirements on the core connections, however strength requirements on the vertical core joints at outrigger level will further increase. An exponential relationship has been derived between the lateral deflections, peak lateral acceleration and the ratio between the effective bending stiffness of the outrigger and the effective bending stiffness of the core as can be seen Figure 3, where 0 and 100% represents a zero bending stiffness and infinitely rigid outrigger respectively.

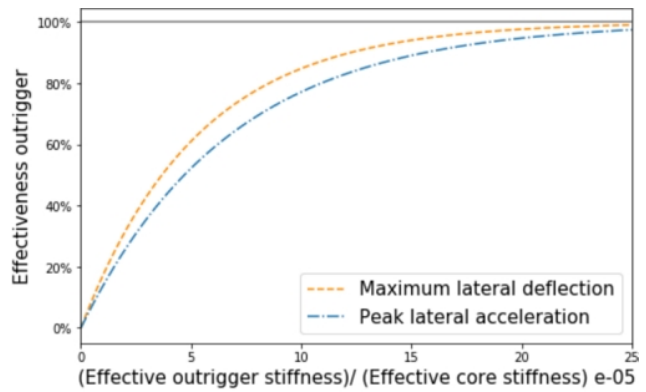


Figure 3. Effectiveness outrigger.

Additionally it was investigated what the critical design parameters are and how the performance of a CLT core building with timber outriggers can be improved. For the design of a CLT core the connection between the core and foundation showed to be critical, having large effects on the lateral deformation. While increasing the stiffness of the vertical connections showed to have little influence on the interaction between core walls due to their respective high interaction factors. In the design of the outrigger it was shown that a two storey outrigger is able to more than double the reduction in deflections compared to a single storey outrigger, further increasing the overall effectiveness of the system. Finally the effectiveness of the system was found to be significantly influenced by the configuration of the outrigger truss, demonstrating a greater impact than increasing member size or connection stiffness.

### 3 Conclusions

By introducing a timber outrigger to a CLT core both deflections and accelerations of the system can be reduced. The effectiveness of the system is largely dependent on the stiffness ratio between the outrigger and the core. Introduction of the outrigger reduces forces in the core connections except for the horizontal connections at outrigger level. Introducing an outrigger to a CLT core could be a viable method to reduce forces in the core and increase lateral stiffness.

### References

- [1] E Karacabeyli and S Gagnon. "Canadian CLT handbook: 2019 edition". In: *FPIInnovations: Pointe-Claire, QC, Canada* (2019).
- [2] Ivana Kuzmanovska et al. "Tall timber buildings: Emerging trends and typologies". In: *2018 World Conference on Timber Engineering*. 2018.
- [3] Xuan Zhao et al. "Numerical Analysis on Global Serviceability Behaviours of Tall CLT Buildings to the Eurocodes and UK National Annexes". In: *Buildings* 11.3 (2021), p. 124.
- [4] Reza Rahgozar, Ali Reza Ahmadi, and Yasser Sharifi. "A simple mathematical model for approximate analysis of tall buildings". In: *Applied Mathematical Modelling* 34.9 (2010), pp. 2437–2451.

## Circularity in bridge engineering

Sharon Deceuninck

Ghent University, Ghent, Belgium

Contact: [sharon.deceuninck@ugent.be](mailto:sharon.deceuninck@ugent.be)

### Abstract

In this paper, the main aspects of circularity in bridge engineering are pointed out. A circular economy means that materials will be recycled or reused at the end of their life time, which results in a waste neutral environment. The focus lies on the different ways to create circularity in the application field of bridge engineering. The goal is to collect data on different reclaimed bridge elements on an entire platform by evaluating the residual strength and performance of existing bridges. Engineers can use this platform as base for new designs. It is important to facilitate the disassembly of bridges to have less damage to the reclaimed elements. Therefore, design guidelines for modular design need to be established.

**Keywords:** circularity, bridges, recycling, residual strength, modular design

## 1 Linear to circular economy

In the scope of the European action plan to create a complete circular economy before the year 2050 [1], a drastic change in the current linear economy is needed. The supply of raw materials is shrinking, while the amount of waste is continually increasing. Eurostat [2] summarises the contribution to waste production of the different sectors of Europe (measured in 2020). The most important impact is from the construction sector which generates more than 1/3 of the total waste.

Especially for bridge engineering, this waste percentage will increase significantly. Just for the European railway bridges alone, already 35 % reached their end of life time in the year 2002 [3]. With the further increasing traffic load, the designed life time will shorten and even more bridges will need to be replaced.

The concept of circularity can be based on the 3R-principle: Reduce, Reuse and Recycle. It challenges designers and engineers to re-think the design and production process. Figure 1 shows the different aspects of circularity in bridge engineering.

## 2 Creating a catalog of reclaimed elements

Instead of demolishing the bridge with heavy equipment, the different elements should be carefully deconstructed for reuse and collected in a bridge catalog. The Netherlands already started a bridge catalog [4], where the offers vary from complete

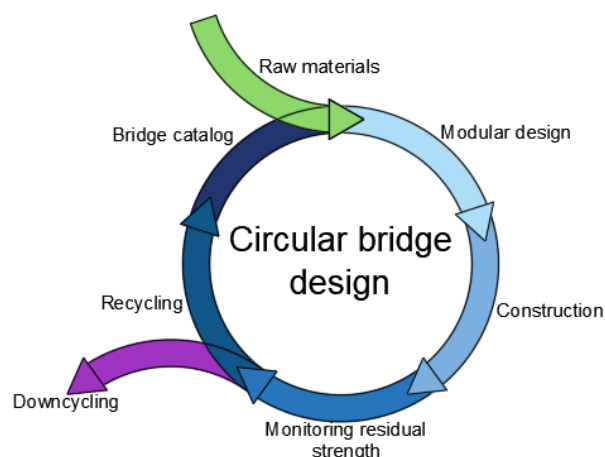


Figure 1. Different aspects of circularity in bridge engineering

recycled bridges to recycled elements such as concrete girders.

In order to have an idea about the ability of reusing elements, it is necessary to have knowledge about the residual strength of these elements. Therefore the structural health and condition of bridges will be monitored and evaluated, to visualise damage such as cracks, delaminations, reinforcement corrosion etc. The monitoring could be done by different types of inspection such as visual, thermal or acoustic inspection. Further research is needed to find the optimal way of inspection to have sufficient knowledge about the residual strength of the bridge elements, within acceptable investment of time and resources.

In addition, it is also important to have a closer look at the influence of deconstruction on the residual strength



of the bridge elements. Different studies have been performed on the deconstruction of buildings in the context of the reuse of the building materials.

The integrated waste management board [5] published a deconstruction manual for buildings. This guideline should be enlarged to infrastructure works to increase the success of circularity.

After deconstructing the bridge, the elements are stocked and collected on the bridge catalog with their corresponding geometrical information and strength condition. The storage of all the recycled elements will be challenging due to the lack of space. Therefore, it would be preferable and more economical to use these elements directly in a new bridge, which will demand a well-conceived logistic system. Designers need to be creative to reuse the reclaimed elements in their new designs.

Research will be done on the influence of possible adaptations of the reclaimed elements on the residual strength. Vergoossen et al. [6] focused in their work on the deconstruction and adaptation of prefabricated prestressed concrete girders. They discussed the possibility to remove the in-situ compression slab, to adapt the angle of skew, to shorten the girders and to create holes. Previous adaptations are possible, but often reduce the performance of the girder. Therefore, they recommend to carefully reflect about the needs for adjustment and try to find some creative solutions.

### 3 Design for reassembly: modular design

Also, the design process of new bridges needs to be adapted to create a circular economy. New design guidelines are necessary to guarantee a modular design. Different companies such as Bailey, Mabey [7] and Acrow [8] are specialised in modular bridge design. They make temporary bridges that are very easy to assemble and disassemble.

One of the challenges in modular design for permanent bridges will be enlarging the expected life time and the span length. Another challenge will be the design of the joints, which require a sufficient stiff connection that can easily be disassembled. For this purpose, prefabricated elements are preferred while cast-in situ is avoided. Several studies of joints in modular buildings can be found in literature [9] [10], which check the performance of the modular joint in the connection. For each joint, the maximum bearing load capacity and rotation capacity are compared with the traditional joints. The application field of these modular joints is still limited to buildings. So, further research will be performed on the use of modular joints in bridge

engineering, where a distinction will be made between steel and concrete joints. Attention needs to be given to the aesthetic possibilities of modular joints as well.

Due to a modular design, repairing bridge elements will be facilitated. Also the construction time will be reduced, which results in less interruption of the traffic.

## 4 Conclusions

This paper gives a global overview of the possibilities to make the bridge infrastructure more sustainable. The reuse of bridge elements needs to be considered as the adaptation in new constructions as well. For the reuse of bridge elements, it is important to be able to summarize the available bridge elements together on a platform. Therefore, further research will be done regarding the residual strength of bridge elements and the impact of deconstruction and adaptations on it.

Next to recycling old bridges, attention needs to be paid to the construction of new bridges. Updated design guidelines are needed to construct modular bridges for easy assembly and especially disassembly.

## References

- [1] "Europees Parlement," 18 01 2023. [Online].
- [2] "Eurostat," 22 08 2023. [Online].
- [3] Brian Bell, R. WP1, "Sustainable Bridges – Assessment for Future Traffic Demands and Longer Lives: European railway bridge demography," 2004.
- [4] "bruggenbank," [Online].
- [5] I. W. M. board, "Deconstruction Training Manual: Waste Management Reuse and recycling at Mather field," California, 2001.
- [6] R. Vergoossen, G.-J. Eck, and D. Jilissen, Re-using existing prefabricated prestressed concrete girders in new bridges, Royal HaskoningDHV, rotterdam, the Netherlands, 2022.
- [7] "mabey bridge," acrow compagny, [Online].
- [8] "Acrow," [Online].
- [9] Xu, C., Qian, X., TAO, R., Wang, R., "Strength of an Improved Connection for modular concrete structures without onsite casting," in *Lecture Notes in Civil Engineering*, Springer, 2022, pp. 221-229.
- [10] G. Nadeem, N. A. Safiee, N. A. Bakar, I. A. Karim and N. A. M. Nasir, "Connection design in modular steel construction: A review," *Structures*, vol. 33, pp. 3239-3256, 2021.

# Renewal of a Station Roof: Using Bio-based Materials

ir. Tijmen Scharff

ProRail B.V., Utrecht, The Netherlands

Contact: tijmen.scharff@prorail.nl

## Abstract

This paper advocates bio-based rain screens in station roof renewals, emphasizing their sustainability over traditional materials. It addresses adoption challenges and encourages collaboration for widespread implementation in infrastructure projects. To give insight in the environmental impact the Environmental Cost Indicator (ECI) is used.

**Keywords:** bio-based materials; carbon footprint reduction; railway stations; Environmental Cost Indicator (ECI); rainscreens; structural projects.

## 1 Introduction

The renovation and renewal of infrastructure facilities, such as railway stations, present a significant opportunity to incorporate sustainable and environmentally friendly materials and technologies. In this context, this project explores recycling existing structural elements and the integration of bio-based materials as rain screens in the refurbishment of station roof at Heiloo. The idea is based on earlier research within ProRail B.V., where bio-based materials are already used in the development of modular electrical substations.

Traditional rain screens, typically constructed using polycarbonate, contribute to resource depletion and environmental degradation. Bio-based materials, derived from renewable sources such as grass, bamboo, or agricultural residues, offer an attractive alternative for rain screen construction. These materials not only reduce the carbon footprint of construction projects, but also contribute to the promotion of a circular economy by utilizing waste and by-products from other industries.

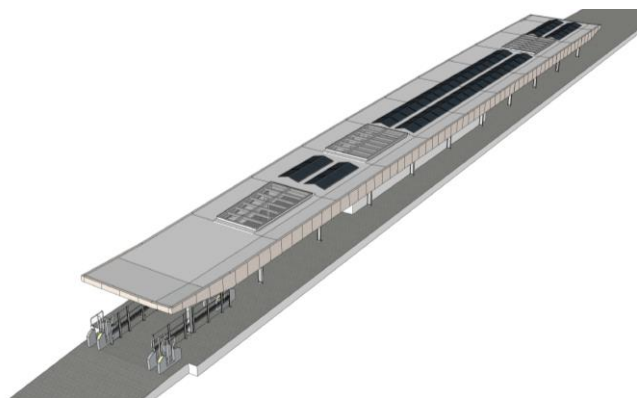


Figure 1: Overview of the upgraded version of Heiloo Station.

## 2 Considerations

The project also addresses challenges associated with the adoption of bio-based rain screens, including cost considerations, regulatory requirements and long-term maintenance. Focus lies on the mechanical and thermal properties, considering factors like durability, resistance to weathering and fire performance. It encourages collaboration between architects, engineers, contractors, and policymakers to promote the widespread adoption of bio-based rain screens in station roof renewal projects and structural projects in general.

## 3 Environmental footprint reduction

To give insight in the environmental impact of this design solution, the Environmental Cost Indicator (ECI) is used. ECI unites all relevant environmental impacts into a single score of environmental costs, representing the environmental shadow price of a product or project. When comparing the bio-based material with the conventional polycarbonate the ECI is reduced by 46,3%. Considering the total amount of building materials, it accounts for 2,3% reduction in ECI.

Table 1. Environmental Cost Indicator (ECI) for different elements of the station roof.

Element	Conventional method (ECI)	Reduced method (ECI)	Relative reduction
Station roof	6893	5986	13,2%
Rain screens	643	345	46,3%



## 4 Conclusions

In conclusion, this project advocates for the use of bio-based materials in rain screens as an innovative and sustainable approach to station roof renewal. Although it contributes 'only' 2,3% reduction to the total ECI, it shows that there is an opportunity in every element of a construction project.

By doing so, it contributes to the development of a more resilient and environmentally responsible transportation infrastructure. This outcome provides valuable insights for professionals in the construction and infrastructure sectors seeking to balance performance, sustainability, and environmental responsibility in their projects.

# Effect of modal coupling on the assessment of footbridge vibrations

Thibaud Bastin, Vincent de Ville de Goyet, Yves Duchêne

Bureau Greisch, Allée des Noisetiers 25, 4031 Liège, Belgium

Contact: [tbastin@greisch.com](mailto:tbastin@greisch.com)

## Abstract

The evolution of pedestrian bridge design is tending towards increasingly flexible and slender structures which are more sensitive to vibrations caused by pedestrians. The accelerations induced by the dynamic response are checked to fulfil the comfort criteria. Traditionally, the calculation is done in the modal basis without modal coupling. This paper shows the limitation of this method and show the benefits of considering it.

**Keywords:** Modal basis, modal interaction, frequency analysis

## 1 Introduction

In the design of footbridges, comfort criteria must be fulfilled. Due to the increasing slenderness of footbridges, the vibrations and accelerations felt during the crossing of pedestrians can be unpleasant. Pedestrian's loading can be considered as a sum of harmonic loads that set the footbridge in motion and can resonate with the footbridge's vibration eigen modes. The acceleration must be bounded to ensure the comfort of pedestrians. To carry out these comfort checks, engineers can rely on the SETRA and HIVOSS guidelines [1],[2].

## 2 Application to a practical example: L'ENJAMBÉE



Figure 1. Footbridge "L'Enjambée"

Namur footbridge "L'Enjambée" [3] was opened in 2020. It is composed of a 2 m wide metal box section with a variable height from 0.4 to 1 m. The structure is a rigid frame bridge with inclined legs that serve as stairs and with two access spans at deck level. It has a main span of 100 m over the Meuse river and is 184 m long.

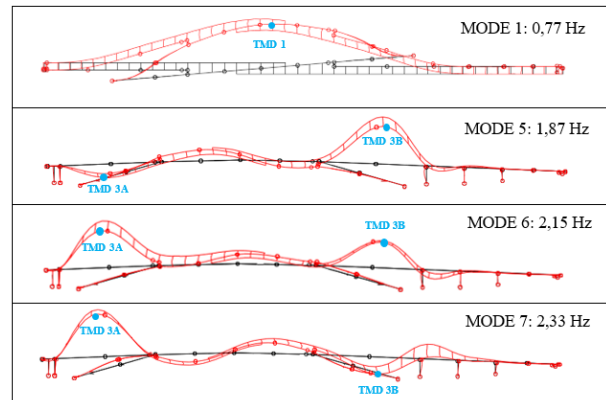


Figure 2. Modes and TMD position

The vibration modes and the TMDs (in blue) placed on the footbridge are given in Figure 2. The mode 1 is transversal and the three others are vertical.

### 2.1 Bridge accelerations without any TMD

Table 1. Footbridge acceleration without TMD

	Mode 1	Mode 5	Mode 6	Mode 7
A [m/s <sup>2</sup> ]	0,8	6,1	4,8	2,9

Without any TMDs, the accelerations calculated with Setra recommendations [1] are above the comfort limits (vertical: 1 m/s<sup>2</sup> & transversal 0.1 m/s<sup>2</sup>)

### 2.2 Footbridge acceleration with TMDs

As the comfort criteria are not respected, TMDs are added to the structure to reduce the accelerations. If no modal interaction is considered, the

acceleration can be obtained by resolving the classical 2 degrees of freedom model.

When modal coupling is considered [4], the TMDs are added to the model. A frequency analysis is done in the modal basis (as in equation 1). The modal matrices ( $M^*$ ,  $C^*$ ,  $K^*$ ) consider TMD and Structural properties.

$$\begin{aligned} \ddot{q}(\omega) &= (-M^* \omega^2 + iC^* \omega + K^*)^{-1} P^*(\omega) \cdot \omega^2 \\ &= H(\omega) \cdot P^*(\omega) \cdot \omega^2 \end{aligned} \quad (1)$$

### 2.2.1 Verification of the transversal mode

On the footbridge “L’Enjambée” only one transversal mode creates large accelerations. No other transversal modes have a close frequency.

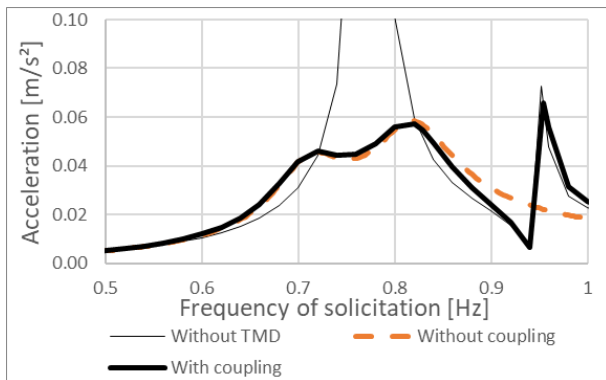


Figure 3. Acceleration observed at TMD 1 position

As shown in Figure 3, both types of resolution give the same type of accelerations. Modal interactions with other modes are negligible. The comfort criterion is fulfilled, with a maximal acceleration of 0.06m/s<sup>2</sup>.

### 2.2.2 Verification of the vertical modes

For the vertical modes, the focus is made on the mode 5,6 and 7 having close natural frequencies. The 3 mode shapes are close together and can be excited by the same pedestrian loads. In Figure 4, only the TMD 3A is placed and accelerations are observed at TMD 3B position.

In Figure 4, the methods with (red curve) and without (green curves) modal interaction gives not the same accelerations. The introduction of TMD 3A impacts the 3 modes, so neglecting the interaction between them and the TMD gives wrong results. In this case, the acceleration at the frequency of mode 5 is overestimated without

modal coupling. At the mode 6 frequency, the accelerations are underestimated without modal coupling.

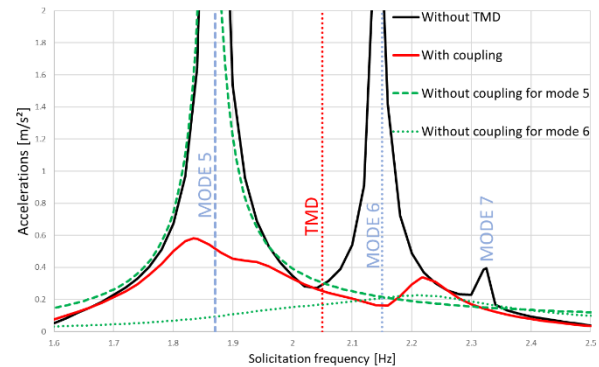


Figure 4. Accelerations at TMD 3B position

## 3 Conclusions

The modal coupling has to be considered if two conditions are met: TMDs are used and impact several modes, the footbridge has modes with close frequencies and mode shapes.

Otherwise, neglecting the modal coupling is sufficient for the assessment of footbridge vibration.

This work was funded by the Service Public de Wallonie as part of the FINELG2020 project.

## References

- [1] Setra: Footbridges – Assessment of vibrational behaviour of footbridges under pedestrian loading, October 2006
- [2] HivoSS: Design of Footbridges – Background, document, September 2008.
- [3] INFOSTEEL : Une emjambée élanée et transparente par-dessus la Meuse, <https://www.infosteel.be/images/magazine/info-steel-65/52/index.html>, 2021.
- [4] Bastin T., Extended vibration serviceability assessment of a footbridge that considers the modal coupling, Eurodyn, 2023



# Optimization of construction sequence by anchoring cofferdam to tunnel

**Wouter Lambrechts**

BESIX Engineering Department, Brussel, Belgium

Contact: [wouter.lambrechts@besix.com](mailto:wouter.lambrechts@besix.com)

## Abstract

To facilitate maritime traffic during the construction of a cut-and cover tunnel, the construction phasing is optimized, involving the anchoring of a sheet pile wall to the new tunnel. The sheet piling wall serves a soil- and water-retaining function while supported by the tunnel. The anchorage system consists of welded steel plates on the sheet pile wall, to which the reinforcement of the tunnel is welded. The design focuses on the dimensioning of the welds, the steel plates and reinforcement to transmit these forces from the sheet pile wall to the tunnel. These interface forces are determined using Plaxis2D on which the tunnel reinforcement is sized. Finally, the welds are calculated on the ultimate tensile strength of the reinforcement.

**Keywords:** cut-and-cover; concrete; sheet pile; retaining; cofferdam; weld; anchoring; maritime; tunnel

## 1 Introduction

In the Nordhavn port in Copenhagen, a 1.4 km cut-and cover tunnel is being prepared, 700 m of which will be submerged. To preserve a 40 m free maritime zone during construction in the channel of 100 m, the excavation is carried out using a cofferdam. Following the construction of the 1<sup>st</sup> tunnel segment, the sheet pile wall of the cofferdam is anchored to it, the excavation is filled and the construction site is mirrored across this sheet pile wall, enabling the construction on the other side and switch the maritime traffic. The design of the anchorage system of the sheet pile wall to the tunnel, is central to maintain the structural integrity and waterproofing of the design and hence, will be the subject of the present paper.

## 2 Methodology

### 2.1 Connection concept

The anchorage system is illustrated in the figure 2 and is envisaged as two welded steel plates on the sheet pile wall, to which the tunnel's reinforcement is welded. The design involves the dimensioning of the following elements: the welds, the steel plates and the reinforcement of the tunnel. These elements will be dimensioned to effectively transfer the forces from the soil-and water-retaining sheet pile wall to the tunnel.

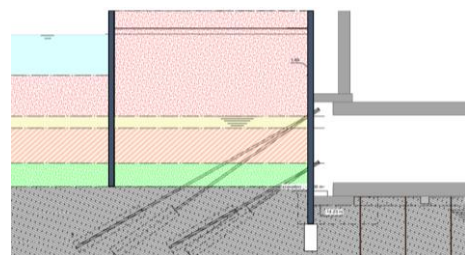


Figure 1 section through the cofferdam and tunnel

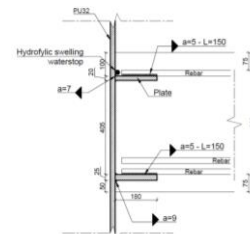


Figure 2 connection detail between sheet pile wall (PU32) and the tunnel's reinforcement

### 2.2 Determination of forces in tunnel

To determine the forces, a distinction is made between the forces that are directly introduced through the sheet pile wall (interface forces) and, on the other hand, external forces due to accidental collision loads, upward water pressures on the tunnel and additional bending moments caused by differential settlements between the sheet pile wall and the tunnel. The current paper only focusses on the former loads.

The interface forces are calculated with Plaxis2D, which is a finite element software specialized in the

geotechnical field. The employed hardening Soil model allows to model the soil with a stress-dependent stiffness. The model covers a detailed modelling of the cofferdam throughout the construction stages. To realistically capture the interface forces, the tunnel slab is modelled with an equivalent translational and rotational stiffness determined in SCIA Engineering. In this regard, the interface forces are directly proportional to the stiffness of the anchorage.

### 2.3 Design of reinforcement

The reinforcement, based on the forces determined in section 2.2, is designed in accordance with [1][2]. Hereby, only the reinforcement due to the interface forces is welded to the steel plate and the reinforcement due to the external forces will not be welded as the welds are only subjected to the forces transmitted from sheet pile to tunnel.

### 2.4 Design of welds between sheet pile and plate

The weld is designed to transmit forces from the sheet pile wall to the tunnel's reinforcement. To prevent brittle fracture upon failure, the weld is dimensioned to the ultimate tensile strength ( $f_u$ ) of the reinforcement, so the reinforcement will yield first. Therefore the weld depends on the amount of reinforcement bars are welded to the steel plates.

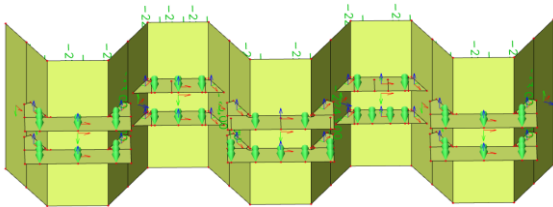


Figure 3 FEM model of sheet pile wall and steel plates subjected to the tensile forces from the reinforcement

The sheet pile wall with the steel plates is modelled in a FEM software (SCIA Engineer), on which point loads are applied in the layout of the reinforcement. These point loads are equal to the ultimate tensile strength of each rebar. The stresses  $\sigma_y$  en  $\tau_{xy}$  are then determined with a plastic calculation, so that when the steel stress exceeds the yield strength, the steel will redistribute the stresses, reflecting a realistic behaviour. The model reveals that the welds are subjected to concentrated stresses in the corners. To stay on the conservative side, the welds are designed to the corner stresses over the full length in accordance with [3].

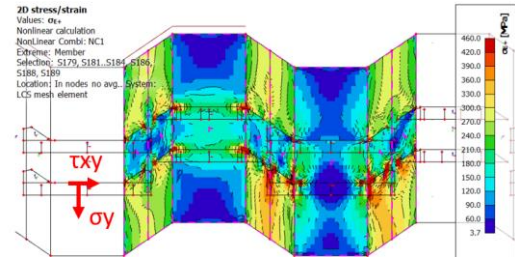


Figure 4 stresses sheet pile wall

## 3 Results

Table 1 shows the governing interface forces for top and base anchoring slab. This results in a respective tunnel under reinforcement of respectively  $\varnothing 25$ -133 en  $\varnothing 25$ -200, for top en base slab (excluding reinforcement due to external forces).

Table 1. Interface forces calculated in Plaxis

Anchorage	Q [kN/m]	M [kNm/m]
Top	215	-370
Base	1605	70

With a steel grade of  $f_u = 594$  MPa, this corresponds to an ultimate tensile strength of 292 kN per rebar at which the weld between sheet pile wall and steel plate is dimensioned. In this layout, there is a maximum of 5 rebars per steel plate. This corresponds to a weld of  $a = 9$  mm.

## 4 Discussion

This construction method guarantees maritime traffic during construction. Nevertheless, this construction is very complex with the required attention points both in design, as proved above, and execution. In particular the custom steel welding work and the dependence on proper execution.

## References

- [1] DS/EN 1992-1-1:2004/A1:2015: Eurocode 2: Design of concrete structures – Part 1-1: General rules and rules for buildings
- [2] DS/EN 1992-1-1 DK NA:2021: National Annex to Design of concrete structures – Part 1-1: General rules and rules for buildings
- [3] DS/EN 1993-1-9:AC:2009: Eurocode 3: Design of steel structures – Part 1-8: Design of joint

# Pile group effect: calculation and impact on design of high-rise buildings

**Niko Verschaeve**

BESIX Engineering Department, BESIX Group, Brussels, Belgium

Contact: [niko.verschaeve@besix.com](mailto:niko.verschaeve@besix.com)

## Abstract

A very common type of foundation used for high-rise buildings is the pile foundation. In the design of such a foundation not only the load bearing capacity is of importance but also the settlement that can be expected. The settlement not only has impact on the internal forces of the structure but also on the surroundings that are located in the influence zone of the settlement trough. Hence, a proper estimation of the settlement is crucial for the design of (high-rise) buildings. When the piles are installed in a dense grid (i.e. when the centre-to-centre distance between the piles is less than ten times the pile diameter [1]) not only the settlement of the individual piles needs to be considered but also the settlement due to compression of the soil layers below the pile tip level. This is the so-called pile group effect for which different calculation approaches are available. This paper discusses and compares different simple calculation approaches followed by a case study.

**Keywords:** High-rise buildings, pile settlement, pile group effect, building damage assessment

## 1 Introduction

The group settlement of pile foundations is defined as the compression of the soil layers below pile tip level and plays an important role in the design of high-rise buildings. While many different methods are available to estimate the settlement, this paper focuses on the equivalent raft method, which can be used as a simple estimation tool. Paragraph 2 discusses the settlement calculations and two different approaches to model the equivalent raft. In paragraph 3 a case study is performed where the results of the equivalent raft method are compared with the results of a 3D Plaxis model in which the piles have been modelled as embedded beam elements. The impact of the pile group effect on the structure of high-rise buildings is also discussed. In paragraph 4 the impact of the settlements on the surroundings is discussed by means of a building damage assessment methodology. Finally some conclusions are given in paragraph 5.

## 2 Calculation approaches to determine group settlement $s_2$

The group settlement can be calculated with the so-called equivalent raft method. This method is based on Terzaghi's formula:

$$s = \frac{1}{C} \cdot H_0 \cdot \ln \left( \frac{\sigma'_v + \Delta\sigma'_z}{\sigma'_v} \right) \quad (1)$$

3D load redistribution is considered, the vertical stress increase  $\Delta\sigma'_z$  is determined for rectangular loading according to Boussinesq. Settlements are calculated until the depth where the stress increase due to vertical loading is less than 20% of the effective soil stress. In the following paragraphs two different approaches are discussed to model the equivalent raft (Figure 1).

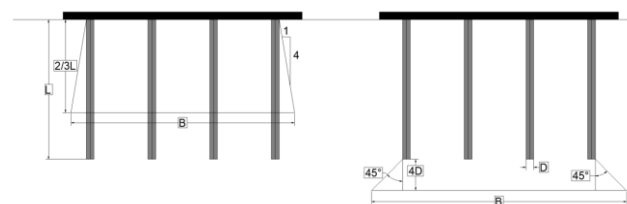


Figure 1. Equivalent raft: Approach at 2/3 of pile length (left) [2] and according to NEN 9997 (right) [1]

### 2.1 Approach with equivalent raft at 2/3 of pile length [2]

In the first approach the pile group effect is estimated by modeling an equivalent raft as shown left in Figure 1. The settlements are calculated for the redistributed load on the equivalent raft starting at a level of 2/3 of the pile length .

### 2.2 Methodology of NEN 9997 [1]

In §7.6.4.2 (k) of the Dutch Eurocode NEN 9997 [1] it is mentioned that the pile group effect should be



determined by calculating the group settlement  $s_2$  in the layers below pile tip level –  $4D$  (with  $D$  the diameter of the piles). The load is redistributed as illustrated on the right in Figure 1.

### 3 Case study

A high-rise building with a height of 100 m is considered for this case study. In the calculations a total SLS load of 1015 MN is considered distributed over a surface of 90 m by 25 m. The piles are considered to have a diameter of 60 cm. The pile tip level is located 23 m below the level of the foundation slab. Below the piles a dense sand layer is assumed with an average cone resistance  $q_c$  of 20 MPa.

#### 3.1 Calculation results

Table 1. Calculation results

	Approach §2.1	Approach §2.2
Settlement at centre	98 mm	108 mm
Settlement at edge	41 mm	46 mm

When the results of both approaches are compared to the results of the first iteration in Plaxis (grey curve in Figure 2) similar results are found for the settlement at the centre. In the first Plaxis iteration the settlement was 115 mm at the centre and 67 mm at the edge. The differential settlement is thus  $115 - 67 = 48$  mm, which is less than calculated with the approaches discussed in §2.1 and §2.2.

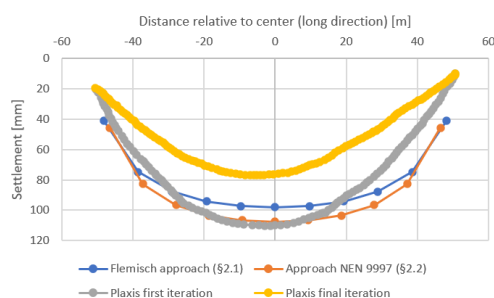


Figure 2. Comparison of results with Plaxis

#### 3.2 Impact of pile group effect on the structure of high rise buildings

Figure 2 shows the importance of soil-structure interaction. Iteration between the geotechnical and structural model was required until the displacements between both models were similar. This resulted in reduced settlements of 75 mm and 47 mm, respectively at the centre and the edge of the slab (yellow vs. grey graph in Figure 2). A more uniform

settlement results in a decrease in forces in the columns and walls of the superstructure. Both the soil and the structure (e.g. the raft thickness) have an impact on the settlement.

### 4 Building damage assessment – CIRIA C760 [3]

The surroundings will also be influenced by the settlement trough due to pile group effect. It is important to determine expected settlements, strains and (greenfield) displacements in the adjoining structures and to discuss allowable limits with the stakeholders. Building damage assessment can be performed according to chapter 6.4 of CIRIA C760 [3] which defines several damage categories, varying from negligible to very severe damage. With the charts of Burland (Figure 3) and the predicted deflection ratio  $\Delta/L$  and horizontal strain the accompanying damage category can be determined.

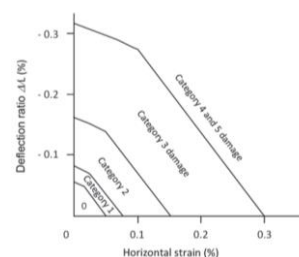


Figure 3. Chart of Burland to define damage category for hogging for  $(L/H) = 1,0$  [3]

### 5 Conclusions

In this paper the results of two simple approaches to determine the settlement caused by pile group effect are compared with Plaxis calculations. For the case study these simple methods give a reasonable estimation (compared to the first iteration) of the settlements at the centre of the slab. The differential settlement between centre and edge was overestimated. The impact of the pile group effect on (high-rise) buildings is briefly discussed, as well as a proposition on how to deal with possible damage in nearby structures caused by these settlements.

### References

- [1] Normcommissie 351 006 “Geotechniek”. NEN 9997-1+C2 Geotechnisch ontwerp van constructies – Deel 1: Algemene regels. 2017.
- [2] Ontwerphandboek Geotechniek – Annexen ontwerp. 16-11-2007. Page C.05.01.00-15/60
- [3] CIRIA. Guidance on embedded retaining wall design. London; 2017

## Piling disease in Amazonehaven

Reza Nejad

Department of Civil Engineering, Delft University of Technology, The Netherlands,

Contact: [r.nejad@iv-infra.nl](mailto:r.nejad@iv-infra.nl)

### Abstract

The removal of Amazonehaven's 'relieving platform quay wall' from 2011 to 2013 revealed a well-known failure in the piling industry. A percentage of 20% of the open-ended tubular piles (primary elements) were severely damaged due to extreme folding close to the pile toe. A 'pile toe failure' to such extent if not limited might lead to dysfunction of the asset during its technical lifetime. To ensure the safety and stability of the quay wall (when operating) counteractions must be taken. These counteractions are either reactive or proactive. The reactive remedies are replacement, early maintenance or a storage capacity reduction. These reactive remedies will bring financial consequences forward. On the other hand, implementing the proactive process-based remedies in the current procedure in the piling industry reduces the probability of the risk event.

**Keywords:** Pile toe failure, open-ended tubular piles, pre-piling, post-piling, relieving platform quay wall,

### 1 Introduction

The Amazonehaven quay wall structure was a so-called 'relieving platform quay wall'. Figure 1 depicts this structure.

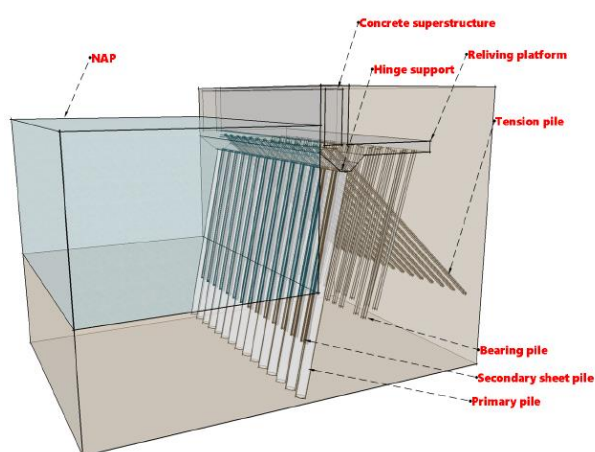


Figure 1. Relieving platform quay wall structure

The main elements in a relieving platform are the open-ended piles and anchors which transfer the load to the subsoil. The combined wall system is consisting of (inclined) open-ended piles and sheet piles in between. The bearing (concrete) piles and the tension (Müller Verfahren) piles are also elements in this system. This type of structure is frequently used in the Netherlands. The advantage of this type of structure is a reduction of forces on the retaining wall, open-ended piles, and the occurring tensile forces.

### 2 Background

After the removal of the Amazonehaven due to new safety regulations [1], it was evident that 20% of the open-ended piles were extremely damaged (a total of 313 piles). The damaged piles were distributed in 20 sections with a length of 45 m. Figure 2 depicts the pile toe failure after the removal.



Figure 2. Pile toe failure Amazonehaven [2]

The open-ended piles were driven into their location with an inclination of 5:1. The piles (1,42 m in diameter, wall thickness of 15 mm and a length of 32,0 m, steel quality X70) were driven first by a Diesel hammer D62 and afterwards a Diesel hammer D100. The usage of D62 resulted in approximately 400 per 25 cm and a driving time of nearly 8 hours. However, when a D100 was used the (number of) blows reduced to 120 strikes per 25 cm and a decrease of driving time to 2 hours [3].



## 2.1 Research

The risk of pile toe failure in the piling industry could be reduced by tackling both the probability and the consequences of the risk event. The consequences of the risk in terms of settlements and instability of the asset appear when the quay is fully operational. However, the probability of the event occurrence could be influenced in the early stages of design and construction.

## 2.2 Pre-piling measures

To reduce the probability of the risk event, process-based alternatives must be undertaken. These are procedures to be taken before to piling as well as during piling activity.

### 2.2.1 Data collection

To reduce the probability of pile toe failure occurrence: (a) carry out sufficient soil investigation, (b) use a piling prediction program together with (c) measurements during piling to carry out a back-analysis and (d) select a correct hammer to bring the piles to its designed toe level.

### 2.2.2 Pre-installation

To reduce the probability of pile toe failure occurrence: (a) use a Just In Time (delivery) system for the piles, (b) protect the pile toe by using an Azobé cover during storage, transport and uplifting (before installation) of the piles. A JIT system is to prevent unnecessary piling up of the piles for a long amount of time in the storage [4].

### 2.2.3 Installation

To reduce the probability of the pile toe failure occurrence: (a) use stiffening rings at pile toe (to protect), (b) in situ checks for out-of-roundness of the pile toe, (c) monitoring system and (d) using a driving procedure.

## 2.3 Post-piling measures

To reduce the consequences of pile toe failure occurrence: (a) carry out replacement of the problematic sections, (b) proceed an early maintenance for the problematic sections (c) implement a capacity reduction of the quay wall. Based on a net present value a decision model is settled to select the most economical remedy for Amazonehaven [5]. In this case, a storage capacity reduction had been economically more attractive to minimize the loss of earnings for the port authority of Rotterdam.

## 2.4 Discussion

In this paper, the probability and consequences of a piling risk event are discussed. The pile toe failure of Amazonehaven is showcased. The post-piling measures are more of a financial burden than the pre-piling measures [6].

## 3 Conclusions

The pile toe failure is a well-known risk event in the piling industry. The counteractions to reduce the risk event of pile toe failure are divided into pre-piling and post-piling measures. The post-piling measures are (1) replacement, (2) early maintenance or (3) capacity reduction. These are financial burdens for the asset manager. However, the pre-piling measures are less expensive. The pre-piling measures are in (a) data collection, (b) pre-installation and (c) (during) installation.

## References

- [1] Broos E.J. and de Gijt, J.G., The demolishing of the EMO quay wall in the Amazonehaven, port of Rotterdam, 2014.
- [2] Mourillon N.K.N., Stability analysis quay structure at the Amazonehaven port of Rotterdam, 2015.
- [3] van Schaik C.N., Ontwerpboek Amazonehaven, Rotterdam: gemeente werken Rotterdam, 1989.
- [4] Davies A., Gann D. and Douglas T., Innovation in megaprojects: systems integration at London Heathrow Terminal 5, 2009.
- [5] de Gijt J.G., A history of quay walls: techniques, costs, types and future, 2010.
- [6] Nejad R., Research into pile toe failure in Amazonehaven, 2017.



## Automation in diaphragm wall design of project Oosterweel Junction

Heng Fang, Bart Rombauts, Benjamin Tytgat

Sweco Belgium, Antwerp, Belgium

Contact: heng.fang@swecobelgium.be

### Abstract

The project Oosterweel Junction (Oosterweelknoop) belongs to a series of large projects that aim at completing the R1 Antwerp Ring Road. Two new tunnels, under the Scheldt and the Albert Canal respectively, will be connected through the junction and close the ring along the north side. To accommodate the elevation of the tunnels, sunken roads are eventually adopted for the junction. Due to the size and complexity of the project, contractors and designers have to work together closely to control the execution cost. However, accompanying the increasing number of stakeholders joining the design procedure, more design iterations are needed. To accelerate the design procedure, a series of automation tools were developed using Python and Excel VBA while performing design tasks of diaphragm wall. In practice, the developed tools are proven to be efficient for engineers without requiring relevant programming skills.

**Keywords:** Diaphragm wall; Ground anchor; Plaxis; Excel VBA; Python; Automation; Structural design.

### 1 Introduction

The first proposal of a construction project intended to complete the ring road in Antwerp, Belgium can be traced back to 1996. The Flemish Government wishes to improve access to the city of Antwerp and to the port meanwhile to relieve traffic congestion which is not unfamiliar when passing through Kennedy tunnel during workdays. After a long time of feasibility investigation and discussion, the current route composed of two new tunnels was eventually approved in 2010 [1]. Overview of the project is shown in Figure 1.

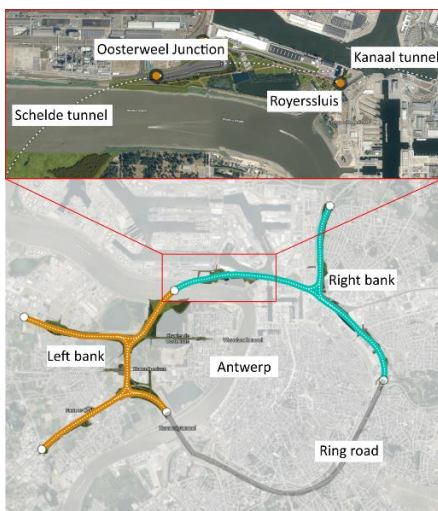


Figure 1. Overview of project Oosterweel Junction

The estimated cost of the project Oosterweel Junction is between 500 to 700 million euro. About 3500 m diaphragm walls, 4200 ground anchors and 300000 m<sup>3</sup> concrete (including the tunnel part) will be used. The design of the project is divided into different cross-sections. One example cross-section is presented in Figure 2.

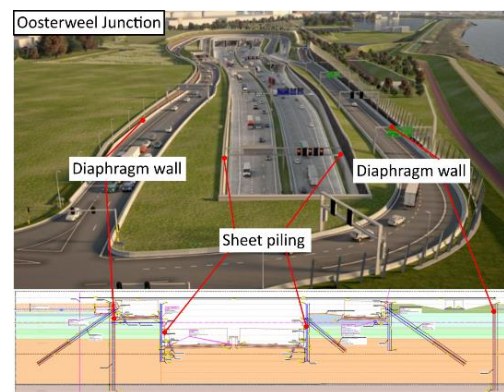


Figure 2. Illustration of design cross-section

Due to the size and complexity of the project, contractors also participate in the design procedure by providing information about execution phases and methods, etc. More stakeholders inevitably increase the number of design iterations. Therefore, accelerating the design procedure with the help of customized automation tools is important as well as necessary.

## 2 Automation in design procedure

In Figure 3, the flow chart of the design procedure gives an overview about how data is transferred between different software. As shown in the figure, the geotechnical calculation for the diaphragm wall design is performed in Plaxis. The input data are mainly stored in the formats that are easy for editing and being exchanged with other parties outside the design procedure.

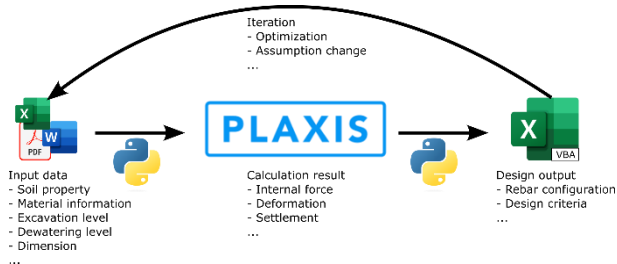


Figure 3. Flowchart of design procedure

Importing soil properties and other prerequisites to Plaxis used to be very time-consuming. In this project, the number of considered soil-layers is about 15. For each layer, the number of soil properties needed for calculation is roughly 30. Through using customized Python scripts, Plaxis is able to read data from excel files and generate the layers automatically. The preprocessing time can be reduced from hours to a couple of minutes meanwhile the possibility of input error is greatly reduced. Furthermore, the structure components can also be generated automatically by reading relevant information from an Excel file or files in other data interchange format such as JSON. This enables the ability of parametric modeling. The parametric modeling method makes changes of the model easily deployed and traceable, which is preferred when a high number of design iterations are needed.

After calculations are finished, investigating and exporting the calculation results can also be time-consuming. The execution time of the project will spread over years, which are composed of complex excavation, dewatering and construction phases. Therefore, the number of phases in modeling can easily exceed 50. Automating the postprocessing procedure by using customized Python scripts makes it possible for engineers to save a large amount of time. Compared with the original report generate function integrated in Plaxis, exporting and labeling the calculation results, e.g. from service limit state (SLS) or ultimate limit state (ULS), can be finished simultaneously with the customized scripts. The well-structured data makes it easy to further develop

corresponding spread sheets for design purpose and data visualization.

In this project, the final design of diaphragm walls is performed by spread sheets programmed in Excel VBA, as shown in Figure 4. Simply importing the generated result files, the rebar calculation can be performed within 10 minutes. Automatically generated results such as rebar usage, rebar configuration, resisting capacity, crack width calculation, etc. can easily be exchanged with other teams. More importantly, the influence of the construction procedure is also taken into account, which makes the design output more reliable and economical.

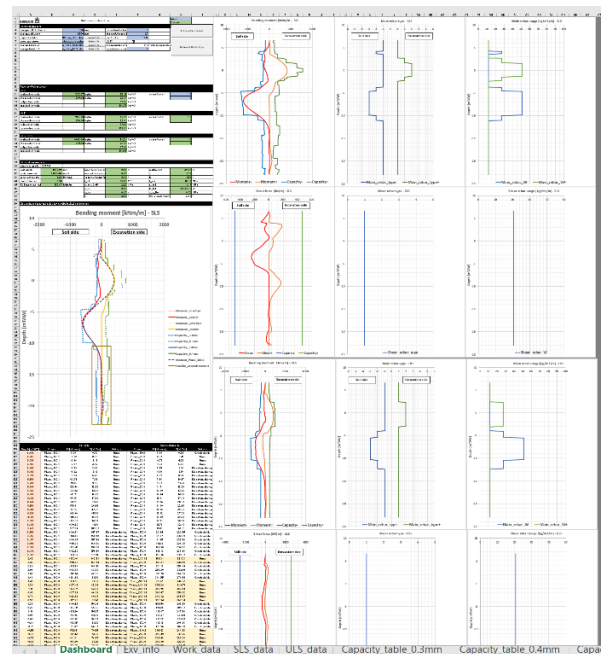


Figure 4. Developed spread sheet for diaphragm wall design

## 3 Conclusions

This paper gives a brief introduction about the automation attempts developed when performing diaphragm wall design for project Oosterweel Junction. For large and complex projects, proper automation tools are able to accelerate design procedure and increase productivity. Engineers with limited or no previous programming experience can also benefit from the developed tools with proper instruction.

## References

- [1] Project website Oosterweelberbinding, <https://www.oosterweelverbinding.be/> (accessed on 29/09/2023)

# Structural design and analysis of Tour Triangle

**Maarten Van Craenenbroeck**

BESIX SA/NV, Brussels, Belgium, BE

Contact: [maarten.vancraenenbroeck@besix.com](mailto:maarten.vancraenenbroeck@besix.com)

## Abstract

The design and structural analysis of the 180 m high high-rise building Tour Triangle, currently under construction in Paris, poses a number of specific engineering challenges. The asymmetric geometry and inclined façades in particular impact the long-term global deformations and introduce the requirement for a staged analysis model for the design of the principal load-bearing elements. The presented work explores the project-specific engineering challenges as well as the utilised design and analysis process.

**Keywords:** high-rise buildings, FEM, structural analysis, long-term deformations, concrete design

## 1 Introduction

After the construction of the Tour Montparnasse in 1973, the city council of Paris imposed a height limit of 37 m for new constructions, to preserve the city skyline. With this height limit revoked in 2010, the construction of high rise buildings within the Paris city centre became once again possible.



Figure 1 – Concept render of Tour Triangle showing the defining triangular geometry. [1]

The 180 m high Tour Triangle high-rise building, designed by the Suisse architecture firm Herzog & De Meuron, aims to fill in the need of office spaces within the city limits. Upon completion, the tower will provide a net floor area of 95 245 m<sup>2</sup> which will house, amongst

others, 71 100 m<sup>2</sup> of office spaces as well as 120 hotel rooms (8089 m<sup>2</sup>).

## 2 Design and analysis

As the project is structured as a turnkey project, the structural design is carried out entirely by the BESIX Engineering Department. Aside from project-specific engineering challenges, the scale of Tour Triangle presents a large quantity of structural elements to be calculated and documents to be produced: 3400 beams, 1900 columns, 2600 structural drawings, and >100 calculation notes.

### 2.1 Structural model and analysis

The structural analysis of the tower is carried out in SCIA Engineer FEM software, and IDEA Statica for the concrete and reinforcement design of the beams and columns.

The tower is constructed as a skeleton system with a central core: outside the core area, vertical loads are transferred through the beam-column system while the core walls ensure horizontal rigidity.

The SCIA model contains the complete structure and utilises a staged construction model containing 42 stages.

### 2.2 Project-specific challenges

#### 2.2.1 Transfer beams

In various locations of the project's lower levels, we find large transfer beams (>10 for this project). These beams which, due to their nature, often have a high depth-to-span ratio, require detailed analysis. In this project strut-and-tie models are used to design these beams



and ensure the required reinforcement does not interfere with, for instance, openings that are required in the beams.

### 2.2.2 Building asymmetry

Whereas typically floor plans of core-stabilised towers are designed to be symmetrical around the core to avoid eccentric loads, Tour Triangle has been designed as an asymmetric structure: not only are three of the four façades inclined (the west façade is the only vertical one throughout the full height of the tower), but each superstructure floor is also distinctly asymmetrical around the core wall.

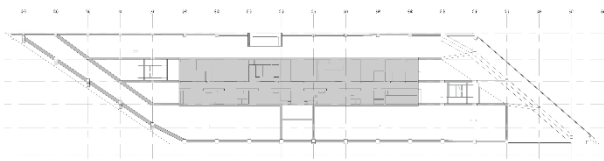


Figure 2 – Typical asymmetric floor plan.

This asymmetry directly impacts the global deformation of the tower under gravity loads: in addition to the initial vertical settlements, a significant rotational deformation around its vertical axis is noted as well as a 60 mm horizontal deformation towards the west.

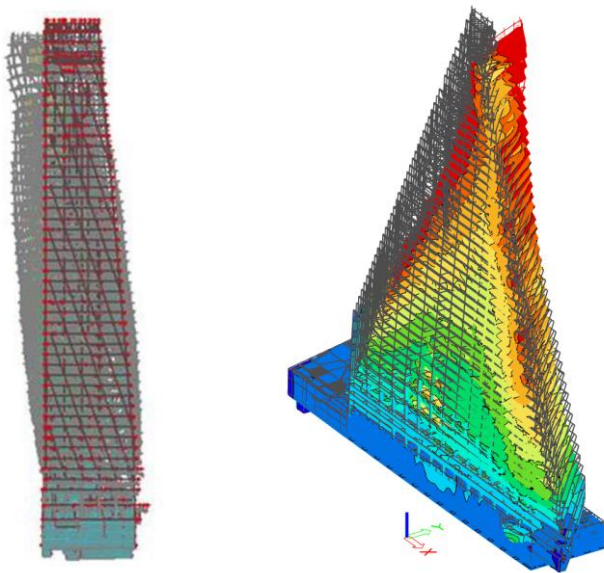


Figure 3 – Due to its asymmetry, the tower shows significant horizontal and rotational deformations.

### 2.2.3 Inclined façades

With the areas outside the core wall designed as a skeleton system, the asymmetric shape of the tower and the inclination of the north, east, and south façade directly impacts the design of the columns. Due to the global deformation of the tower, various columns will -

depending on the construction phase and load combination- experience traction.

Additionally, at different floors, the inclination of specific columns changes which introduces a considerable amount of traction in the concrete slabs. This traction, which exceeds 10 000 kN ULS on certain floors, requires the addition of designated traction rods in the floor slabs (up to 8 rods with a diameter of 63 mm).

### 2.2.4 Global deformations and long-term effects

As mentioned above, the tower presents significant deformations under self weight and permanent loads (presetting). This presetting is determined by four aspects :

- Elastic deformation of the concrete
- Settlement of the foundations
- Shrinkage of the concrete
- Creep of the columns and walls

Due to the triangular shape of the tower, and the long-term nature of these deformations, the vertical deformation is function of the floor level where the largest deformation (67 mm) is not located at the top floor, but rather at R+26.

To offset (part of) the vertical presetting, a floor-by-floor level compensation is introduced where the theoretical level for a specific floor is increased with a value between 20mm and 60mm during concrete pouring. During execution the presetting deformations are continuously monitored to allow correction during execution, if necessary.

## 3 Conclusions

This paper presents the overall design approach of the Tour Triangle high-rise project in Paris, as well as a number of project-specific challenges.

Due to its asymmetric geometry, the resulting eccentric loads, and the large presetting, some specific approaches need to be taken during the structural design and execution of the project.

## References

- [1] Triangle, La ville créative. <https://www.tour-triangle.com> (22/10/2023)

# Structural Assessment of Historical Verbundträger Bridge Decks

**Berber Renckens, Ane de Boer**

*Municipality of Amsterdam, Amsterdam, The Netherlands*

Contact: [b.renckens@amsterdam.nl](mailto:b.renckens@amsterdam.nl)

## Abstract

This study investigates the structural behaviour of historical steel-concrete bridges in Amsterdam, termed ‘Verbundträger bridges’, which fail to meet current NEN-EN 1994 detailing requirements due to the absence of a proper steel-concrete coupling method. The research combines in-situ experiments, laboratory tests, and numerical simulations to assess the structural behaviour. Results confirm significant transverse load distribution and validate a conservative numerical model for assessing structural safety of existing historical steel-concrete bridge decks.

**Keywords:** Amsterdam, Bridge decks, Concrete testing, Experimental testing, Finite Element Method, Historical bridges, NL-FEM, Steel-concrete composite, Steel-concrete composite bridges

## 1 Introduction

Historical steel-concrete ‘Verbundträger bridges’ in Amsterdam, do not comply with the current detailing requirements of NEN-EN 1994 [1]. An estimated 30 of these bridges were designed without any mechanical connectors, they consist only of shrinkage reinforcement in both directions on the top layer of concrete. As a result, the effectiveness of the composite cross-section cannot be verified with the aforementioned design rules. A visual representation of a Verbundträger bridge deck cross-section is provided in Figure 1.

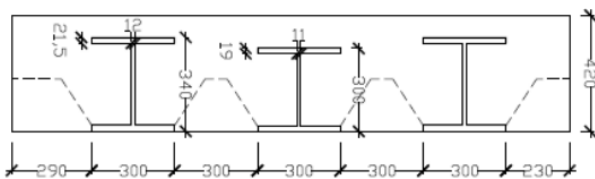


Figure 1. Partial cross-section of a Verbundträger bridge (Bridge 70)

The current assessment method employed by the Municipality of Amsterdam relies on a (presumed) conservative assumption regarding the load distribution in the transverse direction, as the extent of the transverse load distribution has not been conclusively demonstrated.

Inspection of these bridges reveals minimal damage from traffic loads, including possible overloading. To prevent unnecessary disapproval,

there is an urgent need for a generally applicable and practical method to verify the ultimate limit state of Verbundträger bridges in Amsterdam.

## 2 Methodology

### 2.1 In-situ and laboratory research

To assess the behaviour of Verbundträger bridges, in-situ research was performed on Bridge 70. This involved subjecting a sawed-out section, comprising six girders, to a series of load cycles with varying wheel positions and magnitudes.

Consequently, laboratory research was conducted on three specimens sourced from the same bridge. Each specimen, consisting of three girders, underwent a four-point bending test to replicate a Eurocode two-axle vehicle load configuration [2]. Through the utilization of load measurements, displacement tracking, strain monitoring, and deformation analysis, these experiments aimed to comprehend the bearing capacity and structural response of Verbundträger bridge decks.

### 2.2 Numerical model

The experiments are numerically simulated to validate a finite element model, including both 3D solid and 2.5D shell models.

### 3 Results

The in-situ experiment analysis reveals a significant transverse load distribution. Figure 2 illustrates the normalized vertical displacements of the six girders for five in-situ experiments, with a wheel load positioned between girder 3 and 4.

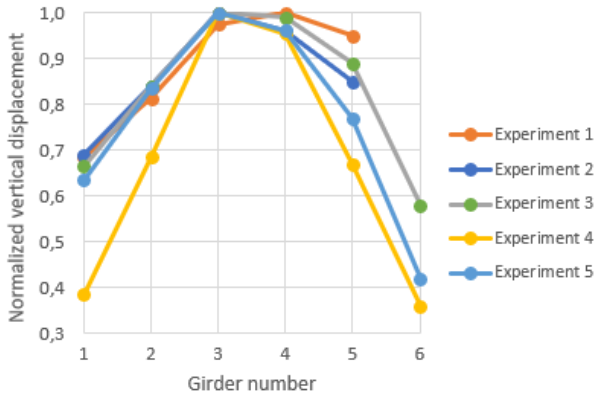


Figure 2. Normalized vertical displacements of six girders under a wheel print load of 475 kN

Numerical simulations employed a physically non-linear 3D solid model with quadratic elements for concrete and steel, incorporating compatible plane-interface elements. The test specimens were loaded to the setup's maximum capacity of 1400 kN. The results, presented in Table 2, reveal a strong alignment between these simulations ( $F_{FEM-3D}$ ) and the laboratory tests ( $F_{Exp}$ ), indicating a conservative approach.

Table 2. Maximum load obtained in experiments ( $F_{Exp}$ ) and with numerical model ( $F_{FEM}$ )

	Exp. 1 [kN]	Exp. 2 [kN]	Exp. 3 [kN]
$F_{Exp}$	1843	1746	1400
$F_{FEM-3D}$	1828	1680	1330
$F_{FEM-2D-600mm}$	N/A	1410	1190
$F_{FEM-2D-300mm}$	N/A	1410	1190

Given the prevalence of 2.5D computational models in engineering practice, the model was adapted to a non-linear elastic 2.5D beam grid model with elastoplastic concrete behaviour. The grid spacing was tailored to match observed crack patterns in the relatively weak concrete, dating back to 1920. Crack patterns typically occurred at a centre-to-centre distance of 0.6 meters. Results for grid spacings of 600- and 300-millimetres, denoted

as  $F_{FEM-2D-600mm}$  and  $F_{FEM-2D-300mm}$  in Table 2, consistently yield conservative outcomes.

### 4 Discussion

Further research into steel-concrete bridges with partial mechanical connections is advisable.

### 5 Conclusions

This study successfully established an assessment methodology for Amsterdam's historical steel-concrete 'Verbundträger bridges', which lack mechanical connections and do not conform to current NEN-EN 1994 detailing requirements. The methodology adopted a holistic approach, integrating in-situ experiments, laboratory tests, and numerical simulations. This comprehensive strategy validated the presence of significant transverse load distribution in the bridge decks.

The ultimate limit state analysis, conducted using a 3D model, yielded conservative results compared to the experimental data, with even greater conservatism observed in the 2.5D beam grid model. This shows that the developed numerical model provides a reliable method for assessing Amsterdam's historical Verbundträger bridges.

### References

- [1] NEN-EN 1994-1-1:2005. *Eurocode 4: Design of composite steel and concrete structures - Part 1-1: General rules and rules for buildings.*
- [2] Jørgensen, A., Poliotti, M., & Yang, Y. *Experiment report on steel-concrete-composite bridge deck without mechanical connectors (Verbundträger).* TU Delft; 2022.

# Construction of the new Verbindingsbrug in Zeebrugge

**Steffie Rooms**

SBE nv, Sint-Niklaas, Belgium

Contact: [steffie.rooms@sbe.be](mailto:steffie.rooms@sbe.be)

## Abstract

This paper discusses the design of the new Verbindingsbrug in Zeebrugge. This new bridge must be suitable for heavy port traffic and manoeuvrable under high wind loads. It consists of two concrete bridges and one swing bridge which is also the largest movable steel bridge of Europe. During the design and the execution many challenges came up like the geometrical and functional requirements, the interaction of all structures, working on water and a tight deadline. Proper communication between all parties and an extensive BIM model were key elements to the successful completion of the project

**Keywords:** Prestressed I-girders, flexible plate joint, movable steel bridge, prefabrication, BIM model.

## 1 Introduction

In 2019, Port of Antwerp-Bruges commissioned by a Design and Build contract a new bridge over the Verbindingsdok which had to replace the temporary one and should be suitable for heavy port traffic and manoeuvrable under high wind loads.

The Verbindingsbrug has a total length of 400 m and consists of two concrete bridges with a length of 170 m and 100 m and a movable part of 130 m, which is the largest movable steel swing bridge in Europe. The width varies from 17 to 25 m. In the project also the building of a new quay wall of 100 m, a composite bicycle bridge and a guiding structure is included.



Figure 1. Overview project

The project was assigned to the contractors Artes Depret, Victor Buyck and Besix Unitec at the end of 2019. SBE was responsible for the studies of the general design and concept of all bridges, the BIM coordination, environmental permit and studies of all hydraulic and civil structures. Stendess did the detailed calculations for the steel structure of the movable bridge.

Construction works started in October 2020 and finished in April 2022.

## 2 Geometry

### 2.1 Concrete bridges

The concrete bridges exist out of 11 fields with a maximum span of 33 m. Every field has 6 prestressed I-girders with a maximum height of 1,9 m and a bridge deck on top with a thickness of 25 cm. The I-girders are supported on a beam on top of steel tubular piles.



Figure 2. Concrete bridges during construction

All fields are connected with a flexible plate joint as there could only be joints at the abutments and in contact with the movable part. This type of joint allows the transfer of horizontal loads through the top plate but all fields will still act isostatic vertically.

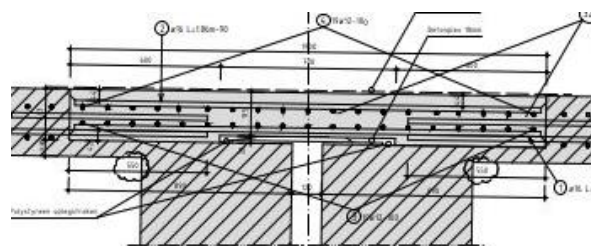


Figure 3. Flexible plate joint

## 2.2 Movable steel bridge

The swing bridge has a total weight of 1800 t and consists of two massive steel beams with secondary beams and an orthotropic deck. The main beams have a height varying from 3,3 to 4,3 m with bottom flanges of 1,5 m wide and varying thickness between 50 and 150 mm.



Figure 4. Construction of steel swing bridge

The middle island is the main foundation of the steel bridge and exists out of a concrete plate with dimensions 15 m x 15 m x 1,50 m which rests on top of 8 steel tubular piles with a diameter of 2 m. Due to the limited height and large reaction forces of the swing bridge the concrete plate is heavily reinforced.

## 3 Challenges in the design

### 3.1 Geometrical and functional challenges

The construction height was limited due to geometrical limitations, e.g.: the water level, the longitudinal slope of the road and the ground level. All control and command rooms also needed to be watertight and at a safe level above water.

The requirements of a passage clearance of 55 m, combined with unlimited free height, led to the design of the swing bridge. Also this type of bridge doesn't require an expensive and time-consuming basement below water level and can be manoeuvred even by strong storm winds.

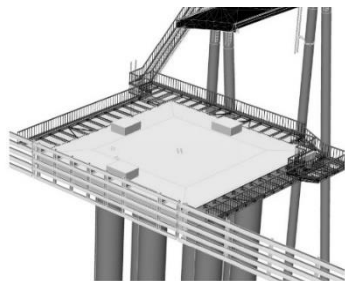


Figure 5. BIM model of middle island

Inspection and maintenance needed to be possible without the use of vessels and during maintenance always one lane must be available for traffic. An extra platform is created at the middle island which is accessible at all times via the extended bicycle bridge and a stair which acts also as cable ladder.

During the project an extensive BIM model with all structures, EM and accessories was used to visually check all requirements and to perform clash controls.

### 3.2 Interaction of all structures

A major challenge was to accurately predict the interaction between all models, as the foundation is very flexible with piles which are freestanding at 20m above ground level. This has a large influence on joint movements and forces. This required a good alignment and connection of the models, which was challenging for the design team.

### 3.3 Working above water

As it is more difficult, expensive and time-consuming to work above water than on land, the bridge decks, foundation beams and middle island were therefore partly prefabricated to reduce working time on water.

The bridge decks were split in two halves as the lifting weight was limited to 400 t. The zone in between the two halves was cast in situ with the use of a lost formwork which was already placed on land. The middle island is also partly prefabricated and had a weight of 400 t.



Figure 6. Middle island during construction

The steel bridge was made in Eeklo and dragged to Zeebrugge along the River Scheldt and the Belgian coast using barges. In order to limit the navigation interruption, the placing of the bridge had to be done in only one weekend.

### 3.4 Other challenges

Other challenges were the limited construction time, heavy fatigue loading, minimal functioning time of the swing bridge and a very tight deadline.

## 4 Conclusions

The construction of the Verbindingsbrug in Zeebrugge imposed a lot of challenges as well for the design as for the construction. Proper communication between all parties and an extensive BIM model were key elements to the successful completion of the project

# Structural assessment of masonry arches

**Thomas Harrewijn**

Royal HaskoningDHV, Rotterdam, The Netherlands

Contact: [thomas.harrewijn@rhdhv.com](mailto:thomas.harrewijn@rhdhv.com)

## Abstract

This paper focuses on evaluating the structural integrity of masonry arch bridges in the Netherlands, particularly in historic city centres with canals. Nonlinear finite element analysis using PLAXIS is employed to assess the bridges' ability to withstand motorized traffic, including heavy vehicles. The research demonstrates that many of these historic bridges can still safely accommodate current heavy traffic loads, offering the potential for lifetime extension.

**Keywords:** masonry arch bridge, NLFEA, PLAXIS, structural assessment, residual lifetime, proof-loading

## 1 Introduction

The masonry arch bridge, one of the oldest known types of bridge structures, plays a significant role in the historic cities of the Netherlands. These bridges have evolved from accommodating pedestrians and horses to handling modern motorized traffic, including heavy vehicles. However, many of these structures lack comprehensive data on their geometry, material qualities, design criteria, and design loads. Two municipalities in the Netherlands, 's-Hertogenbosch and Utrecht, have commissioned research to assess the structural safety of these masonry arch bridges.

The existing calculation methods and programs for assessing these bridges often underestimate their true strength, neglecting soil-structure interaction. A unified approach for evaluating the bearing capacity of masonry arch structures is yet to be established in the Netherlands. To address these challenges, research has been conducted, involving the comparison and validation of various software programs. Among these, Plaxis, a finite element analysis program focused on geotechnical structures, was found to be the most suitable.

## 2 Structural assessment

The structural assessment of masonry arch bridges is conducted using Plaxis, a specialized software program with a focus on geotechnical engineering. This assessment employs a physical and geometrical non-linear finite element analysis to model the failure behaviour of the arch structures.

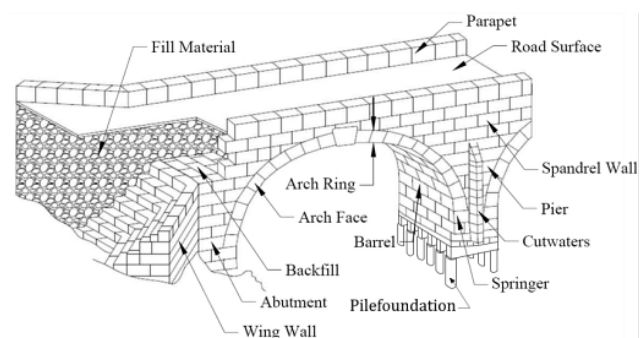


*Fig.1. Terminology of a masonry arch bridge on a wooden pile foundation, by T. Siwowski (2018).*

### 2.1 Geometry and Modelling:

The arches are continuously modelled, including backfill, as a 1.0 m wide strip. A 2D non-linear plane strain Finite Element Analysis (FEA) is utilized. An updated mesh is applied, where the deformed mesh from previous load steps serves as the starting point for subsequent steps.

### 2.2 Masonry Modelling

Masonry is modelled using the Mohr-Coulomb model with specific parameters. Cohesion is set to half the compression strength of the lower limit value. The angle of internal friction is set to zero. The tension cut-off (maximum tensile stress) corresponds to the flexural tensile strength perpendicular to the ribbon joint. The Poisson value is set to 0.2. To prevent overestimation of the failure load in the Ultimate Limit State (ULS), a low tensile strength value of 0.005 N/mm<sup>2</sup> is applied. For the Serviceability Limit State (SLS), the lower limit value from the NPR9998+C1 2020 is used for tensile strength.

An alternative modelling approach is presented using a Concrete model. This approach relies on the tensile strength according to the code without

overestimation of the failure load. However, it's noted that low values for the fracture energy (0.01 kN/m or lower) may lead to numerical instability and longer calculation times.

### 2.3 Soil Modelling

The material properties of the soil are based on available soil surveys or open-source data. A Hardening Soil model is applied when the bridge is founded on sandy soil. The Hardening Soil model provides a more accurate description of soil stiffness than the Mohr-Coulomb model. It considers three different input stiffness parameters:  $E_{50}$ ,  $E_{ur}$ , and  $E_{oed}$ , accounting for stress-dependency of stiffness moduli. Initial soil conditions, including preconsolidation, are considered in the initial stress generation from construction phasing.

## 3 Safety Philosophy

Three methods from the FIB Modelcode are used to examine the non-linear behaviour of masonry. Global Resistance Factor (GRF) Estimation of coefficient of variation of resistance method (ECOV). The limit states indicate impending failure, beyond which a structure ceases to perform its intended function satisfactorily, in terms of either safety or serviceability.

### 3.1 Ultimate Limit State:

The Ultimate Limit State assesses the destructive load of masonry arch bridges. The GRF and PF-methods are applied to the non-linear finite element analysis for safety verification. Various traffic loads are considered, and the bridge is symmetrically and asymmetrically loaded. Multiple plastic hinges occurring in the arch signal failure, and various failure mechanisms are possible.

### 3.2 Serviceability Limit State

In addition to the Ultimate Limit State, the Serviceability Limit State is considered for durable conservation. It aims to assess the risk of cracking of the masonry due to overloading by traffic. The criteria include exceeding the flexural tensile strength of the masonry and deflections. Cracks tend to be perpendicular to the driving direction, and an inspection is recommended when heavy traffic crosses the bridge.

## 4 Results

Failure in the masonry arch becomes evident when multiple plastic hinges form due to the compression strength of the masonry being exceeded. This failure is characterized by the crushing of the masonry material within a small portion of the cross-section. Notably, the Mohr-Coulomb model does not account for the material's crushing. Nevertheless, the approximation of the failing masonry is clearly visible.

Figure 2 illustrates the compression stresses within a masonry bridge subjected to a design tandem load of 600 kN and a distributed mobile load of 9.0 kN/m. The maximum compression stress ( $\sigma_{c,max}$ ) for the Global Resistance Factor (GRF) method is calculated as the characteristic value divided by the partial factor for masonry strength and the required load factor ( $\sigma_{c,max} = 5000 / (2.2 * 1.2) = 2725 \text{ kN/m}^2$ ). This stress leads to the initiation of three plastic hinges at the extrados beneath the applied load and two at the intrados of the arch.

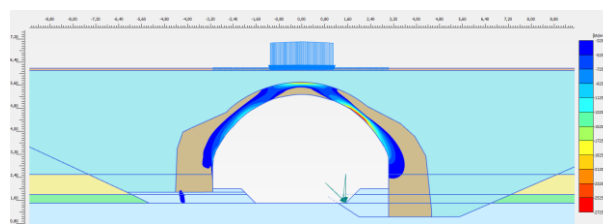


Fig.2. Example of compressive stresses ( $\sigma'1$ ) in an arch due to traffic load.

## 5 Conclusion

This comprehensive approach ensures that the assessment of masonry arch bridges considers multiple factors, including geometry, material properties, soil conditions, and safety considerations, to determine their structural integrity under various load scenarios.

## References

References should be listed in a dedicated section at the end of the paper. They should be listed in the order in which they appear in the paper and provided with a reference number in square brackets [1]. References should be made in the paper using the appropriate reference number in square brackets.

- [1] Siwowski, T., 2018. Bridge Engineering – Selected issues. [https://www.researchgate.net/publication/326132087\\_Bridge\\_Engineering\\_-\\_Selected\\_Issues](https://www.researchgate.net/publication/326132087_Bridge_Engineering_-_Selected_Issues). Accessed 20-02-202



# Risk management on historical quay walls in Amsterdam

**Rick Voortman**

*Gemeente Amsterdam, Amsterdam, Netherlands*

Contact: [r.voortman@amsterdam.nl](mailto:r.voortman@amsterdam.nl)

## Abstract

The city centre of Amsterdam contains a network of 200 kilometres of quay walls of which many are considered potentially unsafe. To gain a better understanding on different typologies of quay walls, inspection and monitoring data are combined to form risk profiles. The profiles are combined to prioritise inspections, renewal, maintenance work on quay walls and improve asset management strategies.

**Keywords:** quay walls; Amsterdam; data-driven; asset management; monitoring; typologies; pile foundation.

## 1 Introduction

Amsterdam contains an extensive network of historical quay walls, totalling over 200 kilometres within its urban area. These quay walls are divided over 1700 segments (“assets”) managed by the Municipality of Amsterdam. Due to their age and change in use, many quay walls are to be considered as potentially unsafe. In 2018, the need for addressing the structural issues of quay walls led to the Program of Bridges and Quay walls (Programma Bruggen en Kademuren).

Over the past three years, an intensive inspection program has been started. For about 1000 of the 1700 segmented quay walls an in-depth re-examination of archives has been completed. Additionally, on 400 quay walls submerged diving inspections have been performed, an exercise that is still ongoing. With a newly developed risk assessment tool, the Amsterdam Riskbased Quay Wall tool (Amsterdamse Risicobeoordeling Kademuren, ARK), approximately 200 quay walls have been evaluated by structural and/or geotechnical engineers. ARK is a qualitative assessment tool comprising of scores for various performance indicators and criteria, which are aggregated (using expert-based weighing factors) to obtain a safety assessment per asset. Furthermore, using data obtained by satellites from the past five years, nearly all quay walls are monitored.

Recently, a project started combining and analysing all the collected data through the use of Geographic Information System (GIS). The objective of the data analysis is to generate risk profiles for different types of quay walls within Amsterdam. It will facilitate a comprehensive understanding of the overall results and risks identified in inspection reports on asset level. Also, it will aid in prioritizing quay walls typologies for inspections, renewal and potential safety measures, creating a long term efficiency on areal level.

## 2 Quay wall typologies in Amsterdam

Although the 1700 quay walls segments in Amsterdam show a large variety, they can be subdivided in two major typologies. The first typology is a masonry wall, built on timber floors with vertical timber foundation piles, typically founded on the first sand layer in Amsterdam at a depth ranging from -7 till -9 meters below NAP. These types of quay walls are predominantly constructed before the 1920’s.

The second typology is a concrete L-shaped wall. The building of these structures started in the 1920’s and continues till today. Over a century of development since the introduction, multiple variations and construction methods within this category can be seen. For example, beneath the concrete L wall, there are timber foundation piles, but also concrete and steel piles. The earliest timber piles are founded on the first sand layer, the newest concrete and steel piles are founded at the second sand layer in Amsterdam at a depth of -20 metres NAP.

To gain a better understanding of the risk profiles associated with the majority of the quay walls, the two typologies mentioned above can be subdivided in approximately 20 typologies. These subdivisions are based on extensive archival studies and diving reports. The variants consist of differences in piles, angle of the foundation piles, height of the retaining wall, building

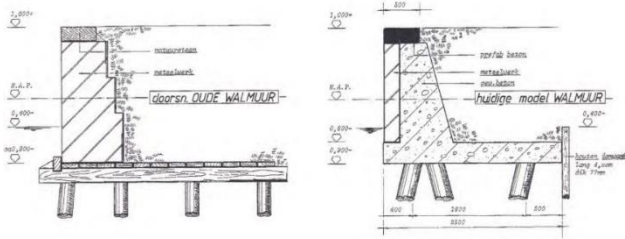


Figure 7: Main typologies of quay walls in Amsterdam: masonry- (L) and concrete L-shaped

period and the presence or absence of a small vertical retaining wall at floor level to prevent sink holes.

Together, the masonry and the L-shaped concrete wall, as displayed in figure 1, account for about 75% of quay wall assets in Amsterdam. The remaining 25% of the quay walls assets consist of steel sheet piling and soil slopes.

### 3 Combining inspection and monitoring data

The diving inspections on 400 quay walls result in a database containing over 10,000 wood samples extracted from timber foundation piles in Amsterdam. These samples, along with their respective reports, provide critical data on the degradation, pile diameter, pile angle and connection to the floor. Together with monitoring data and inspections to the structural state of the masonry, a risk assessment is performed.

In the current ARK assessment tool, both its condition and function are considered. The condition reflects the probability on a quay wall failure, while the function assesses the severity of the consequences of such failure.

The ARK tool employs four risk classifications, ranging from low to very high risk. Quay walls with a low risk remain under periodic maintenance schedule. Those assessed being at very high risk need urgent action, i.e. a fast but comprehensive evaluation where decisions are made regarding the necessary and appropriate (short term) safety measures. In this evaluation not only the structural safety is taken into account, but also the impact on



Figure 2: Gis based risk assessment

the environment (the citizen), sustainability and financial costs. Quay walls with a medium risk, proceed to a quantitative assessment through structural verification calculations.

### 4 First steps to data-driven asset management: GIS and Risk Profiles

This year, a project started combining all the collected data through the use of Geographic Information System (GIS). By doing so, the quay walls categorized into distinct typologies from archival researched are visually displayed with the results of diving inspections, and (satellite) monitoring data. To get an understanding of the project, in figure 2, the pile foundation data is plotted. This is not only an advantage into the structural assessment of a single asset, but is the starting point of risk management on all assets. Also, for decision-makers it gains a comprehensive view of the condition and functionality of each quay wall.

### 5 Conclusions

By combining all the data per typologies, a comprehensive view of each typologies' condition and functionality is achieved. The automation of data analyses will lead to a data-driven risk assessment approach that allows for the identification of high-risk areas requiring immediate attention and low-risk sections that can continue with periodic maintenance, much faster than the current object-based risk assessments. This provides a structured framework for prioritizing actions, ensuring an efficient and informed asset management strategy.



## Lock Renovation in Auvelais (Belgium) – Miter Gates

**Dubucq Robin**

Greisch (Project Leader), Liege, Belgium

**Bonivers Michaël**

Greisch (Project Director), Liege, Belgium

Contact: [rdubucq@greisch.com](mailto:rdubucq@greisch.com)

### Abstract

The lock of Auvelais is being renovated to improve its accessibility for vessels of 2000t. The miter gates have been modernized and optimized.

**Keywords:** Lock, Miter Gates, Gates, Renovation, Steel, Mechanics, Valves

### 1 Introduction

The lock of Auvelais, on the Basse-Sambre, is being renovated to improve its accessibility for convoys of Class CEMT Va (110 m x 11.4 m, 2000 t vessels). The renovation consists of the lowering of the lock's downstream miter sill, the replacing of the miter gates, and the rectifying of the upstream and downstream navigation walls. This project is co-funded by the European Union. Both gates are being replaced and the downstream one is now 50 cm taller. The gates have been modernized as well as the gates valves. This paper aims at explaining the parts of the gates for which a new design has been studied.

### 2 Main Renovations

*“As name refers, Miter gates are made up of two gate leaves that provide closure at a “miter” or angle pointed towards the upstream side of water flow.[1]”*

The previous miter gates were unsealed and it was difficult to guarantee the water level in the lock chamber. Moreover, the downstream miter sill had to be 50cm lower in order for bigger vessels to access the lock, from 1350T to 2000T. The object of the study on the miter gates was to:

- Improve the robustness by adding a defence system. The gates are designed to handle an accident by a vessel which doesn't stop in the lock;
- Reduce the number of longitudinal and vertical stiffeners and simplify the global structure;
- Improve the static scheme of the gates by ensuring that each element is assuming one function (adding punctual blocks, separating the rotation and displacement at the pivot);

- Add elastic anchor for the top pivot in order to reduce the shocks during the shutting or opening of the gates;
- Place the gates valve at the upstream side and the skin plate at the downstream side;
- Ensure a good sealing by a soft seal;

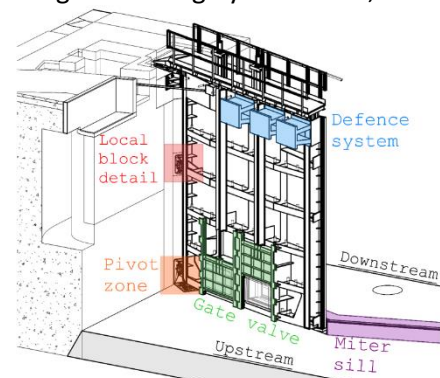


Figure 1 Sketch of the different elements

#### 2.1 Gates

The previous gates were using a wood to ensure the sealing and the equilibrium of the reaction since the blocks were parallel to the gates. A part of the miter reaction force had to be handled by the woods. As function of the wear of the wood, the static scheme of the gate is modified and the good sealing is no more guaranteed.

The new design of the metal structure is based on the horizontal reactions on the concrete. Horizontal steel beams are placed between the blocks. Vertical stiffeners transfer the water reaction to the horizontal beams. There are three layers of blocks on the downstream gates, two on the other ones.

The miter reaction is transferred to the concrete thanks to punctual blocks (blue on the figure below) and their

orientation is based on the resultant of the main force (water) applied on the gate ( $F_1$ ). The elements used to transfer the miter force reaction and to ensure the sealing have been separated in punctual blocks and a P rubber seal instead of wood. The static scheme of the gate is therefore clear.

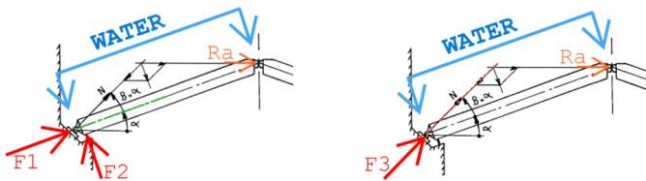


Figure 2 Static scheme of a miter gate (old – modern)

The angle  $\alpha$  is the miter angle and the resultant has the same angle to the gate  $\beta = \alpha$ .

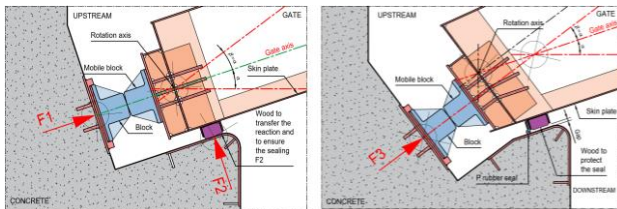


Figure 3 Local block detail (old – modern)

At the bottom pivot, the male and female elements had two different diameters. A horizontal movement was observed between the grey and orange parts. Nowadays, it is better to limit the role of the pivot to the rotation of the gates and the handling of the vertical reaction from the gate's dead load. There is a gap between the spherical bearing and the door and no more between the pivot and the spherical bearing. The sliding contact is now located between the orange and the green parts.

This gap is important to avoid the pivot gets unwanted stresses when the pression of the water is increasing. The miter force should go through the blocks and not the pivot.

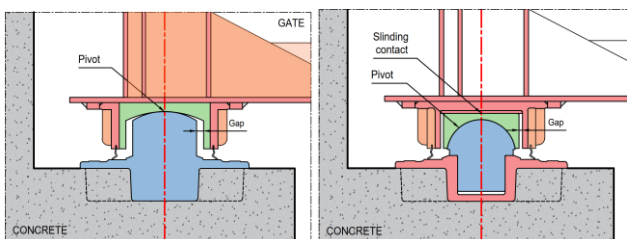


Figure 4 Old pivot - Modern Pivot

## 2.2 Gates Valves

The gates valves have been located at the upstream side of the gate in order to ensure a natural sealing thanks to the water reaction.

The rubber seal of the gate valve and the gliding stainless-steel of the gate have an angle of  $1.3^\circ$  from the vertical to ensure a quick clearance between the rubber and the gate. The rubber seal is preserved and the contact between the steel and the rubber is limited.

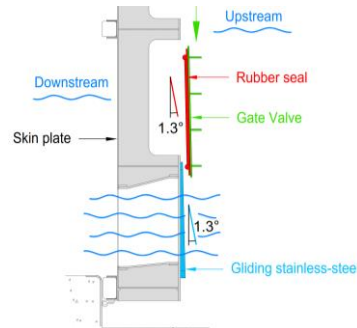


Figure 5 Gate valve

For the record, the skin plate is placed downstream to avoid any vertical reaction under the door when the water level is lower downstream. In fact, the position of the skin can affect the vertical reaction on the bottom pivot during the operations.

## 2.3 Blocks

It was asked by the client to use GE300 steel as material for the blocks. The standardisation between all the different elements was also a wish. It has been proposed to use standard crane rails. The maximal tensile strength for a GE300 is  $602 \text{ N/mm}^2$  in comparison to  $880 \text{ N/mm}^2$  for the crane rail.

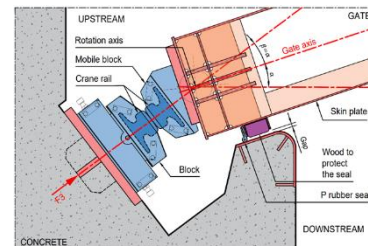


Figure 6 Crane rails used as blocks to ensure the transfer of the miter reaction force

## 3 Conclusions

The static scheme of the new gates is clearer and each element has one function. The miter gates are more robust and the sealing is ensured by appropriate materials.

The lock of Auvélais is able to raise and lower vessels up to 2000t as the other locks on the Basse-Sambre, against 1350t before the renovation.

## References

- [1] Jashindia. (2021, 27 septembre). *MITREGATE–Jashindia*. <https://jashindia.com/products/mitre-gate/>
- [2] FRT 103- Composants critiques et mécaniques des portes busquées

## Pont Patton – Ettelbrück – Luxemburg

**Ir. Koen Calleyl**

Victor Buyck Steel Construction – Senior Project Engineer

Contact: [koen.calleyl@victorbuyck.be](mailto:koen.calleyl@victorbuyck.be)

### Abstract

Located in Ettelbrück (LU), the existing Patton Bridge was replaced by a weathered steel-concrete infrastructure in 2020. The entire steel superstructure (drawing, assembly, erection engineering, installation) turned out to be extremely challenging and got assigned to Victor Buyck Steel Construction (VBSC) [1].

**Keywords:** weathering steel, fabrication, CAD, incremental launching, heavy lift, box girder, cantilevers, strong curvature, engineering, software

### 1 Project description

The new Patton Bridge is a composite steel-concrete deck with three hyperstatic spans. While being integrally connected to two intermediate steel piers, both ends support on an abutment. All built in weathering steelwork (1090T).

The longitudinal profile has a circular curve, which changes to a linear slope towards one abutment. In plan view, the bridge deck is circular (R120m), contains a transition curve (clothoid) and a straight segment.

The part with a constant curvature was incrementally launched on temporary trestle towers in order to cross the neighbouring river and railways. The remaining part was lifted in.

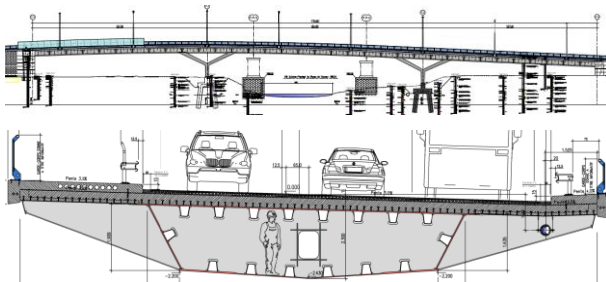


Figure 1. Global image of the Patton Bridge

### 2 Design and fabrication

The Patton Bridge consists of a constant cross section (box girder) that is longitudinally reinforced with trapezoidal stiffeners. The web plates are heavily inclined whereas the bottom flange is 'roof-pitched'. The box is internally and externally stiffened with diaphragms and cantilevers every 5,00m. The unpainted interior remains inspectable by access openings throughout the entire length.

Even though consisting of a through-stiffened deck plate, the design (Schroeder & Associés) is not to be considered as an 'orthotropic carriage deck'.

#### 2.1 Establishment of CAD Drawings

To establish CAD Drawings, the bridge wireframe is programmed in Rhino3D (Grasshopper) which holds the flexibility of amending geometric changes, which requires a tight involvement between draftsmen, project engineer and designer, until all is permanently settled.

In a second stage, VBSC imports the wireframe into Tekla, or a direct Rhino – Tekla link is established, to start shedding the frame with steel plates.

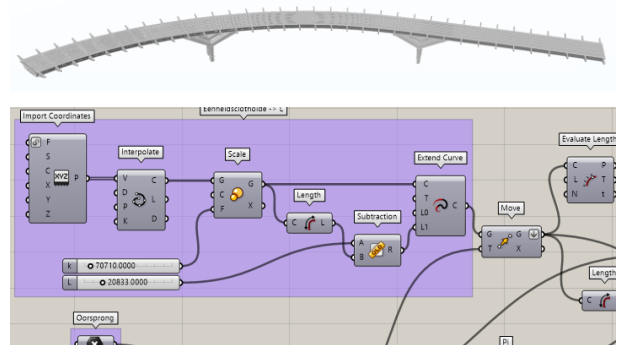


Figure 2. Rhino3D/GH Geometry extract

#### 2.2 Fabrication

The bridge deck was constructed into 20 segments (each segment ( $\pm 50T$ ) being half a bridge section) and 70 cantilevers. The piers were separated into 4 column bases and 4 V-shaped top parts. Translating the clients design correctly to a buildable and weldable steel structure is one of the major tasks of a steel contractor's project engineer.



Figure 3. Workshop assembly

### 3 Launching and the engineering

#### 3.1 About launching

Launching belongs to the most challenging erection methods, as they often demand a thorough design preparation and require a lot of logistics and auxiliary steel, in order to assemble and move the bridge in a few 'increments'. Among others, a few particularities are listed which make the Patton Bridge even more complex than the average launching:

- Extreme curvature (120m plan radius)
- Torsion-stiff box section
- The lack of classic (concrete) piers
- Full-depth cantilevers

#### 3.2 Design preparation

The incremental launching method brings the moving bridge deck in a different stress state with every bit of advancement. An Excel-based VBA link was programmed between Rhino3D and SCIA Engineer (Non-linear) to exchange between the three software systems. This allowed the 131m launch to be evaluated in-depth in steps of 1m.

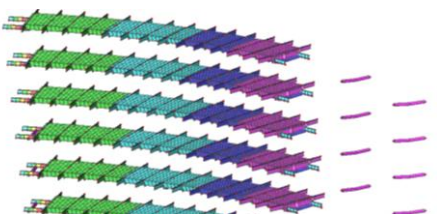


Figure 4. Impression of calculation model – 4 steps

#### 3.3 Auxiliary steel

The list of auxiliary steel designed and verified for the combined erection methods of a single bridge project seems endless: on-site assembly supports, lifting &

fixing equipment, site and craning layout, launching platform, launching supports, launching nose and tails, propulsion, guides, ... All to be thoroughly engineered within a strict programme.



Figure 5. Temporary Launching equipment

### 4 Discussion and conclusions

Bridge launching proves to be a very effective (yet often more costly) method to cross rivers, railways, highways, ... with limited interruption. It requires a lot of in-house knowledge, expertise and customized equipment with a very active role for a structural engineer.

I would like to express my deepest gratitude to the entire VBSC crew to get me involved in four complex launches already as a Young Engineer.

#### References

- [1] VBSC, *Victor Buyck construira le nouveau Pont Patton à Ettelbruck*, <https://victorbuyck.be/nl/blog/victor-buyck-construira-le-nouveau-pont-patton-a-ettelbruck>



## Structural Assessment of Historic Masonry Cellars in Utrecht

Peter Vos

Antea Nederland B.V., Heerenveen, NL

Contact: [peter.vos2@anteagroup.nl](mailto:peter.vos2@anteagroup.nl)

### Abstract

The city centre of Utrecht is home to approximately 1000 masonry cellars and little is known about their structural capacity. This paper presents a method to determine their structural capacity. A non-linear analysis is performed in DIANA FEA using the GRF-2 method. Results reveal distinct failure patterns, aiding in a better understanding of the structural behaviour of the cellars during heavy vehicle passage.

**Keywords:** structural capacity; masonry cellars; DIANA FEA; parametric design; automation.

### 1 Introduction

The city centre of Utrecht is home to approximately 1000 masonry cellars, with new discoveries still unfolding. *Figure 1* provides a schematic representation of a typical masonry cellar in Utrecht. Some of these cellars are more than 900 years old, some of them neglected for decades which has taken a toll on their condition. During those years a lot has changed: a growing population, development of cars and trucks, fluctuating water levels and various types of work in and around the cellars to name a few. The masonry cellars were originally not designed for this and currently there is little knowledge about their structural capacity which can potentially lead to unsafe situations. This paper will present the approach that was used to determine the capacity of the historical masonry cellars in Utrecht.

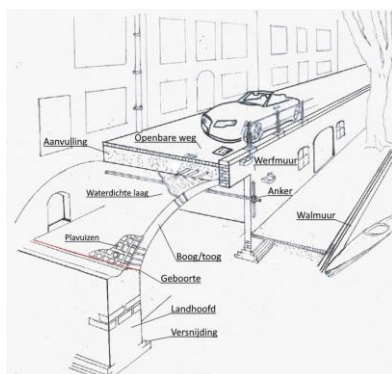


Figure 1: Typical masonry cellar in Utrecht [1].

### 2 Modelling Approach

The structure is assessed in accordance with the Eurocode and the Dutch NEN 8700 series for existing structures. The masonry cellar exhibits predominantly non-linear elastic behaviour due to factors such as crack formation in the masonry, the intricacies of arch deformation, and the ground-structure interaction. Consequently, a non-linear calculation is conducted to

provide a more realistic depiction of the structural behaviour and occurring failure mechanisms.

The structural assessment is done in DIANA FEA. A 2D plane strain model (infinitely extended constant cross-section) is used with a width of 1m as shown in Figure 2. The non-linear finite element method (NLFEM) is used for the calculation in combination with the Global Resistance Factor-2 (GRF-2) method as described in [3].

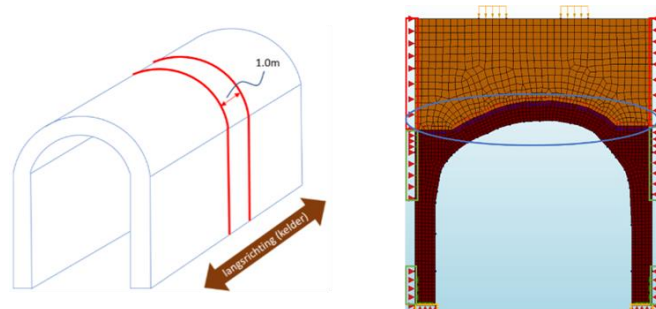


Figure 2: Schematic of the plane strain model (left) and the model in DIANA FEA (right).

The GRF-2 method employs the masonry's characteristic strength, reduced by a factor. The masonry is modelled based on a Total Strain Crack Model (TSCM) in which the crack orientation can rotate. In accordance with [2], an exponential softening curve has been chosen for the tensile behaviour and a parabolic curve for the compressive behaviour. The residual strength after cracking is set to zero for both tension and compression.

The geometry of the cellar and ground above are modelled in Diana using a 3D point cloud. The other elements are modelled as springs in the boundary conditions. Figure 2 shows the model and the boundary conditions with the: ground (red), adjacent cellars



(green), foundation (yellow), the ground-masonry interaction (blue) and the load of the wheels on top.

### 2.1.1 Limit states

The structural assessment is carried out considering both the Ultimate Limit State (ULS) and the Serviceability Limit State (SLS). In the ultimate limit state, a progressively increasing load is applied until structural failure is achieved. The serviceability limit state is determined by (1) a deformation criterion ( $L/300$ ) and (2) a crack width criterion ( $<1\text{mm}$ ).

### 2.1.2 Automating the Simulation Process

A sensitivity analysis is conducted in the form of a simplified Monte Carlo Simulation to assess the influence of the input parameters on the model output. In this process, automation is applied to systematically vary various factors such as boundary conditions, wheel load(s) position, and material properties within predefined ranges. The failure load for each simulation is subsequently determined by examining the load-displacement curve.

## 2.2 Results

Failure of the masonry arch is characterized by the following sequence of events:

1. Initialization of hairline cracks at low load levels;
2. Crack development leading to a reduced cross-section of the arch to distribute the load;
3. Reaching masonry compressive strength at multiple locations (formation of plastic hinges);
4. Further development of cracks (tensile regions) and plastic hinges (compressive regions);
5. Structural failure.

Table 2-1 shows an overview of the results with the wheel load at multiple locations ranging from left (LL) to right (RR). For the normative load case the cracks and compressive stresses are shown in Figure 3.

Position wheel load:	LL	L	M	R	RR
Reaching the masonry compressive strength [kN]	287	373	560	545	480
Failure load [kN]	797	890	1117	966	980

Table 2-1: Results for the normative load case.

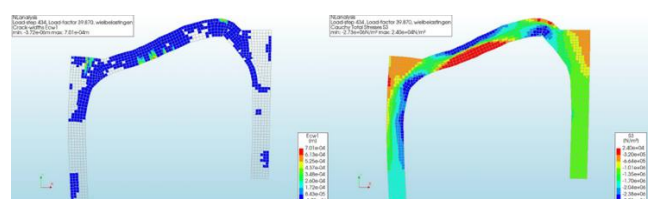


Figure 3: Crack formation (left) and compression stresses (right), deformations increased by a factor 5.

The highest failure load occurs with a centrally placed load, while its weakest point is when the load is placed on the far left. The asymmetrical loading results in increased deformation, hindering the arch from functioning at its best as illustrated in Figure 3. Because the arch has a larger span on the left compared to the right side, the left side is the normative load case for the cellar in this example.

In every load scenario, cracks initiate in the upper part of the arch, in a direction perpendicular to the cross-sections illustrated in Figure 3. The initial hairline cracks appear at relatively low load levels, well in advance of reaching the compressive strength of the masonry. Even when the compressive strength of the masonry has been reached, the structure still retains significant structural capacity until it ultimately fails. This insight enables more effective inspection procedures for identifying cracks caused by over-loading of the structure.

## 3 Conclusions

This document outlines a methodology for evaluating the structural integrity of masonry cellars in Utrecht by determining their maximum capacity. The analysis employs a non-linear finite element approach within DIANA FEA, utilizing a 2D plane strain model and the Global Resistance Factor-2 (GRF-2) method. The findings unveil specific failure patterns when overloading of the structure happens. These are characterized by cracks in the upper part of the arch and in a direction perpendicular to the cross-section. This contributes to a deeper comprehension of how the cellars respond to the passage of heavy vehicles, the potential risks and what to look for when there is a concern that the cellar might be overloaded.

## References

- [1] Report on basements in the city centre of Utrecht, October 2020. Drawn up by the City Engineers City Companies department of the municipality of Utrecht.
- [2] Hendriks MAN, Roosen MA. (2020). Guidelines for nonlinear finite element analysis of concrete structures (RTD 1016-1:2020). Ministry of Infrastructure and the Environment—Rijkswaterstaat.
- [3] Aanpak constructieve beoordeling metselwerk boogbruggen 's-Hertogenbosch, RHDHV/ Nebest, Witteveen+Bos, Iv-Infra, 23-07-2020.



# Assessing concrete structures after repair: a chloride ingress forecasting model

Karel Van Den Hende, Stef Helderweirt, Wouter Botte, Stijn Matthys and Robby Caspeele

Department of Structural Engineering and Building Materials, Ghent University, Ghent, Belgium

Geert Lombaert

Structural Mechanics, Civil Engineering Department, KU Leuven, Leuven, Belgium

Contact: [karel.vandenhende@ugent.be](mailto:karel.vandenhende@ugent.be)

## Abstract

Chloride migration in reinforced concrete is a significant factor leading to reinforcement corrosion, which can compromise the structural integrity and service life of concrete structures. This paper presents an overview of analytical models designed to predict and assess the effectiveness of repair methodologies for chloride ingress, including coatings, repair mortar overlays, and partial cover replacement by repair mortar. These models enable a practical evaluation of each repair method, facilitating informed decision-making for an optimal repair strategy.

**Keywords:** Chloride-induced corrosion, concrete repair, analytical modelling

## 1 Introduction

Chloride migration in reinforced concrete is one of the main reasons why reinforcement inside of concrete structures starts to corrode. In order to extend the lifetime of a structure, several repair methodologies are available to reduce the ingress of chlorides. In this work, an overview is given of analytical models to predict the chloride profile after application of a coating, repair mortar overlay or partial cover replacement by repair mortar. This enables the assessment of each repair method, which can be used to make a well-based decision on the final repair strategy.

## 2 Modelling of chloride ingress

### 2.1 Chloride ingress before repair

Regarding modelling of chloride ingress through a concrete substrate, general consensus has been achieved. The transport of chlorides through the concrete substrate is typically described by the one-dimensional solution of Fick's second law of diffusion:

$$C(x, t) = C_s \left[ 1 - \operatorname{erf} \left( \frac{x}{2\sqrt{Dt}} \right) \right] \quad (1)$$

where  $C(x, t)$  is the chloride concentration at depth  $x$  and time  $t$ ,  $D$  the diffusion coefficient,  $C_s$  the surface concentration which follows from the environmental conditions and  $\operatorname{erf}(\cdot)$  the error function.

### 2.2 Chloride ingress after repair

#### 2.2.1 Repair strategies

The working principle of each repair methodology is illustrated in Figure 1, which shows the influence of the intervention on the ingress of chlorides.

The first repair method considered is a coating which creates an additional barrier on the concrete surface. This barrier is harder to penetrate than the usual concrete and hence reduces the introduction of new chlorides into the concrete. Alternatively, a layer of repair mortar can be applied to the concrete surface which reduces the introduction of new chlorides, but also part of the already penetrated chlorides will migrate back to this new "clean" layer.

The last possible repair method considered here, is replacement of part of the contaminated concrete by a repair mortar. In the same way as the previous methods, fewer chlorides will migrate from the exterior because a more dense layer is located at the surface. Additionally, part of the chloride-contaminated zone is removed, which reduces the chloride content.

#### 2.2.2 Modelling

Modelling of the chloride-ingress after repair can generally be calculated as [1]:

$$C(x, t) = C_s + \sum_{n=1}^{\infty} A_n f_n(x, \lambda_n) \exp(-\lambda_n^2 t) \quad (2)$$

The coating application is considered to be a convection-diffusion problem, and hence the variables are defined as [2]:

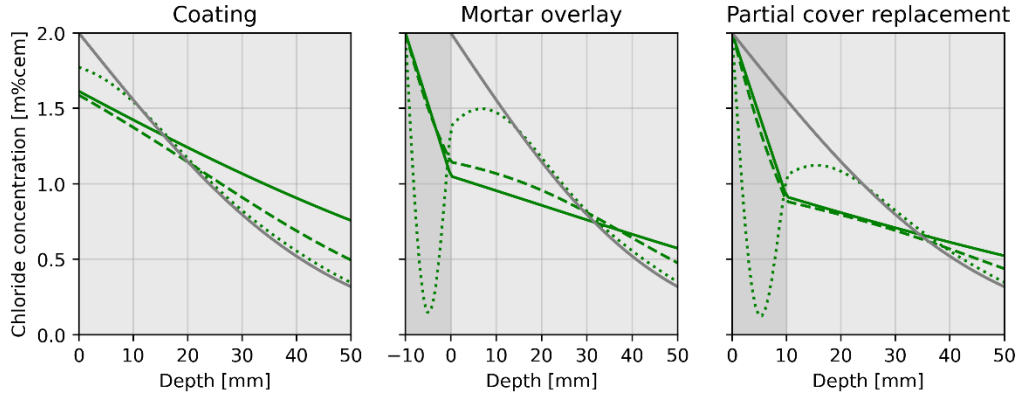


Figure 1: Result of analytical models to study the influence of repair strategies on ingress of chlorides

$$f_n(x, \lambda_n) = \sin\left(\frac{\lambda_n x}{\sqrt{D_2}}\right) + \frac{\sqrt{D_2}}{h_s} \lambda_n \cos\left(\frac{\lambda_n x}{\sqrt{D_2}}\right) \quad (3)$$

$$A_n = \frac{\int_0^{h_1} [C_{t=0} - C_s] f_n(x, \lambda_n) dx}{\int_0^{h_1} f_n(x, \lambda_n)^2 dx} \quad (4)$$

$$\frac{1}{\sqrt{D_2}} \cos\left(\frac{\lambda_n h_2}{\sqrt{D_2}}\right) = \frac{\lambda_n}{h_s} \sin\left(\frac{\lambda_n h_2}{\sqrt{D_2}}\right) \quad (5)$$

Whereas the application of mortar is modelled as a two-material diffusion process, this leads to the following terms [1]:

$$f_n(x, \lambda_n) = \begin{cases} \frac{\cot\left(\frac{\lambda_n h_2}{\sqrt{D_2}}\right)}{\sin\left(\frac{\lambda_n h_1}{\sqrt{D_1}}\right)} \sin\left(\frac{\lambda_n x}{\sqrt{D_1}}\right), & 0 \leq x \leq h_1 \\ \frac{1}{\sin\left(\frac{\lambda_n h_2}{\sqrt{D_2}}\right)} \cos\left[\frac{\lambda_n(x-h_1-h_2)}{\sqrt{D_2}}\right], & h_1 < x < h_1 + h_2 \end{cases} \quad (6)$$

$$A_n = \frac{\int_0^{h_1+h_2} [C_{t=0} - C_s] f_n(x, \lambda_n) dx}{\int_0^{h_1+h_2} f_n(x, \lambda_n)^2 dx} \quad (7)$$

$$\tan\left(\frac{\lambda_n h_1}{\sqrt{D_1}}\right) \tan\left(\frac{\lambda_n h_2}{\sqrt{D_2}}\right) = \sqrt{D_1/D_2} \quad (8)$$

Where  $C_{t=0}$  is the chloride profile at the moment of the repair governed by Eq. (1),  $h_1$  the thickness of the repair mortar,  $h_2$  the design space of the concrete substrate typically chosen equal to 300 mm,  $D_1$  and  $D_2$  the diffusion coefficient of the mortar and concrete respectively, and  $h_s$  the convection coefficient of the coating.

### 2.3 Optimization of interventions

With the models derived in this work, chloride profiles as shown in Figure 1 can be easily derived and the effect of a repair strategy can be quantified. The choice of

repair strategy can be based on the probability of depassivation, i.e. the probability that the chloride content at the reinforcement exceeds a critical threshold. This requires the ingress of chlorides to be quantified in a probabilistic context, taking into account the variability of all parameters involved. Due to the analytical nature of the models given in this paper, probabilistic modelling becomes practically feasible.

### 3 Conclusions

In this work, analytical methods are given which enable to assess the influence of a repair strategy on the migration of chlorides. Due to the simple and analytical nature of the equations, it allows for easy implementation in practical software (e.g. MS Excel), which makes it practical for the daily engineering practice.

### References

- [1] Wang T., Zheng J.J. and Dai J.G. Analysis of time-dependent chloride diffusion in surface-treated concrete based on a rapid numerical approach. *Structure and Infrastructure Engineering*. 2022; **19**(3): 332-344.
- [2] Van Den Hende K. et al. Probability-based service life design of repair mortar overlay in case of chloride-induced depassivation risk. *Proceedings Life-Cycle of Structures and Infrastructure Systems*. 2023; 2371-2378



## Modern trends in Bridge Health Monitoring (BHM)

Muhammad Farjad Sami, Hans De Backer, Amelie Outtier  
Universiteit Gent, Gent, Belgium

Contact: Muhammadfarjad.Sami@UGent.be

### Abstract

Bridges are exposed to harsh environmental conditions and require more robust monitoring to ensure their safety. With the current technological advances many new monitoring approaches are considered. Some of them include smart sensors, fiber optics, and computer vision based technologies and machine algorithms. Unmanned aerial vehicles (UAVs) and robotic vehicles have also been employed successfully with the advantage being easy access and fast data acquisition. However it is important to understand the nature and limitations of each technique.

**Keywords:** Bridge health monitoring (BHM), Smart sensors, Computer vision, Unmanned aerial vehicles (UAVs)

### 1 Introduction

Bridges are among the most monitored civil engineering structures as they sustain excessive structural degradation caused by several factors, including harsh environment, traffic collisions, and increasing traffic volume and load. Bridge health monitoring (BHM) is a multi-discipline field developed to predict and detect damage at the early stages. Traditional BHM involves onsite evaluation, requires substantial field labour, experience, and operational interruptions. Therefore, developing a cost effective, accurate, and automated noncontact solution for efficient and reliable BHM has been an emerging research topic. This paper presents a brief summary of various techniques and procedures used in the last two decades for BHM

### 2 Global and local Health Monitoring of Bridges

Damage at a local level may be considered as changes in the effective material properties or conditions such as crack, spalling, corrosion. Ultrasonic measurement, impact-echo and tap tests are well proven technologies that are used to evaluate local conditions [1]. Global health monitoring methods are centred on finding shifts in resonant frequencies or changes in structural mode shapes. Various techniques are used for global. These include, but not limited to: 1. Observing natural frequency shift 2. Change in mode shape 3. Ritz vectors 4. Matrix update method 5. Statistical pattern recognition approach using Bayes theorem.

### 3 Modern techniques used in BHM

With the technological advancement many new approaches have been employed for BHM. Some of the

most promising techniques are briefly discussed along with their limitations and advantages.

A novel method to monitor cracks is the use of imaging and pattern recognition. The fact that Cracks reflect or absorb light differently from the neighbouring region is used. X-rays and Gamma rays are used to get visual images of the interior of structures such as steel cables and slabs. The size of the equipment makes it difficult to reach locations with difficult access. These techniques require access to both sides of a structure, however use of back-scattered signals has mitigated this problem [1]. Radar technology has recently seen many new innovations in the area of sensing. Major innovations include the development of ground penetrating radar and broadband radar. Infrared thermography is also employed to detect debonding of steel bars[1]. However dependence on the thermal emissivity, effects of the external temperature reduce the accuracy of the measurements and allow for qualitative investigations only [2]. Elastic waves are generated by a material experiencing internal changes. By monitoring the acoustic emission of these elastic waves, it is possible to monitor the structural health of bridges even with a limited coverage of the structure [2]. The recorded data by application of actuators and sensors such as piezoelectric materials for long term monitoring is extensive and requires costly processing. Hence smart sensors are employed which can process the data before the output is recorded. Another class of smart sensors consists of those sensors that can communicate with each other and are capable of communicating among themselves and communicate the sensed data wirelessly by hopping from one sensor to another. Wired sensors need to be installed during construction thus affecting the use of structure and also limiting the number of sensors deployed [1]. Fiber optics have made distributed sensing possible. The chemical coated fiber optics can be used to



detect the corrosion in reinforcement [1]. Flexibility, Electromagnetic Interference Immunity, and scalability are among the advantages [2]. However expensive data acquisition equipment, complicated installation process are among disadvantages. These can be avoided by using coaxial cable as sensors. For efficient BHM very large amount of data is collected. ML algorithms and Convolutional Neural Network (CNN) are being developed to process this huge data and provide real-time feedback. The template matching technique, feature matching technique and optical flow are the most common algorithms for obtaining displacement time histories with high accuracy. Modal 3D algorithm is used for Image processing. Mask R-CNN is used for component identification. Examples of CNN include custom CNN, Xception, and AlexNet for detection of concrete deterioration.

## 4 Vision Based techniques

With the advances in image processing techniques, researchers have employed photogrammetry and computer vision based techniques to overcome the limitations of the number of data collection points, accessibility and interference with the normal functioning of bridge. Digital image correlation (DIC) involves applying camera detectable patterns on the surface to measure displacements. Light detection and ranging (lidar) uses light in the form of a pulsed laser to measure and quantify variable distances. Digital twins (DTs) are used to create a virtual representation or digital counterpart of an entity, which can be an object or a procedure. Computer vision (CV) is another low-cost, long-distance, contactless process. Fig 1 shows a framework for CV based BHM [3].

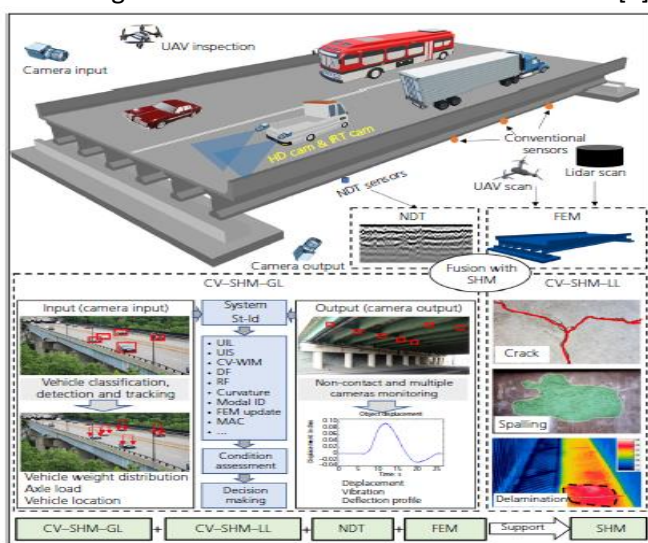


Figure 1: Framework for CV based BHM [3]

## 5 UAV and robotics sensing systems

Unmanned aerial vehicles (UAVs) and robotic vehicles have the ability to expedite the optical-based measurement process with increased accessibility, and reduced interference. UAVs can fly autonomously, remotely controlled by computers, humans or both. These small-sized aircraft have been used increasingly in a variety of civil applications. These include inspection of pipelines, bridges, roads, capturing images for 2D and 3D DIC analysis, combined area virtual models, 3D orthogonal mapping [2], etc. On the other hand ubiquitous bridge inspection robot systems (U-BIROS) have a robotic arm with a camera installed, used to scan and generate a crack map for bridges. Similarly with the help of a mounted camera and an integrated edge detector software, robotic crack inspection and mapping (ROCIM) was able to autonomously inspect bridge decks. A wall-climbing robot was employed successfully for monitoring and corrosion detection in reinforced concrete. Metric learning support vector and impact-echo techniques were used for the functioning of this robot.

## 6 Conclusions

None of these technologies offer a solution to solve all problems in bridge engineering. It is essential to define the problem and the desired end goals before considering which technology to use. Understanding the capabilities and limitations of the technologies, some of which are briefly described here, is also a critical step towards achieving the end goal. In addition, some of these technologies can be employed and combined in an integrated manner.

## References

- [1] Chang, Peter C., Alison Flatau, and Shih-Chii Liu. "Health monitoring of civil infrastructure." *Structural health monitoring* 2.3 (2003): 257-267.
- [2] Reagan, Daniel, Alessandro Sabato, and Christopher Niezrecki. "Feasibility of using digital image correlation for unmanned aerial vehicle structural health monitoring of bridges." *Structural Health Monitoring* 17.5 (2018): 1056-1072.
- [3] Catbas, Necati, and Onur Avci. "A review of latest trends in bridge health monitoring." *Proceedings of the Institution of Civil Engineers-Bridge Engineering*. Vol. 176. No. 2. Thomas Telford Ltd, 2022



## Research: Use of innovative techniques in bridge inspections

**Thomas Plumet**

*Agentschap wegen en verkeer, Evere, België*

Contact: [thomas.plumet@mow.vlaanderen.be](mailto:thomas.plumet@mow.vlaanderen.be)

### Abstract

Innovation in bridge inspections is currently ongoing, employing various inspection techniques. Drones are being utilized for inspections of water-carrying conduits and box girders. Drones offer significant safety advantages, particularly in confined spaces. However, the introduction of new techniques also presents new challenges, which we have endeavored to address through innovative approaches.

**Keywords:** bridges; inspections; box girder; ROV; drones; crawler.

### 1 Introduction

In the field of inspections we are continuously looking for opportunities to improve our bridge inspection techniques. For example the use of drones and ROVs (remotely operated vehicles). The possibility for a more efficient inspection and a safer inspection are the main reasons that we do our research. This paper gives an overview of the research that has been conducted by the Flemish Agency for Roads and Traffic (AWV) in Belgium.

### 2 Methods

We conducted experiments to explore the diverse range of applications for drones. Our investigations included inspections both above and below the water's surface. One of our key endeavors involves developing a system for inspecting the interior of bridge caissons. We are also exploring the use of various tools to enhance operational efficiency and effectiveness.

### 3 Descriptions

#### 3.1 ROV inspections

The use of Remotely Operated Vehicles (ROVs) is gaining increasing prominence in the field of bridge inspections. We primarily employ ROVs to inspect water-carrying conduits that are otherwise inaccessible to our personnel. This eliminates the need for our inspectors to enter these confined spaces, significantly enhancing job safety. Another valuable benefit of ROV inspections is the ability to obtain visual data both above and below the waterline without the need for divers as shown in figure 1. This capability allows us to better assess and map the splash zone. ROV inspections do come with their inherent limitations. In cases where

there is uncertainty regarding the data captured by these devices, it still necessitates the presence of an inspector to perform a follow-up assessment. This means that we are still required to send personnel into confined spaces when doubts arise. The tactile assessment of concrete surfaces by physically feeling and tapping them remains a valuable source of information, particularly in cases where the extent of damage is in question.

Ultimately, it remains crucial to prioritize the creation of high-quality deliverables. The use of ROVs offers a wide range of inspection possibilities. For certain applications, above-water inspections may suffice, while others require the use of underwater sonar. The most comprehensive applications may necessitate the generation of a complete point cloud with indications of damages and cross-sections. Making a well-informed assessment of these factors is essential before proceeding with the execution of an inspection.



*Figure 1 Under and above water image with ROV*

#### 3.2 Developing interior inspections of bridge caissons

This has been one of our most challenging projects – inspecting box girders in bridges. These box girders are often extremely inaccessible. Accessing them requires a cherry picker, but cherry pickers are typically restricted to use by the fire department for entry. Another option is using a ladder, but climbing a 5-meter ladder and then performing an entry of the box girder is not particularly



safe. Additionally, these box girders are treated as confined spaces, necessitating the presence of an attendant at the manhole at all times which is hard on a ladder. All of these factors make manually inspecting these box girders cumbersome. That's why we turned to drones to work more efficiently, safely, and with high quality.

Our first pilot project involved a brief demonstration with the ELIOS 3 drone at the Goedinge Bridge over the Leie River in Ghent. The images were of low quality due to the kicked-up dust, and we could only inspect three compartments of the box girder. The signal deteriorated significantly later on. However, we did achieve positive results in terms of positioning accuracy, and the live stream feature, which allows an inspector to follow the inspection in real-time, was an advantage. All of these factors motivated us to further investigate and refine our approach.

The second pilot project was a proof of concept that we wanted to carry out. We aimed to determine whether it was possible to conduct a comprehensive inspection of a box girder using flying drones. This took place at the bridge over the E17 in Bontinckstraat, a type of bridge that is common in the AWW infrastructure.

Unfortunately, we primarily obtained poor results with this approach. The box girders in this type of bridge are larger, resulting in a significant amount of dust, which severely affected the image quality as shown in Figure 3. Another challenge was that the drone was too large to fit through the internal manholes. In the case of this bridge, the drone could only navigate through the first compartment, as there was a high risk of it getting stuck in the second compartment. Retrieving the drone from the second compartment would require a manual entry. Following the proof of concept with flying drones, we decided not to proceed with this approach.



Figure 2 Dust problem in boxgirder

Keeping the challenges in mind, we explored alternative solutions, eventually leading us to consider ground-based drones, crawlers, or multipurpose drones. Initially, we looked into types like SPOT, which moves like a four-legged animal. This approach seemed promising for overcoming the issue of high crossbeams without requiring additional attachments. However, it

turned out that the market lacked sufficient experience in this area, so we continued our search.

Our investigation eventually led us to a project at Caltech where they had developed a combination of a flying and ground-based drone. This concept seemed like it could address our problems. Unfortunately, this solution was not cost-effective in the short term, and the drone was still in the conceptual stage.

We decided to conduct a second Proof of Concept (POC) on the Bontinck Bridge, this time using crawlers. The results with crawlers were largely positive. The crawler is suspended from a wire, eliminating any battery concerns, and it can be easily pulled out of the bridge girder in case of emergencies. The only issue we encountered was that the crawler couldn't navigate over the crossbeams. After discussions with the manufacturer, we developed a solution as shown in figure 4. Crawlers have a high torque capability, allowing them to overcome steep obstacles. For metal bridges, magnetic crawlers provided a suitable solution, while for concrete bridges, we opted for a conceptual solution involving ramps.

This necessitated a final testing site, the Mylle Bridge in Bruges. This bridge featured extremely high crossbeams and very short compartments. The test proceeded smoothly, with the only issue being that the high torque caused the ramps made of tear plate to shift. However, this is easily resolved by securing them to the manhole. It has been decided to move forward with this approach, and there is an ongoing project to fully equip the first bridge with this concept and conduct a comprehensive inspection. If these results prove positive, there will be no obstacles to inspecting bridges with box girders efficiently using unmanned devices.

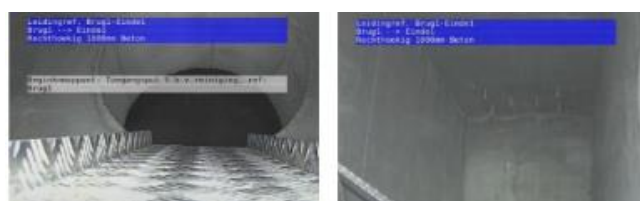


Figure 3 Footage of the crawler

## 4 Conclusions

In summary, it's evident that there is a focus on innovation in the niche field of bridge inspections. Through our research and experimentation, we have identified a valuable addition to the toolkit for inspecting water-carrying conduits. We believe that by using crawlers to inspect bridge girders, we can reduce the need for manual entries, reserving tactile inspections only for cases of significant doubt.



# Renovating the IJ-viaduct while keeping Amsterdam Central Station in operation – A case study

Stakeholders: the difference between building in theory and building in the outside world

**Ir. Laura van der Hoeven**

ProRail

[laura.vanderhoeven@prorail.nl](mailto:laura.vanderhoeven@prorail.nl)

**Keywords:** Renovation, Viaduct, Station, Railway, Stakeholder management, System Engineering

## 1. Context

The IJ-viaduct is a viaduct that finds itself under the railway boxes of tracks 13, 14 and 15 of Amsterdam Central Station (Figure 1). The viaduct, which was built in 1924, is a 320 meter long and 20 meter wide steel construction surrounded by concrete (Figure 2). After almost one hundred years the IJ-viaduct is nearing the end of its technical lifespan. Therefore, the IJ-viaduct needs to be renovated. Apart from this project, five other large projects are doing construction work on and around Amsterdam Central Station. However, as the IJ-viaduct is located in one of the most important stations of the Netherlands, the station cannot be closed off completely. Therefore, there needs to be coordination with all the involved stakeholders; such as the Dutch railway provider (NS), the municipality of Amsterdam and the other projects of ProRail. This paper uses the IJ-viaduct renovation project as a case study to argue that taking into account stakeholders and their requirements makes building in the outside world different than building in theory.

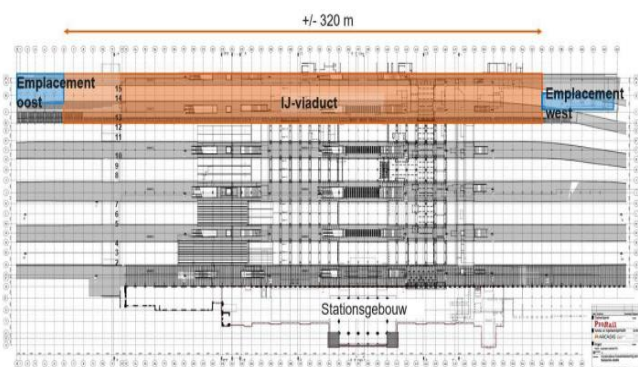


Figure 1. The location of the IJ-viaduct within Amsterdam Central



Figure 2. The construction of the IJ-viaduct in 1924.

## 2. Objectives

The scope of the project is to extend the lifespan of the IJ-viaduct until 2070, while keeping Amsterdam Central Station in operation and without preventing the other ProRail projects from doing their work.

RQ 1: Which parts of the structure need to be renovated in order to expand the lifespan of the IJ-viaduct with 50 years?

RQ 2: Which are the constraints in order to keep Amsterdam Central Station in operation?

RQ 3: How to renovate the scope parts while meeting the requirements of keeping Amsterdam Central Station in operation?

RQ 4: What would theoretically be the most ideal solution on renovating the scope parts?

## 3. Theoretical framework

After concluding which parts need to be renovated (RQ 1), a solution can be developed on how to renovate the parts. When working in theory the most ideal solution can be selected, which is the solution that is most favourable in terms of quality. However, in the real world this solution might not be a viable one as it does not reckon with the circumstances of the outside world. These circumstances are represented by the interests of the stakeholders. These



stakeholder interests can be summarised in a so-called CRS, which stands for a client requirement specification. When building in the real world, a solution should meet the formulated CRS. Therefore, the selected solution on how to renovate the parts, is probably not the most efficient one, as it is restricted to requirements such as money, time and other stakeholder interests.

#### 4. Methodology

In the exploration phase of the project an engineering company examined the viaduct and wrote an maintenance report. Based on this report the scope of renovation parts were determined. In the project development phase the CRS was compiled by talking to the different stakeholder parties such as the NS, the municipality of Amsterdam and the other projects of ProRail. Based on the CRS a solution was found on how to renovate the determined scope parts. In the interest of this paper the renovation solutions of the outside world was compared to the theoretical solutions.

#### 5. Key findings

The key findings are summarized in table 1, photos of the scope part can be found in the paper itself. When comparing the theoretical solution with the outside solution there can be concluded that the outside solution is a adjusted version of the theoretical one and therefore a less ideal solution in terms of time and money.

#### 6. Conclusions

When building in theory the best renovation solution can be selected on time, money and other interests, but in the real world a renovation solution needs to meet certain requirement. These requirements are formulated by stakeholders and can be summarized in a client requirement specification (CRS). The real world renovation solution is for this reason often not the ideal renovation solution. Therefore, building in the outside world differs from building in theory. As is shown by the case study of the renovation of the IJ-viaduct.

Table 1: Three of the determined scope parts, their theoretical solution and their outside solution, based on the user requirements given by the stakeholders.

Scope part	Theoretical solution	User requirement (Stakeholder)	Outside solution
Replace retaining wall platform 15	Demolish monumental wall in front and replace the retaining wall	The monumental wall needs to remain its value (Municipality of Amsterdam)	Before replacing the retaining wall, carefully take apart the monumental wall and store it so it can be reused
Restore steel coating bottom side IJ-viaduct	Remove all cables and pipes and repair from the bottom up	The cables and pipes have to remain their function (NS)	Repair mostly from the top down
Replacing the girders of platform 13 and 14	Replacing the girders at the same time	Platforms 13, 14 and 15 cannot be closed off at the same time (Other ProRail projects)	Replacing the girder of platform 13 in a different phase than replacing the girder of platform 14



# Cycling bridge ‘Vijfstraten’: using parametric design in bridge engineering

Ronan Pieters

SBE nv, Sint Niklaas, Belgium

Contact: [ronan.pieters@sbe.be](mailto:ronan.pieters@sbe.be)

## Abstract

This paper presents the design for a new cycling bridge in Sint Niklaas. Since the architect desired an organic hole pattern on inclined plates, it became clear that traditional design methods would be inefficient. They would also be perilous for correct data sharing between architect, engineer and draftsman.

To enable efficient data sharing, a central geometric model was used to which all involved parties could refer. This ensured that all data models (FEM, BIM, visual, ...) were equivalent. This geometric model was built in a parametric way to establish the organic pattern based on (*pseudo-*) random values.

**Keywords:** Parametric design, organic architecture, structural design, BIM model, steel bridge

## 1 Introduction

For the F4 cycle highway between Ghent and Antwerp, a new cycling bridge is constructed over the Vijfstraten intersection in Sint-Niklaas. The steel bridge, consisting of 2 spans and a total length of 93m, is designed as a single U-shaped profile with a continuous transverse section. For aesthetics, decorative perforations were added on the parapets.

As the envisioned bridge became geometrically complex, new methods were explored to create it efficiently. The complex geometry also proved an obstacle for data sharing between everyone involved.

## 2 Central geometric model

The central geometric model was created with Rhino - Grasshopper. This enables for a programmable geometry based on dependencies and formulas.

### 2.1 Axis based geometry

All bridge structures can be (more or less) described as axis based geometries. This axis, along with the positions of supports, will be the input for the parametric model.

A first step consists of defining stations along the axis. These stations are planes with (1) the origin on the axis, (2) the local z tangent to the axis and (3) local x in the global xy-plane. Primary stations define the positions of the abutments and pilar, secondary stations are used for cross-sectional plates.

The ‘points of interest (POI)’ for the cross section are then mapped to all the stations. Then, corresponding points can be linked together to form plates between stations and within stations.

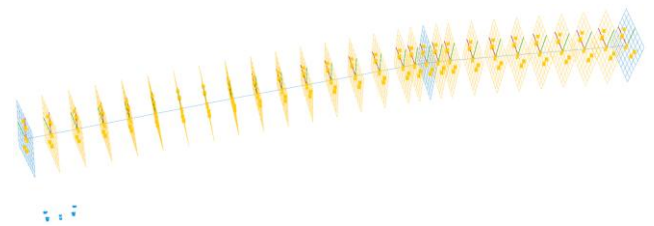


Figure 1. Axis with primary stations (blue) and secondary stations (yellow)

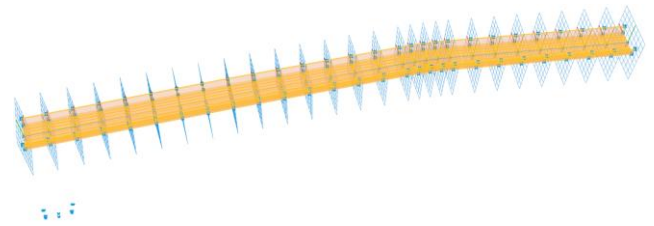


Figure 2. Plates after linking mapped POI (yellow)

### 2.2 Organic pattern

The base shape of the cut-pattern in the bridge is the triangle used for signaling the bicycle highway ‘F4’ to which the bridge is a part. These triangles are preset to four different possible sizes (none, small, medium and large cut). The triangles are positioned in a hexagonal pattern. An important engineering boundary condition is to reduce the amount of removed material in areas where large shear forces are present (near abutments



and pillar). Lastly, it is important to avoid conflicts of the cut pattern and other structural elements like the handrail stiffeners.

To comply with all the goals described above, the following algorithm was constructed. First, all panels (between two rail stiffeners) were subdivided in a hexagonal pattern and for each triangular position a (pseudo-) random value was assigned. These random values determined the cut shape at that position:

- [0,00 ; 0,25[ => no cut
- [0,25 ; 0,50[ => small triangle
- [0,50 ; 0,75[ => medium triangle
- [0,75 ; 1,00] => large triangle



Figure 3. Hexagonal base pattern

A scaling of the random values is still necessary to make sure that little or no material is removed at the zones of the abutments and the pillars. Therefore, each triangular position was assigned its relative location within its span (between 0 and 1). Depending on this position, a quasi-parabolic function was used to rescale the random values and these scaled values were eventually applied resulting in the organic pattern.

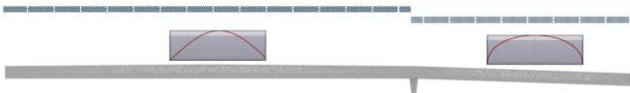


Figure 4. Scaling functions



Figure 5. Close up of resulting pattern

### 3 Export to FEM model

Once the algorithm was made, a first line-model for structural design could be exported to SOFiSTiK. Based on this model, a preliminary design was conducted. A later stage called for a more detailed area-model in which all remaining checks could be performed.

It goes without saying that with every design step, adjustments were made to the input parameters of the central geometric model.

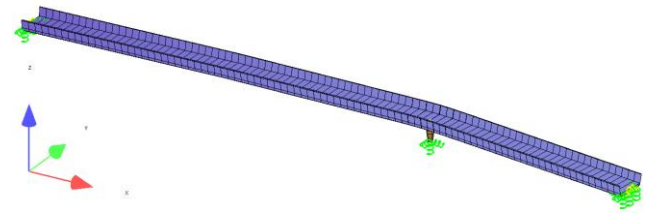


Figure 6. Beam model

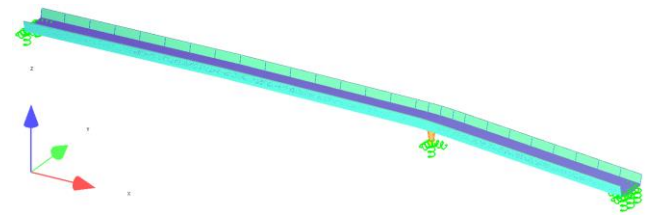


Figure 7. Quad model

## 4 Export to BIM model

Once the results from the FEM were satisfying, an export of the geometric model to a BIM software (here Tekla Structures) could be performed. Since both FEM and BIM model come from the same source, the risk of human error in redrawing a structure from engineering sketches was eliminated.

It should be noted that there were of course still additions to be made to the BIM model by a draftsman, e.g. the joints and support bearings.

## 5 Awards

This project had received the 'Construsoft BIM Awards 2023' [\[link\]](#) for its use of the aforementioned methods.

Also a 'Belgian Construction Award for Communication' [\[link\]](#) was obtained for this project. It was awarded for the citizen participation with central aspect a cycling simulation. A key aspect for this VR-model was the geometric and BIM-model.

## 6 Conclusions

For the purpose of model sharing, especially between more than two parties, a central geometric model proved reliable.

Furthermore, parametric modelling was an efficient method to create complex geometries based on dependencies and formula